



# Design, build, and testing of a multicolour CNC drawing machine

Mechatronic Project 478  
Final Report

Author: Mia Ham  
25872214

Supervisor: Dr. M Neaves

2025/10/22

Department of Mechanical and Mechatronic Engineering  
Stellenbosch University  
Private Bag X1, Matieland 7602, South Africa.

# Executive Summary

<b>Title of Project</b>
Design, build, and testing of a multicolour CNC drawing machine.
<b>Objectives</b>
Formulation of requirements, concept generation, concept evaluation and final design of a functional CNC drawing machine. Software development and user interface design for effective control of the system. Manufacture, assembly, and testing of machine movement and drawing ability.
<b>What is current practice and what are its limitations?</b>
Current implementations of CNC drawing machines exist as DIY projects or expensive high-end pen plotters. Commercial products available are not capable of automatic tool change for multicolour drawing.
<b>What is new in this project?</b>
This project developed an automatic stylus exchanger for changing between colours mid-drawing, enabling the production of multicolour drawings without user intervention. The machine was developed using affordable, locally sourced components to deliver a more cost-effective solution than what is currently commercially available.
<b>Was the project successful? How will it make a difference?</b>
The project was successful, as it was completed on time and within the provided budget for procurement. The completed project can form the basis for further development of an affordable drawing machine product to be used by people with disabilities for art expression, by clothing makers for pattern drawing and by educators as a geometric teaching aid.
<b>What were the risks to the project being a success? How were these handled?</b>
The biggest risks to the project's success were difficulties with procurement and a tight time schedule due to late design changes. These risks were handled by proactively seeking out suppliers and working on software, assembly and integration in parallel to save time.

<b>What contributions have/will other students made/make?</b>
No contributions from other students were made, but the project will likely repeat or be expanded on in the next year.
<b>Which aspects of the project will carry on after completion and why?</b>
The project will be used at Stellenbosch University's open days to showcase to prospective students what is possible with an engineering degree from the university. If the supervisor wishes, the project may be developed further by future students, reusing components sourced during the course of this project.
<b>What arrangements have been/will be made to expedite continuation?</b>
A comprehensive report documenting the project's design process, implementation and testing was compiled. This report, along with presentation slides and the assembled machine may be used by future students to build on the project. A <a href="#">GitHub repository</a> with the project's software, a video tutorial and this report has also been made publicly available.

# Plagiarism Declaration

I have read and understand the Stellenbosch University Policy on Plagiarism and the definitions of plagiarism and self-plagiarism contained in the Policy [Plagiarism: The use of the ideas or material of others without acknowledgement, or the re-use of one's own previously evaluated or published material without acknowledgement or indication thereof (self-plagiarism or text-recycling)].

I also understand that direct translations are plagiarism, unless accompanied by an appropriate acknowledgement of the source. I also know that verbatim copy that has not been explicitly indicated as such, is plagiarism.

I know that plagiarism is a punishable offence and may be referred to the University's Central Disciplinary Committee (CDC) who has the authority to expel me for such an offence.

I know that plagiarism is harmful for the academic environment and that it has a negative impact on any profession.

Accordingly all quotations and contributions from any source whatsoever (including the internet) have been cited fully (acknowledged); further, all verbatim copies have been expressly indicated as such (e.g. through quotation marks) and the sources are cited fully.

I declare that, except where a source has been cited, the work contained in this assignment is my own work and that I have not previously (in its entirety or in part) submitted it for grading in this module/assignment or another module/assignment. I declare that have not allowed, and will not allow, anyone to use my work (in paper, graphics, electronic, verbal or any other format) with the intention of passing it off as his/her own work.

I know that a mark of zero may be awarded to assignments with plagiarism and also that no opportunity be given to submit an improved assignment.

Signature: 

Name: Mia Ham Student no: 25872214

Date: 22/10/2025

# AI Use Declaration

1. I am convinced and can support my claim that my assessment product is an indication of my own learning, knowledge, skills, and understanding.
2. Where I have used AI tools for enhancing my own creation of ideas and words, I acknowledge that I have to declare it.
3. Where I have used AI tools for generating new ideas, words, code, image-prompts for other AI Image-generating tools, or structure and even presentations (or other AI tools that can be used as assistants to the knowledge building and representing process), I have declared and documented the use of such tools and I am prepared to talk about the process I used and what it contributed to my learning and insights.
4. I am aware that the lecturer can ask me to demonstrate my learning, for example through explaining the choices I made in terms of approach, content used, literature selected, conclusions drawn, etc. through an additional assessment like an oral (for example).
5. I understand that if I am not able to agree to the above points, there is a chance that my academic behaviour will be deemed unethical and might lead to a disciplinary case being brought against me on the grounds of cheating or plagiarism and that the standard procedures for such behaviour will be followed.
6. As per the Disciplinary Code of SU (par. 10.2.1 and 10.2.2), I understand that I take responsibility for the integrity of my work, which includes the obligation to ask for clarification from an academic member of staff if I am unsure of anything, and that I strictly adhered to all instructions received in the course of the academic assessment by relevant and authorized staff (whether the instruction is in oral or written format).
7. I understand that when I am not able to document and declare my use of AI tools, this behaviour will be deemed as cheating in examinations and assessments (Disciplinary Code 1.1 c.) as I referred to “unauthorized notes, books, electronic devices or other reference material”.

Signature: 

Name: Mia Ham Student no: 25872214

Date: 22/10/2025

# ECSA Self-Assessment

Table 2: ECSA graduate attribute self-assessment for project activities

<b>GA1. Problem Solving</b>
The problem of designing, building and testing a multicolour CNC drawing machine was solved in this project. This was done by defining the problem and identifying stakeholder, functional and performance requirements for the machine (Section 3.1). Multiple solutions were then developed, including two movement system concepts (Section 3.3) and three stylus exchanger concepts (Section 3.4). Concepts were evaluated qualitatively and quantitatively (Section 3.5) and the solution was designed in detail (Chapter 4). A problem-solving approach was also applied to software development, where the problem of converting images to G-code was solved (5.3). Problems such as rail alignment and homing difficulties, were encountered and solved during the implementation of the project (Section 4.5).
<b>GA2. Application of Scientific and Engineering Knowledge</b>
During the design phase, physical laws and knowledge of the physical world were applied in the project's design calculations (Appendix D) to inform design decisions, such as component selection and structural design. Mathematical and numerical analyses were applied in the development of the image conversion software, to extract paths from polynomials and optimise drawing paths with mathematical algorithms (Section 5.3). Various areas of engineering science were applied to this project, such as machine design (calculations), mechatronics (motor control), embedded systems (microcontroller programming) and computer science (software development).
<b>GA3. Engineering Design</b>
A unique multicolour CNC drawing machine was designed by first planning the project activities (Section H.2) and assessing relevant literature to execute the design process (Chapter 2). After the evaluation of possible solutions (Chapter 3), the detailed design was created by performing quantitative analyses (Appendix D) and exercising engineering judgement, as communicated in Chapter 4. Other than the design of a unique machine with an innovative stylus exchanger, custom image conversion software (Chapter 5) and benchmark tests (Section 6.2) were also designed.

<b>GA5. Engineering Methods, Skills and Tools, Including Information Technology</b>
Computer aided design (in Autodesk Inventor Professional 2025) was used to develop concepts and the final design (Chapters 3 and 4). The image converter was programmed in Python (Section 5.3), with the GRBL firmware modified in C++ (Section 5.4) and vector graphics edited in XML (Section 6.2). Computer numerical control (CNC) was implemented to control the machine with G-code instructions and an executable program was created to develop a user-friendly image converter (Chapter 5).
<b>GA6. Professional and Technical Communication</b>
Effective written communication of technical information is demonstrated throughout this report, which follows a clear structure, utilises graphics effectively and uses appropriate professional language. This is further supported by the inclusion of professional meeting minutes in the project file and usage instructions in the project's <a href="#">GitHub repository</a> . Effective oral communication is demonstrated by progress- and project presentations, utilising appropriate language and visual aids.
<b>GA8. Individual, Team and Multidisciplinary Working</b>
Effective individual work is demonstrated by the successful completion of the project within the set timeframe and budget (Chapter H). All project objectives were achieved with moderate supervision, and the project remained focused on its main objectives.
<b>GA9. Independent Learning Ability</b>
Independent learning ability is demonstrated in the sourcing and evaluation of relevant information during the literature review (Chapter 2), especially concerning topics not covered in formal instruction, such as the intricacies of G-code generation from images (Section 2.4). Programming languages such as Python, LaTeX, G-code, C++ and XML were learnt and applied independently during software development (Chapter 5), testing (Section 6.2) and report consolidation. Knowledge of CNC machining and toolpath generation acquired independently through vacation work was also applied during the project.

# Acknowledgements

First and foremost, I would like to thank God for my talents and abilities that have brought me this far, as well as for the strength and perseverance to complete this degree. A big thank you to my parents, Cori and Hannél, for supporting me (both financially and emotionally) and to the rest of my family (Philip and Vicky), for their continued encouragement. This project would also not have been such a success without the guidance and support from my supervisor, Dr Neaves. Thank you all for believing in me.

To the sisters from res (Lucy, Nikolaa and Jule), thank you for the late night cups of tea, McDonald's trips and overall clownery. To Aloise, Nina and Robyn, thank you for all the roadtrips, hikes, sokkies, concerts and many more adventures. Last but not least, Chavan, Camryn and Johann, thank you for facing this monster of a degree with me. It was all about the climb.

# Table of Contents

<b>List of Figures</b>	<b>xii</b>
<b>List of Tables</b>	<b>xiv</b>
<b>1 Introduction</b>	<b>1</b>
1.1 Background . . . . .	1
1.2 Objectives . . . . .	2
1.3 Motivation . . . . .	2
1.4 Use of Generative AI . . . . .	3
<b>2 Literature review</b>	<b>4</b>
2.1 Current CNC Drawing Machines . . . . .	4
2.2 Current CNC Tool Exchangers . . . . .	6
2.3 G-code Instructions . . . . .	8
2.4 Image to G-code Conversion . . . . .	9
<b>3 Concept Selection</b>	<b>12</b>
3.1 System Specifications . . . . .	12
3.1.1 Stakeholder Requirements . . . . .	12
3.1.2 Engineering Requirements . . . . .	13
3.2 System Decomposition . . . . .	15
3.3 Movement Subsystem Concepts . . . . .	15
3.3.1 Lead Screw Motion . . . . .	16
3.3.2 Belt Driven Motion . . . . .	17
3.4 Stylus Exchanger Subsystem Concepts . . . . .	18
3.4.1 Side Gripper . . . . .	18
3.4.2 Claws . . . . .	19
3.4.3 Revolver . . . . .	20
3.5 Concept Evaluation and Selection . . . . .	22
3.5.1 Qualitative Evaluation . . . . .	22
3.5.2 Quantitative Evaluation . . . . .	23
<b>4 Detailed Design and Implementation</b>	<b>25</b>
4.1 System Overview . . . . .	25
4.2 Movement Subsystem . . . . .	26

4.3	Stylus Exchanger Subsystem . . . . .	27
4.4	Electronics . . . . .	30
4.5	System Assembly . . . . .	31
<b>5</b>	<b>Software</b>	<b>33</b>
5.1	Overview . . . . .	33
5.2	User Interface . . . . .	34
5.3	Image to G-code Converter . . . . .	35
5.4	G-code Sender Application . . . . .	38
<b>6</b>	<b>Calibration, Testing and Validation</b>	<b>40</b>
6.1	Calibration . . . . .	40
6.2	Testing . . . . .	41
6.2.1	Functionality Test . . . . .	42
6.2.2	Resolution Test . . . . .	43
6.2.3	Repeatability Test . . . . .	43
6.2.4	Accuracy Test . . . . .	44
6.2.5	ATC Precision Test . . . . .	45
6.2.6	Software Test . . . . .	45
6.3	Validation . . . . .	47
<b>7</b>	<b>Conclusions</b>	<b>49</b>
7.1	Objectives Achieved . . . . .	49
7.2	Recommendations for Future Work . . . . .	49
7.3	Closing Remarks . . . . .	50
<b>A</b>	<b>Decision Rationale</b>	<b>51</b>
A.1	Performance Requirements . . . . .	51
A.2	Quantitative Evaluation Scoring System . . . . .	53
<b>B</b>	<b>Sources for CAD Models</b>	<b>55</b>
<b>C</b>	<b>Cost Estimation</b>	<b>56</b>
<b>D</b>	<b>Calculations</b>	<b>57</b>
<b>E</b>	<b>Estimation of Drawing Force</b>	<b>63</b>
<b>F</b>	<b>Wiring Diagram</b>	<b>64</b>
<b>G</b>	<b>Photographs</b>	<b>65</b>
G.1	Assembly and Calibration Photographs . . . . .	65
G.2	Testing Photographs . . . . .	66

<b>H Techno-Economic Analysis</b>	<b>67</b>
H.1 Budget . . . . .	67
H.2 Planning . . . . .	70
H.3 Technical Impact . . . . .	71
H.4 Return on Investment . . . . .	71
H.5 Potential for Commercialisation . . . . .	72
<b>I Responsible Use of Resources and End-Of-Life Strategy</b>	<b>73</b>
<b>J Risk Assessment</b>	<b>74</b>
J.1 Assembly Procedure . . . . .	74
J.2 Activity Based Risk Assessment . . . . .	75
<b>List of References</b>	<b>76</b>

# List of Figures

2.1	UUNA TEK 3.0 Pen Plotter Drawing Robot . . . . .	4
2.2	Bantam Tools NextDraw 1117 Pen Plotter . . . . .	5
2.3	Tbot movement system . . . . .	6
2.4	Drum-type ATC . . . . .	7
2.5	Chain-type ATC . . . . .	7
2.6	Disc-type ATC requiring changer arm . . . . .	8
2.7	Different orders of Bézier curves . . . . .	10
2.8	Progression of 2-opt algorithm from (a.) to (f.) . . . . .	11
3.1	Simple system diagram of CNC drawing machine . . . . .	15
3.2	CAD model of lead screw motion concept . . . . .	16
3.3	Close-up of lead screw concept . . . . .	16
3.4	CAD model of belt driven motion concept . . . . .	17
3.5	Close-up of belt driven motion concept . . . . .	18
3.6	CAD model of side gripper concept . . . . .	18
3.7	CAD model of stylus stand . . . . .	19
3.8	CAD model of claws concept . . . . .	20
3.9	Close-up of claws concept showing (a.) open position and (b.) closed position . . . . .	20
3.10	CAD model of revolver concept . . . . .	21
3.11	Close-up of revolver concept showing (a.) servo motor retracting and (b.) servo motor pushing stylus down . . . . .	21
4.1	CAD model of final design of CNC drawing machine . . . . .	25
4.2	CAD model of final stylus exchanger subsystem . . . . .	28
4.3	CAD model of lead screw assembly to adjust height of stylus exchanger . . . . .	30
4.4	Photo of assembled CNC drawing machine . . . . .	32
5.1	Flow diagram of software elements . . . . .	33
5.2	Screenshot of user interface for image converter . . . . .	34
5.3	Comparison of (a.) a raster image and (b.) the G-code path generated from it . . . . .	36
5.4	Flow diagram of image to G-code converter script . . . . .	36
5.5	Screenshot of GRBL-Plotter user interface . . . . .	39

6.1	Results of functionality test on different surfaces: (a.) white-board, (b.) MDF board, (c.) white paper, (d.) cardboard, (e.) cotton fabric, (f.) felt fabric . . . . .	42
6.2	Resolution test results for three different colours . . . . .	43
6.3	Repeatability test results showing absolute deviations from first run . . . . .	44
6.4	Heatmaps of deviations in (a.) width and (b.) height for each square in the accuracy test . . . . .	44
6.5	Two of the circles drawn during the ATC precision test . . . . .	45
C.1	Screenshot of the Microsoft Excel sheet used to estimate cost of concepts . . . . .	56
F.1	Wiring diagram of the CNC drawing machine . . . . .	64
G.1	Rail alignment using a square . . . . .	65
G.2	Calibration verification of x- and y-axes . . . . .	65
G.3	Calibration of z-axis with protractor . . . . .	65
G.4	Marker making contact with drawing surface . . . . .	65
G.5	Testing setup with tracing paper taped down . . . . .	66
G.6	Rectangle drawn in the repeatability test . . . . .	66
G.7	Grid drawn in the accuracy test . . . . .	66
G.8	Circles 3 and 4 drawn in the ATC accuracy test . . . . .	66
G.9	GRBL-Plotter test image used in the software test . . . . .	66
G.10	Six squares image used in the software test . . . . .	66
H.1	Cost of all components used in project . . . . .	68
H.2	Planned budget of project . . . . .	69
H.3	Actual budget of project . . . . .	69
H.4	Gantt chart of project planning . . . . .	70

# List of Tables

2	ECSA graduate attribute self-assessment for project activities . . . . .	vi
3.1	Stakeholder requirements . . . . .	13
3.2	Functional requirements . . . . .	13
3.3	Performance requirements . . . . .	14
3.4	Quantitative evaluation of movement subsystem concepts . . . . .	23
3.5	Quantitative evaluation of stylus exchanger subsystem concepts	24
6.1	G-code path lengths for each image . . . . .	46
6.2	Validation of performance requirements . . . . .	48
E.1	Results of marker drawing force test . . . . .	63

# Chapter 1

## Introduction

### 1.1 Background

CNC, or computer numerical control, has revolutionised the manufacturing industry. The technology started off in 1949 when John T. Parsons developed a machine with motorised axes that received its instructions from punched tape. Later, the evolution of computers in the 1960s and 70s made the processing of machining instructions much faster and simpler (Smoothy, 2024). Today's CNC machine has a microcomputer inside its machine control unit (MCU) that receives G-code and tells the machine what to do. G-code instructions come in the form of coordinates, feed rates and speeds. Many modern machines such as lathes, mills, routers and 3D printers use CNC (Goodwin University, 2024).

While CNC machines certainly have great use in manufacturing plants, their smaller implementations are growing increasingly popular under hobbyist woodworkers. In fact, the global desktop CNC machine market size is expected to grow from \$0.5 billion in 2024 to \$1.11 billion in 2033 (Businessresearchinsights.com, 2025). The availability of desktop machines such as routers and 3D printers has undoubtedly helped many small businesses cut down on time and manufacturing costs.

However, these machines do not exclusively have to be used for prototyping or manufacturing. CNC can be implemented in any application where movement according to a coordinate system is required. An interesting use of this type of machine is for drawing or writing on a surface. That is exactly what Das *et al.* (2024) designed and built: a budget CNC machine that can effectively write on paper, wood and cardboard. Although their focus was on design applications, such as printed circuit board (PCB) design, these machines can be developed for more artistic purposes.

While there exist some commercially available CNC drawing machines, such as the AxiDraw series by Evil Mad Scientist (2023) and the iDraw and iAuto ranges from UUNA TEK CO., LIMITED (2025a), they are not widely available in South Africa. These machines are only capable of drawing with one stylus (pen, marker or pencil) at a time. This makes drawing multicolour

images complicated, as the stylus must be changed manually during operation, and colour layers must be separated into different runs.

This project aims to design and build an artistic multicolour CNC drawing machine capable of sketching complex and colourful images on various mediums. The work in this project forms part of M. Ham's final year Mechatronic Engineering 478 Project and will be completed from 3 February to 24 October 2025. Manufacturing and assembly will be done in the Mechatronics Workshop at the Mechanical and Mechatronic Engineering Department of Stellenbosch University, with an allocated procurement budget of R5,000.00.

## 1.2 Objectives

The aim of this project is to design, build and test an operational multicolour CNC drawing machine. Several objectives have to be met to achieve this aim. They are identified below and will be used to measure the extent to which the project is completed successfully:

**OBJ1** Formulation of requirements and specifications

**OBJ2** Generation and evaluation of various concept designs

**OBJ3** Selection of suitable materials and components for the final design

**OBJ4** Manufacture of custom parts and construction of the final design

**OBJ5** Development / adaptation of CNC software, and user interface design

**OBJ6** Testing and verification through production of colourful, sufficiently complex drawings

The scope of this project is limited to what can be achieved by a final year mechatronic engineering student within the allocated 450 working hours, over a period of nine months. It is also limited to resources and manufacturing equipment available within the Mechanical and Mechatronic Engineering Workshop (MMW). Additional resource acquisition cannot exceed a total of R5,000.00. Therefore, the quality of the final design is limited to the quality of components within that budget.

## 1.3 Motivation

The concept of a CNC drawing machine and similar products do exist but can be very expensive. UUNA TEK, who sell their drawing machines in America, have prices ranging from R5,500.00 to over R200,000.00 (UUNA TEK CO., LIMITED, 2025a). With a budget of only R5,000.00, this project aims to deliver a product that is more affordable and that utilises local suppliers.

As mentioned, current machines on the market do not have the ability to automatically change between styluses, thereby limiting the user to single-colour drawings, or complicated operations involving separate colour layers and manual intervention. By developing a multicolour drawing machine that utilises an automatic stylus exchanger, this project fills that gap in the market. This leads to more possibilities in terms of the colour complexity of drawings, thereby enhancing the drawing machine as an artistic tool. With no manual intervention required, higher accuracy and better alignment of colour layers is also possible.

Other than developing a tool for artistic expression, this machine can be of use to people with reduced hand mobility and writing abilities. Writing letters, drawing concepts or even signing signatures can be made easier using a CNC drawing machine.

In small clothes-making and tailoring businesses, patterns often have to be drawn by hand onto textiles and then cut out. This process can be very inaccurate and often leads to material waste. A drawing machine that can accurately outline a desired pattern will save these business owners time, as well as material costs.

This tool also holds educational value. Since it will be designed with affordability in mind, it can be used in schools to teach students geometry concepts, coding basics and safe machinery practices. A machine such as this does not yet exist at Stellenbosch University, and it could be very valuable in teaching prospective students about engineering.

These possible use cases can all be achieved with a single, affordable design. This project aims to ensure that the design is successfully developed and capable of performing all the functions mentioned above.

## 1.4 Use of Generative AI

No sections of this report were written using generative AI tools. All text, except where credited, was typed by the author. Only references in BibTeX format were generated with GitHub Copilot, but duly checked. AI tools, such as GitHub Copilot and ChatGPT 4, were consulted to assist in learning and debugging LaTeX code for the compilation of this report. All photos and diagrams were either taken by the author, made by the author using Autodesk Inventor or Draw.io, or sourced from articles and cited. Thus, no images were generated using AI tools. ChatGPT 4 was used to assist in debugging and optimising code for the image to G-code conversion program. Where code was generated by AI tools, it was duly checked and rewritten by the author with modifications, not copied.

# Chapter 2

## Literature review

### 2.1 Current CNC Drawing Machines

While many do-it-yourself (DIY) CNC drawing machine tutorials are available on the internet, few established commercial solutions exist. The commercial market is mostly dominated by UUNA TEK, who describe themselves as the primary supplier of pen plotter drawing robots, which is their iDraw product range. They also invented the iAuto range, which they describe as a world-first, being able to do “true automatic handwriting” in bulk. Their iAuto machines can “hand-write” up to 80 cards, invitations, letters or envelopes at a time (UUNA TEK CO., LIMITED, 2025b).

The most expensive and newest desktop pen plotter available from UUNA TEK is their UUNA TEK 3.0 (Figure 2.1). It comes pre-assembled and can be ordered in a variety of sizes, ranging from A3 to A0 paper sheet sizes. The A3 version is priced at \$1,899.00 (R32,893.63 as on 16 October 2025). It makes use of three belt systems; two for the Cartesian y-axis and one for the Cartesian x-axis. Each belt system is driven by a stepper motor, with the y-axis motor being dual-shafted and driving a belt on either side of the x-axis. Three cast aluminium rails with self-lubricating plastic balls ensure high precision and speed (UUNA TEK CO., LIMITED, 2025c).

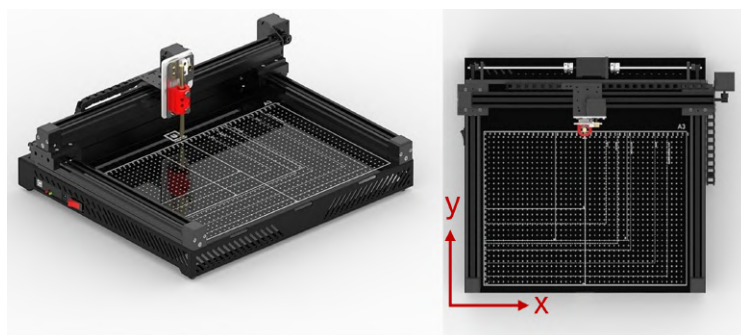


Figure 2.1: UUNA TEK 3.0 Pen Plotter Drawing Robot  
(UUNA TEK CO., LIMITED, 2025c)

UUNA TEK provides their own custom software to generate G-code instructions from uploaded image files. Their machines are also compatible with instructions generated by other softwares, such as Inkscape, UGS, Lightburn and LaserGRBL. Instructions can be uploaded via USB connection, over WIFI (with an extra module), or by inserting an SD card for offline jobs. This specific version boasts very quiet operation, making less than 60 dB of noise (UUNA TEK CO., LIMITED, 2025c).

Bantam Tools, another American company, have reinvented the AxiDraw series mentioned earlier. AxiDraw, which competed directly with UUNA TEK, is no longer in production, but Bantam Tools' versions are almost identical. Their pen plotter series is called NextDraw and exhibits three models. The models are identical in design but differ in size; with options of A4, A3 and A1 drawing areas. The Bantam Tools NextDraw 1117 (Figure 2.2) is their A3 size option, priced at \$1,349.00 (R23,366.77 as on 16 October 2025) (Bantam Tools, 2025a).

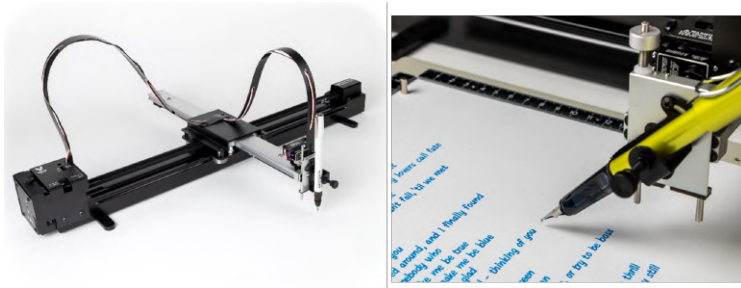


Figure 2.2: Bantam Tools NextDraw 1117 Pen Plotter (Bantam Tools, 2025b)

These pen plotters do not have a fixed frame like the UUNA TEK model. They only have one fixed crossbar, serving as the x-axis. The bar that the pen attaches to moves back and forth over this fixed bar. This means that the plotter can be placed on drawing surfaces bigger than the machine itself. Another feature of this pen plotter is the option to rotate the pen up to 45° and draw at an angle, which is useful when drawing with fountain pens. The NextDraw pen plotters also come with their own software for uploading images and converting them to machine instructions (Bantam Tools, 2025b).

NextDraw utilises a Tbot movement system, which consists of a single looped belt driven by two stationary stepper motors, as shown in Figure 2.3. Similar to a Core XY movement system, powering one motor at a time produces diagonal motion. When both motors spin in opposite directions, the pen moves back or forth along the y-axis. When the motors spin in the same direction, the pen will move left or right along the x-axis. Combining diagonal and axial motion allows the machine to move to its next location quicker, taking the shortest path (Rossing, 2014).

Both the UUNA TEK and NextDraw machines have adjustable pen holsters, allowing for different pens to be inserted up to a maximum cross section.

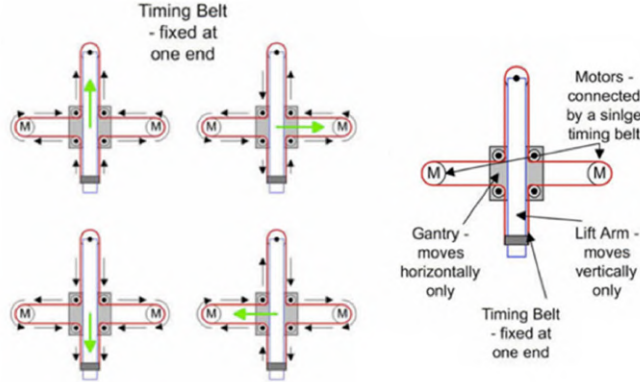


Figure 2.3: Tbot Movement System (Rossing, 2014)

However, neither of these machines have the ability to change between pens automatically.

## 2.2 Current CNC Tool Exchangers

In heavy industrial settings, CNC machines are required to machine complex parts at high speeds. These machining jobs can be complicated and may require different tools to be used in a single job, necessitating tool changes during operation. User interaction during a machine's operation is a major safety concern as the user is prone to serious accidents resulting from mechanical or tool failures (Rogelio and Baldovino, 2014). To shorten machining time, improve safety and reduce labour costs, various automatic tool changer (ATC) systems have been developed for use in conjunction with CNC machines. The general requirements for a CNC ATC system is that it has a short tool change time, exhibits high functional and operating reliability, and can store a large number of tools as required for a typical workpiece (Trajkovski, 1985).

An ATC system typically consists of a tool magazine, tool holders and an ATC. The ATC usually comes in the form of an arm that moves between the indexable tool magazine and the machine's tool holder. Some ATCs simply make use of a gripper arm that is separate to the machine and replaces tools in the same way a human operator would. Other ATCs are categorised by the type of tool magazine they use. Common tool magazine types include rotary drums, chain magazines, disc magazines and turret heads. Turret head magazines are specifically employed in CNC lathes, whereas the other types can be used in mills, routers and engravers too (Abraham, 2023).

Drum-type ATCs are composed of a vertically oriented rotary drum magazine and a cam gearbox (Figure 2.4). A drive arm on the cam gearbox rotates between the tool holder and the magazine to exchange tools (Choi and Lee, 2020). Tools are placed in tool ports on the periphery of the rotating drum, and the cam gearbox makes use of roller gears and grooved plate cams to ex-

change them (Abraham, 2023). This type of ATC boasts faster operating times and shorter unit lengths compared to chain-type ATCs. They are also more rigid and require fewer parts. This means that they are more cost-effective, with lower servicing costs (Choi and Lee, 2020).

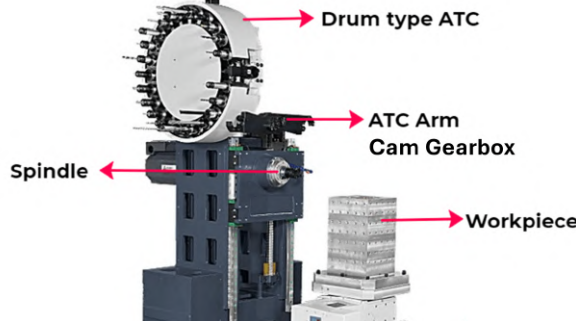


Figure 2.4: Drum-type ATC (Abraham, 2023)

Chain-type ATCs are often used in heavy machining applications, particularly when a large number of tools are required. Where drum-type ATCs are usually restricted to 30–60 tools, chain-type ATCs can hold more than 100 tools (Darji and Shil, 2017). Tools are arranged in tool ports along a chain, as shown in Figure 2.5. The chain moves in its track until the correct tool is indexed in front of the headstock. Some chain-type ATCs do not require a swivel arm to move the tool to the tool holder. Rather, machining is done with the tool remaining in the chain (Abraham, 2023). Other chain-type ATCs make use of a swivel arm driven by a cam and bevel-gear assembly to move tools to and from the tool holder (Xiaohong *et al.*, 2014). While this kind of ATC performs well in heavy machinery and mass production settings, it usually exhibits slow tool search speeds due to the large tool-filled chains moving slowly (Abraham, 2023).



Figure 2.5: Chain-type ATC (Abraham, 2023)

Disc-type ATCs are also known as carousel-type ATCs and can be divided into two kinds: those with a changer arm and those without. In disc-type ATCs with a changer arm, the disc only indexes and stores the tools (Figure 2.6).

A separate changer arm moves tools between the disk and the tool holder. Disc-type ATCs that do not require a changer arm may have the disc mounted vertically next to the tool holder and require the tool holder to rotate towards it (Gökler and Koç, 1997). Like drum-type ATCs, tools are held along the periphery of a disc and the disc rotates to index tools. A disc-type ATC system may have multiple discs located within reach of a changer arm. This allows for large tool-holding capacity and quick tool changes (Abraham, 2023).

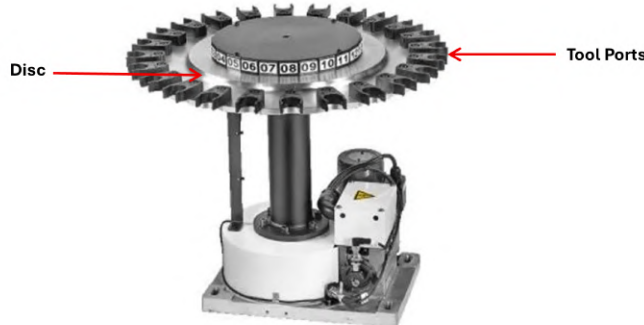


Figure 2.6: Disc-type ATC requiring changer arm (Abraham, 2023)

## 2.3 G-code Instructions

G-code, or geometric code, is a programming language used by most CNC machines. It is a simple line-by-line language that gives machines what-, which- and how-type instructions. Invented in the late 1950s at the Massachusetts Institute of Technology (MIT), it is one of the oldest programming languages still in use today. The language was standardised in the early 1960s by the Electronics Industries Alliance and later became what is now known as the standard RS-274D language (Awati, 2024). G-code is simple in the sense that it does not have decision functions, variables or loops. However, its simplicity makes it highly customisable, and many CNC machines have a different “dialect”, with functions defined to be machine specific. While RS-274D is the standard used in the United States, it may differ from the international standard, ISO 6983, and that may differ from the German DIN 66025 standard that it was derived from. Many commonly-used commands are, however, similar across standards and manufacturers (Acu and Ciocarlie, 2014).

Machine instructions in G-code are written in an alpha numeric pattern. A line of code will typically be presented in the following format:

N## G## X## Y## Z## F## S## T## M##

where ## represents numbers.

Each letter represents a different part of the command, defined as:

- N – Line number

- G – Type of motion
- X – Horizontal position
- Y – Vertical position
- Z – Depth
- F – Feed rate
- S – Spindle speed
- T – Tool selection
- M – Miscellaneous functions

In the context of a CNC drawing machine, spindle speed (S) is not relevant, as the stylus usually does not rotate. Feed rate (F) refers to the speed at which the axes move, and should not be confused with 3D printing applications where it defines the speed of the filament extruder. Miscellaneous functions (M) are normally machine specific. They will typically be defined to switch actuators and coolant on or off, stop program execution, initiate a tool change or change the direction of a spindle (Rathbone, 2020).

There are three basic types of motion that a CNC machine can do, and they are defined by the designation of the G parameter:

- G0 – Linear move to an XYZ-defined position at maximum feed rate
- G1 – Linear move to an XYZ-defined position at a specified feed rate
- G2/G3 – Clockwise or anti-clockwise circular move at a specified feed rate

## 2.4 Image to G-code Conversion

Scalable vector graphics (SVG) files are the most common file type used to create G-code instructions for CNC drawing machines. The SVG file format was developed by the World Wide Web Consortium (W3C) and recommended as a standard in 2001. It utilises extensible markup language (XML) to define shapes in images. Shapes in SVG files are defined mathematically, making them infinitely scalable without losing quality. While the SVG format natively supports some basic geometry elements such as rectangles, circles, ellipses, lines, polylines and polygons, any 2D shape can be defined using Bézier curves as '`<path/>`' elements (Neumann, 2008).

Bézier curves are parametric curves constructed with Bernstein polynomials as their basis functions. They do not have shape parameters, but are defined by a set of control points (Maqsood *et al.*, 2020). The positions of these control points relative to each other determine the shape of the curve. With

more control points, more complex curves can be constructed. The linear, quadratic and cubic Bézier curves are defined as shown in Figure 2.7. Each curve is essentially a weighted sum of its control points, with the weights being Bernstein polynomials (Melo, 2021). Thanks to their mathematical definition, points on Bézier curves can be calculated easily, making them ideal for CNC toolpath generation.

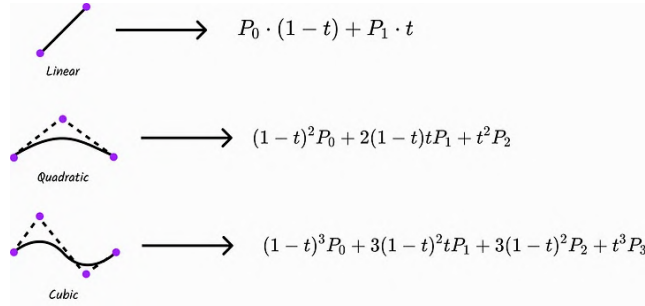


Figure 2.7: Different orders of Bézier Curves (Melo, 2021)

When defining toolpaths from SVG files, the order in which paths are drawn is important. Machine travel between paths wastes time, increases wear and tear of mechanical components, and increases the file size of G-code instructions. Decreasing the travel distance between paths is known as the travelling salesman problem (TSP), which is a well-known combinatorial optimisation problem. It asks the question: “Given a list of cities and the distances between them, what is the shortest possible route that visits each city exactly once and returns to the origin city?” (Khdeir and Awad, 2025). Many algorithms and heuristics have been developed as attempts to solve this problem; such as the nearest neighbour algorithm, genetic algorithm, simulated annealing, tabu search, ant colony optimisation and particle swarm optimisation (Halim and Ismail, 2019).

The first algorithm introduced to solve the TSP was the nearest neighbour algorithm. It is the most commonly used heuristic and is based on greedy procedures. The algorithm starts at a random point and then moves to the nearest unvisited point. This repeats until all points have been visited. While this algorithm does not guarantee an optimal solution, it is simple to implement and by far the fastest of the TSP heuristics (Halim and Ismail, 2019). Another famous TSP heuristic is the 2-opt algorithm, which performs local searches to improve an existing solution. It does this by evaluating all pairs of non-adjacent edges in a path and swapping their endpoints if the swap results in a shorter total path length. This is illustrated in Figure 2.8, where the path length was reduced from 40 to 28 units by implementing a form of the 2-opt algorithm (Levin and Yovel, 2013). In the figure, numbers in bold represent the distance between points (circles) and dotted lines represent the new optimal connection between points for that step<sup>1</sup>. The 2-opt algorithm is often used

---

<sup>1</sup>Admittedly, this algorithm is easier to visualise with the help of a [video](#).

to improve solutions found by other heuristics, such as the nearest neighbour algorithm. Nuraiman *et al.* (2018) found that combining the nearest neighbour algorithm with 2-opt optimisation reduced error by 10.27% on average when compared to the optimal path for 11 symmetric TSP cases.

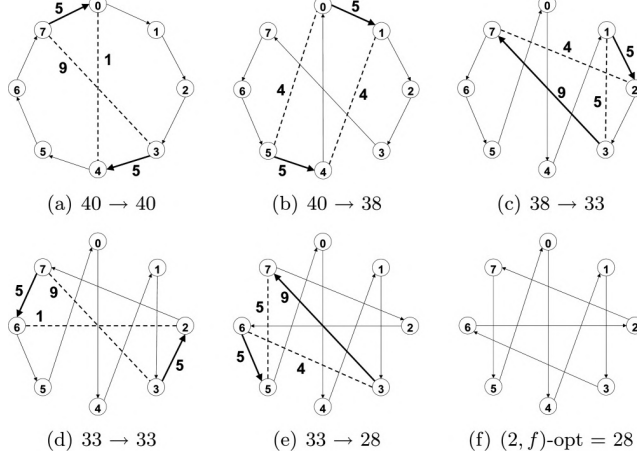


Figure 2.8: Progression of 2-opt algorithm from (a.) to (f.)(Levin and Yovel, 2013)

Another important factor in path generation of multicolour images is colour mapping, which is the process of assigning colours in an image to physical styluses. Colours in images will not match available styluses exactly, thereby necessitating a method of mapping image colours to a limited palette. This can be done by using colour spaces to quantify the “distances” between colours. There are three main colour spaces used in digital imaging: RGB, CMYK and CIE L\*a\*b\*. RGB (red, green, blue) is an additive colour space mainly used in digital displays. It is highly device dependent, meaning that the same RGB values may appear differently on different devices, as devices use different screen technologies. CMYK (cyan, magenta, yellow, black) is a subtractive colour space mainly used in printing. All colours are formed by “subtracting” light from a white background, as is often the case with ink on paper. This colour space is also device dependent, as different printers and inks will yield different results. CIE L\*a\*b\* (or simply Lab), on the other hand, is a device-independent colour space. It was developed by the International Commission on Illumination (CIE) and is based on the human perception of colour (Pantone, 2025). The three parameters of the Lab colour space are L\* for lightness, a\* for a green-red axis and b\* for a blue-yellow axis. This colour space was designed to be perceptually uniform, meaning that a colour change along one axis is perceptually equivalent to a colour change of the same magnitude along another axis. This is very useful when quantifying colour differences, as the Euclidean distance between colours in Lab space is proportional to the human-perceived difference between those colours (Barrington *et al.*, 2024).

# Chapter 3

## Concept Selection

In order to select a suitable final design for the CNC drawing machine, several concepts were developed, considered and evaluated. First, the stakeholder and engineering requirements of the system were identified. The system was then decomposed into its functional subsystems. Multiple concepts were developed for each subsystem. They are described in Sections 3.3 and 3.4. These concepts were then evaluated both qualitatively and quantitatively. Ultimately, the best concepts were incorporated into a final design.

### 3.1 System Specifications

For this project, the main stakeholder is the Department of Mechanical and Mechatronic Engineering at Stellenbosch University, as represented by the project supervisor, Dr Melody Neaves. The finished CNC drawing machine will be used by undergraduate and prospective students of Stellenbosch University, with it mainly operating at the university's Open Day. It may also be used at educational facilities, such as schools, where educators will operate it. At the end of its life, when the CNC drawing machine is being disposed of, it will have an impact on the environment and people involved in the disposal process. Thus, all these stakeholders had to be considered when designing the drawing machine.

#### 3.1.1 Stakeholder Requirements

The requirements, as identified by stakeholders and users, are contained in Table 3.1 below. Each stakeholder requirement (SR) was assigned a priority level (1–3) based on the following rating scale:

1. Required for successful operation
2. Required by stakeholders, but not essential to function
3. Preferred by stakeholders

Table 3.1: Stakeholder requirements

SR	Description	Priority
SR1	The device must make use of CNC	1
SR2	The device must be portable	2
SR3	The device must be capable of drawing on various surfaces	2
SR4	The device must have the capacity to draw on A5- to A3-sized surfaces	2
SR5	The device must produce multicolour drawings	1
SR6	The device must select and exchange colours automatically	1
SR7	The device must have a user-friendly user interface	3
SR8	The user should be able to upload images that the machine draws	3
SR9	The device must be capable of drawing sufficiently complex shapes	2
SR10	The device must be safe to operate	1
SR11	Maintaining the device should be easy and inexpensive	3
SR12	The device must be affordably made (budget of R5,000.00)	1
SR13	The device must be manufactured in an environmentally conscious way	3

### 3.1.2 Engineering Requirements

From the SRs in Table 3.1, functional requirements (FRs) and performance requirements (PRs) were derived. FRs describe what the CNC drawing machine should be able to do and can be found in Table 3.2. PRs, contained in Table 3.3, outline measurable parameters that indicate how well the machine should perform its functions. For each FR and PR, its relevant SRs are indicated in the rightmost column of each respective table. The rationale for determining the acceptable ranges for the PRs are shown in Appendix A.1.

Table 3.2: Functional requirements

FR	Description	Related SR
FR1	Processes user instructions	SR7, SR8
FR2	Generates G-code instructions	SR1
FR3	Draws shapes by moving stylus on surface	SR9
FR4	Selects colours to represent images	SR6, SR8

FR5	Automatically exchanges colour styluses	SR6, SR5
FR6	Constructed out of environmentally safe and recyclable materials	SR13
FR7	Enclosed moving parts	SR10
FR8	Constructed out of lightweight materials	SR2
FR9	Built small enough to be carried by a human	SR2
FR10	Adjustable for drawing on different surfaces and sizes	SR3, SR4
FR11	User interface provided	SR7
FR12	Constructed within provided budget	SR12
FR13	Components are easy to access for maintenance	SR11
FR14	Movement system is precise and accurate	SR1, SR9

Table 3.3: Performance requirements

PR	Description	Target	Range	Unit	Related SR
PR1	Overall machine length	480	430–500	mm	SR2
PR2	Overall machine width	400	330–450	mm	SR2
PR3	Overall machine height	130	40–350	mm	SR2
PR4	Machine weight	10	1–16	kg	SR2
PR5	Drawing area length	420	420–480	mm	SR4
PR6	Drawing area width	300	297–400	mm	SR4
PR7	Total procurement cost	3,500	0–5,000	R	SR12
PR8	Number of colours	6	2–10	colours	SR5, SR6
PR9	Compliance with safety standards	100	-	%	SR10
PR10	Adjustable drawing height	10	2–20	mm	SR3
PR11	Drawing precision	0.5	0.5–2	mm	SR9
PR12	Recyclable and reusable parts	80	60–90	%	SR13
PR13	Power consumption	15	2–50	W	SR13, SR11
PR14	Image processing time	60	0–300	s	SR8, SR7
PR15	Maximum RAM <sup>1</sup> usage	2	0.01–4	GB	SR8

<sup>1</sup>Random access memory

## 3.2 System Decomposition

For a complicated system such as a CNC drawing machine, it is much easier to divide it up into subsystems and develop concepts on a subsystem level. The proposed machine was divided into three subsystems, as listed below:

1. User interface and controller subsystem
2. Movement subsystem
3. Stylus exchanger subsystem

The interactions of these three subsystems with each other and with the environment, are illustrated in the system diagram in Figure 3.1. Each subsystem is represented in a different colour. As shown, the user inputs commands or uploads images to the user interface, which then sends G-code instructions to the microcontroller. The microcontroller controls motors through motor drivers. These motors are what drive the movement system, where rotational motion converts to translational motion. The stylus holder is translated by the movement system, effectively drawing on a sheet or other drawing surface. Styluses are inserted into the exchanger system, which will automatically exchange the stylus in the stylus holder, as commanded by the microcontroller. The user interface, microcontroller, motor drivers and exchanger system are all powered by a power supply, which draws power from the electrical grid.

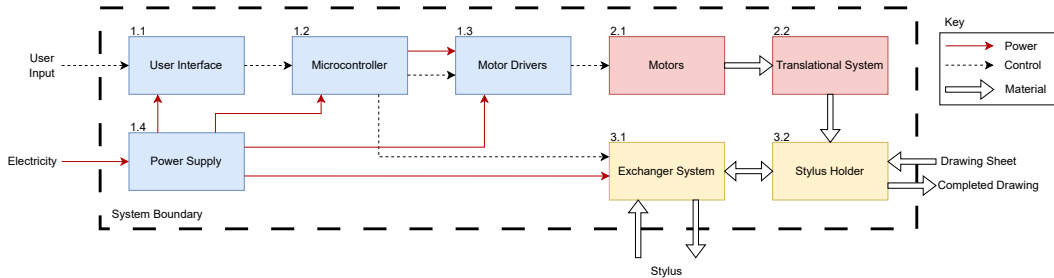


Figure 3.1: Simple system diagram of CNC drawing machine

Concepts were developed for the movement and stylus exchanger subsystems. These concepts are detailed in the sections that follow. The CAD models shown were developed with standard components from GrabCAD for visual purposes only and do not necessarily represent the final components that will be used. Artists of GrabCAD models are credited in Appendix B.

## 3.3 Movement Subsystem Concepts

The movement subsystem includes all components necessary to translate rotational motion from motors to translational motion for movement in the Cartesian plane. Only Cartesian movement systems with separate x- and y-axes were considered, as this coordinate system lends itself best to CNC.

### 3.3.1 Lead Screw Motion

This concept makes use of two lead screw assemblies to produce translational motion in both the x and y directions. These axes are defined as shown in the CAD model in Figure 3.2. Parts are shown in different colours for better clarity in the description that follows.

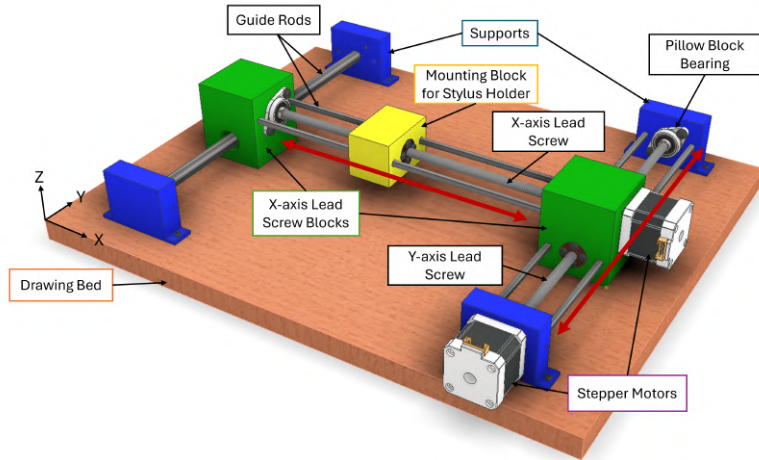


Figure 3.2: CAD model of lead screw motion concept

The y-axis lead screw system is mounted onto the drawing bed by four supports (blue) that are bolted down. The stepper motor that drives the y-axis lead screw mounts to one of these supports. Its shaft is coupled to a lead screw, which is supported at its other end by a pillow block bearing that is bolted to another support. This ensures that the lead screw stays perfectly aligned, while allowing it to rotate. Two guide rods are aligned on either side of the lead screw and press fitted into the corresponding supports.

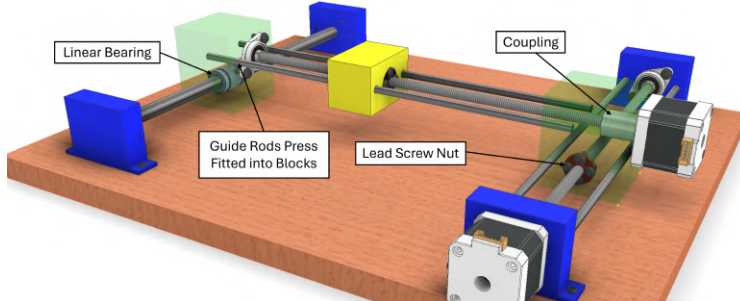


Figure 3.3: Close-up of lead screw concept

The x-axis lead screw system is supported by two blocks (green), as shown in Figure 3.3. One block is moved by the y-axis lead screw and the other runs on a thick guide rod. A linear bearing allows for frictionless sliding along this guide rod, while decreasing the load on the y-axis lead screw. Similar

to the y-axis setup, the x-axis lead screw is also driven by a stepper motor and supported by a pillow block bearing. The stylus holder, with which the machine will draw, mounts onto the yellow block, which moves when the x-axis lead screw turns. As shown in the close-up in Figure 3.3, the two green blocks are designed so that the x-axis lead screw system sits on top of the y-axis system.

### 3.3.2 Belt Driven Motion

In this concept, two belt-and-pulley systems are used to enable motion in the x and y directions, as shown in Figure 3.4. Four supports (blue) are bolted to the drawing bed. These supports serve as both anchorage for the y-axis belt system and as mounts for the linear rails. Two linear rails support a third one and allow smooth movement along the y-axis.

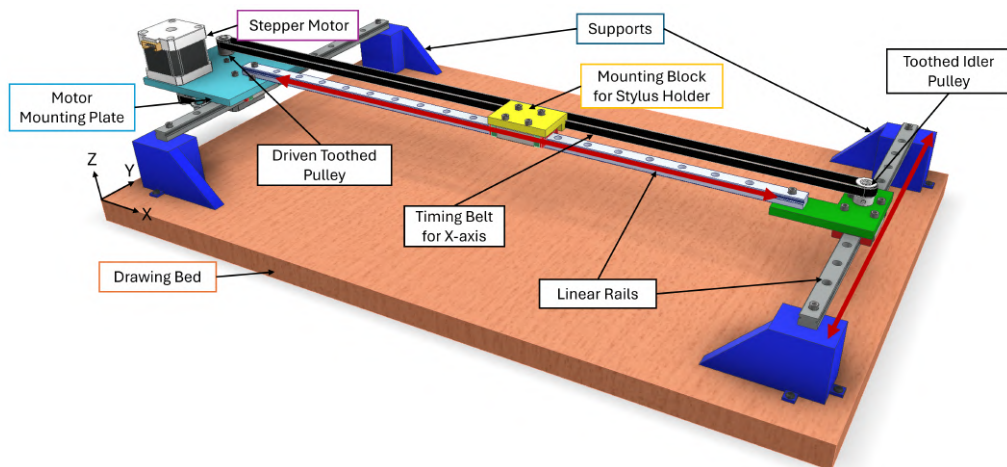


Figure 3.4: CAD model of belt driven motion concept

A motor mounting plate (cyan) supports two stepper motors, one for driving each axis' motion. The y-axis motor sits on top of the mounting plate, driving a toothed pulley underneath the plate. This driven pulley forms a triangle formation with two other idler pulleys under the mounting plate, as shown in Figure 3.5. A timing belt spans from one corner support, around each pulley, to the other corner support. This formation allows the motor mounting plate, along with the rail attached on top of it, to move back and forth along the y-axis as the motor turns.

A second stepper motor mounts to the underside of the mounting plate and it also drives a toothed pulley. This pulley, along with another timing belt and a toothed idler pulley, form the x-axis belt system. The belt forms a loop around the two pulleys, from one side of the stylus holder mount (yellow) to the other. Thus, the stylus holder mount will move left and right along the x-axis when the x-axis motor turns. This mount interfaces with the stylus holder and exchanger system.

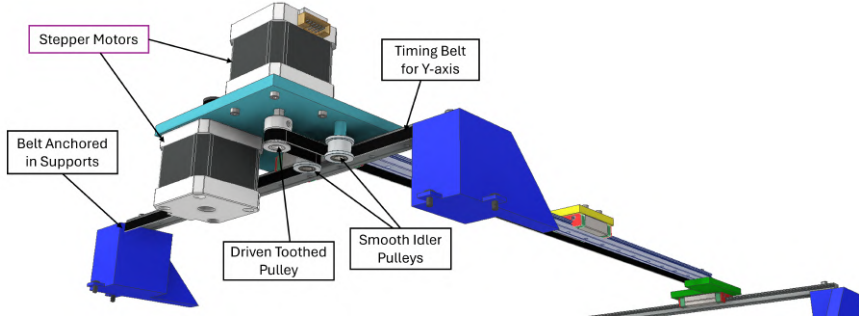


Figure 3.5: Close-up of belt driven motion concept

### 3.4 Stylus Exchanger Subsystem Concepts

The stylus exchanger subsystem refers to all components required to both hold the stylus during a drawing operation and exchange it with a different stylus. A Parrot Products Slimline Whiteboard marker was modelled in Autodesk Inventor from measurements taken with a caliper. This model was used to develop the following three concepts to a realistic scale.

#### 3.4.1 Side Gripper

This concept, illustrated in Figure 3.6, makes use of a small servo motor to hold the stylus in place whilst drawing. The servo motor is attached to a backing plate (blue), with its drive gear exposed through a rectangular hole in the plate. A small tapered arm is fitted onto the motor's drive gear. The backing plate attaches to the movement system either through holes in the plate or by an L-shaped bracket fitted onto a horizontal moving surface.

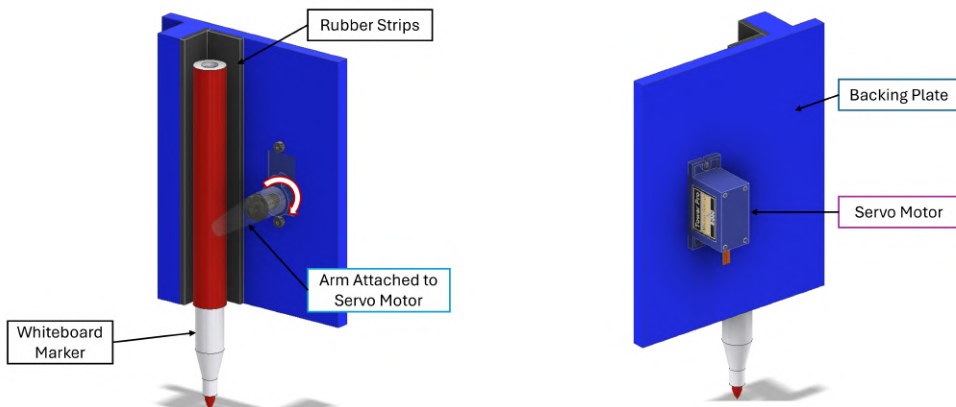


Figure 3.6: CAD model of side gripper concept

During a loading operation, a stylus is aligned upright against the ledge on the backing plate. The servo motor then turns its arm clockwise until it presses the stylus securely against the rubber strips on the plate. These strips ensure

a tight grip and add friction to resist upward forces as the stylus is dragged on a drawing surface. To exchange styluses, the current one is released by turning the servo arm anti-clockwise. The machine will then locate to the new stylus and load it.

This concept requires that styluses be stored in an upright position near the drawing surface for efficient automatic exchange. To enable this, a wooden stand as shown in Figure 3.7 is installed right next to the drawing surface, within reach of the side gripper mechanism. The movement system will move the side gripper to the stand and align it next to a stylus for loading. This stylus stand consists of a backboard with a small shelf fastened perpendicular to it. Clips (black) are bolted to the backboard to hold styluses upright and in position. The shelf ensures that styluses are kept level as they are supported on their points. This means that the styluses, no matter how long they are, will always be picked up at the same height from their drawing point.

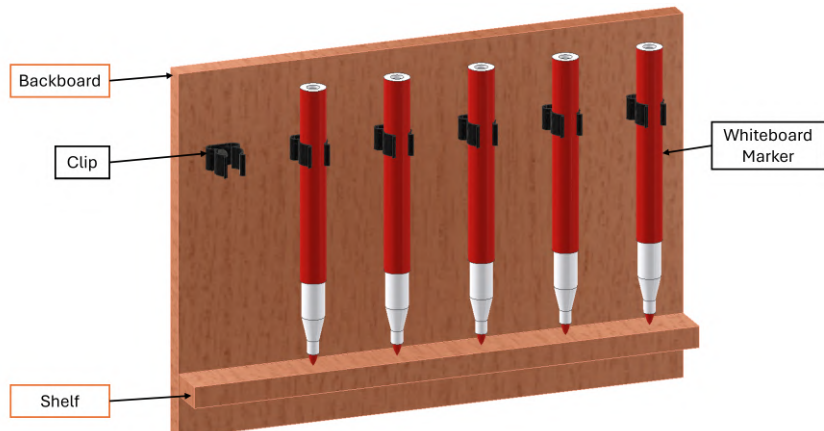


Figure 3.7: CAD model of stylus stand

### 3.4.2 Claws

This concept also makes use of a servo motor to hold the stylus in place. However, it was developed to have a tighter grip. This is accomplished by two opposing “claws” that squeeze the stylus between them, as shown in Figure 3.8. These claws (green) attach to the servo motor, which is in turn fastened to a mount block (blue). This mount block interfaces with the movement system by way of horizontal holes in the block or an L-shaped bracket, depending on the orientation required.

Figure 3.9 illustrates how the claws in this concept work. Each claw has a half-moon shape with a strip of rubber affixed on the inside. The one claw press fits directly onto the servo motor’s drive gear. It has gear teeth that mesh with the other claw. The non-driven claw is held in place with a small pin drilled into a plate that fits over the servo motor’s face. When the servo motor turns clockwise, the claws open. A stylus can then be located between them.

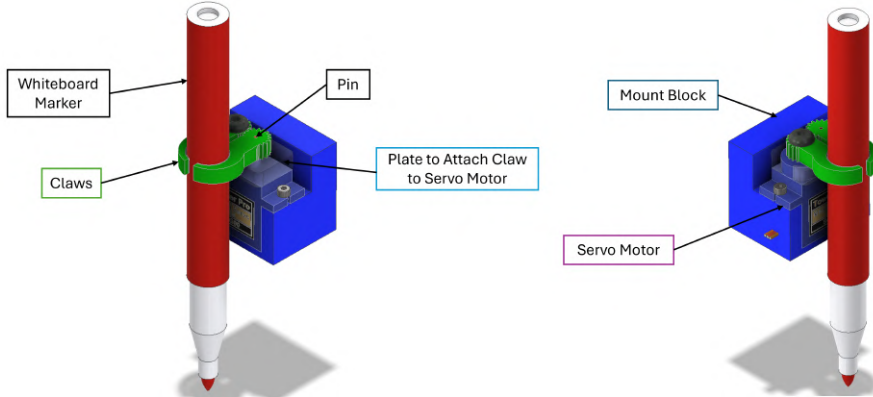


Figure 3.8: CAD model of claws concept

The claws close and grip the stylus tightly when the servo motor turns anti-clockwise. This allows for some self-alignment if the stylus was not picked up in its exact coordinate location. The stylus stand, as described in Section 3.4.1, is also required to ensure upright storage and accurate location for this concept.

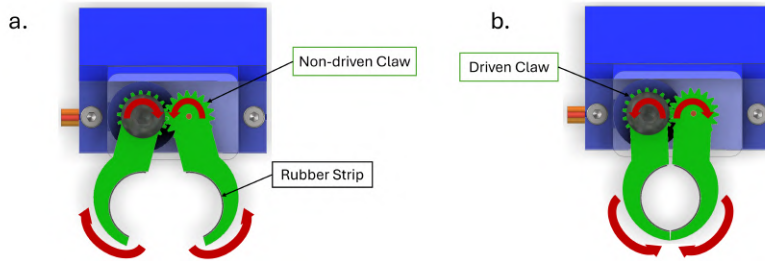


Figure 3.9: Close-up of claws concept showing  
(a.) open position and (b.) closed position

### 3.4.3 Revolver

This concept draws inspiration from the handgun with the same name. It can be categorised as a drum-type ATC, with its chambers each containing a different colour stylus. This allows stylus exchange to happen at the location where the machine is drawing, with no need for movement to a separate stand. The whole assembly, as shown in Figure 3.10, attaches to the movement system either through horizontal holes or a base plate.

A housing (blue) supports and encloses the revolving cylinder (yellow). This cylinder can hold multiple styluses in its chambers. The cylinder is rotated by a stepper motor, which mounts atop a plate fastened to the housing. A square shaft, coupled to the stepper motor, moves the cylinder as it rotates. The square corners of the shaft ensure high friction and prevent the cylinder from stripping loose. This shaft is supported by a small ball bearing seated in the bottom of the housing.

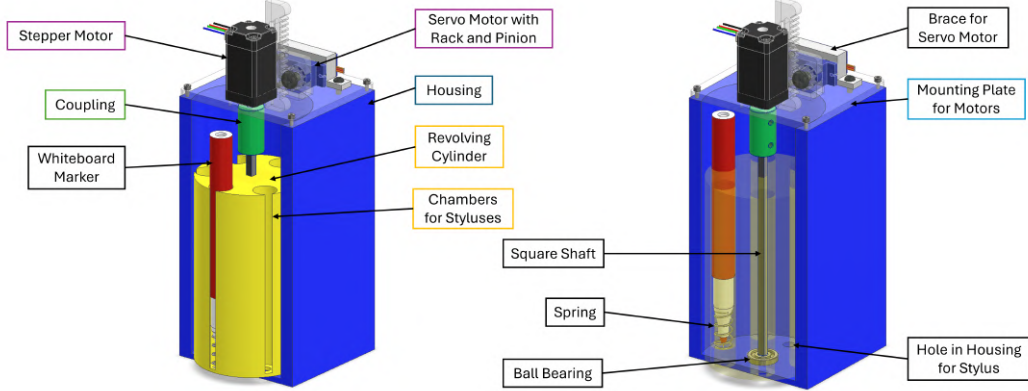


Figure 3.10: CAD model of revolver concept

Within each chamber of the cylinder, there is a small spring. These springs have a smaller diameter than the stylus body, but larger than the stylus tip. This means that when the springs are not compressed, they hold the styluses up inside the chambers. These styluses can then be pushed down onto the drawing surface, through holes at the bottom of the chambers. Once released, a stylus will pop back up into its chamber. To push and hold styluses down onto a drawing surface, a servo motor assembly is used. The workings of this assembly are illustrated in Figure 3.11.

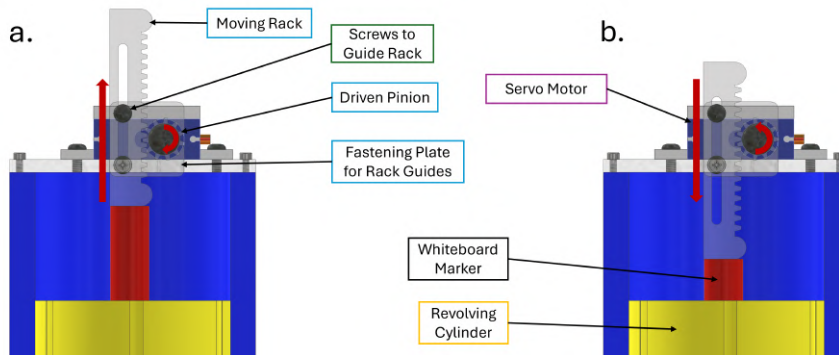


Figure 3.11: Close-up of revolver concept showing (a.) servo motor retracting and (b.) servo motor pushing stylus down

The servo motor assembly includes a rack and pinion that converts rotational motion to translational motion to push styluses down onto a drawing surface. Once styluses have been loaded into the revolving cylinder, the cylinder will rotate until the requested stylus is aligned with a hole at the bottom of the housing, which defines the drawing position. The servo motor will then turn anti-clockwise to push the stylus down onto the drawing surface. Once a drawing operation with the current stylus is completed, the servo motor will turn clockwise to release the stylus. The cylinder can then be rotated to align a different stylus with the drawing position.

## 3.5 Concept Evaluation and Selection

This section presents the evaluation of all the aforementioned concepts and the selection of the best concepts for the final design. Concepts for both subsystems were evaluated qualitatively and quantitatively to determine how well they adhere to stakeholder and engineering requirements.

### 3.5.1 Qualitative Evaluation

#### 3.5.1.1 Movement Subsystem Concepts

Both the lead screw- and belt driven motion concepts can be built to have an A3-sized drawing area and to draw on different surfaces, thereby meeting SR4 and SR3. To draw sufficiently complex shapes (SR9), the machine must be very precise. Lead screw motion is inherently very precise. Belt-driven motion on the other hand, can be less precise due to belt stretch.

Both movement system concepts are designed to be portable (SR2), as they mount onto a drawing bed. However, the lead screw concept will be heavier. While both concepts would require minimal maintenance (SR11), the belt driven concept would have to be checked for belt wear.

In terms of safety (SR10), the belt driven concept presents less likelihood for jamming fingers in between moving parts than the lead screw concept does. It would also be easier for a human to resist the motion of belts versus the motion of lead screws, which are more powerful.

In a general sense, both concepts have intricacies in building them. The lead screw concept is easy to assemble, but its parts are complicated to manufacture. Tensioning the belts correctly for the belt driven concept and aligning its pulleys precisely is difficult, but its parts are easy and quick to manufacture.

#### 3.5.1.2 Stylus Exchanger Subsystem Concepts

All three stylus exchanger concepts can exchange multiple styluses and do so automatically, thus meeting SR5 and SR6. However, the side gripper and claws concepts require the machine to fetch and replace styluses one at a time, whereas the revolver concept can exchange styluses without having to move to a precisely defined location, making it easier to automate.

The side gripper will be the easiest to assemble and maintain, thanks to its very few parts. However, it will not resist upward forces and friction from the stylus dragging along the drawing surface very well. Styluses can also fall out if they are not picked up accurately.

While the claws concept will grip styluses tighter and resist forces and friction better, it will present problems with gear tooth wear when used frequently. This concept will self-align styluses to some extent, but if they are not picked up properly, the servo motor will wear out from forcing the claws closed.

The revolver concept is by far the most complex to build and maintain, requiring the most parts. However, this concept eliminates the need for a stylus stand and ensures that a new stylus will begin drawing at the same location and height of the previous one. While it cannot accommodate a range of stylus types and sizes, it is the most compact and efficient solution.

### 3.5.2 Quantitative Evaluation

A quantitative evaluation of the concepts was performed by scoring each concept on a scale of 1–3 against weighted criteria. The criteria were derived from the SRs, FRs and PRs. Each criterion was assigned a weight by reversing the priority level of its related SR, meaning the most important criterion (ranked 1) received the highest weight (3). Results of the evaluation for the two subsystems are shown in Tables 3.4 and 3.5. More information on how each criterion was scored is provided in Appendix A.2.

To save space, the concept names were abbreviated. The lead screw motion and belt driven motion concepts are represented by “L” and “B”, respectively. For the stylus exchanger concepts, side gripper, claws and revolver are represented by “S”, “C” and “R”, respectively. For the “Cost” criterion, costs were estimated based on quotes from suppliers for typical components used in these applications. A screenshot of the spreadsheet used to estimate costs is shown in Appendix C.

Table 3.4: Quantitative evaluation of movement subsystem concepts

Criterion	Weight	Score		Comment
		L	B	
Cost	2	3	1	Estimated cost of B is R2,261 and of L is R1,318.
Scalability	2	1	3	Linear rails in B are very scalable, but long lead screws bending and misaligning in L is a concern.
Weight	2	2	3	Both concepts are light enough to carry, but L is heavier.
Maintenance requirements	1	2	1	Both concepts require semi-regular lubrication, but B’s belts need additional maintenance.
Safety	3	2	3	Fingers can get jammed in L, but not in B.
Ease of manufacture	2	2	3	L has complicated parts to manufacture, whereas B’s parts are simpler and off-the-shelf.

Ease of assembly	2	3	2	L is easy to assemble, but B's belt tensioning and alignment is harder.
Reusable parts	1	1	2	Both concepts will potentially utilise 3D printing, but L will require more material.
Total	16	15	18	
Weighted Total	48	31	37	

Table 3.5: Quantitative evaluation of stylus exchanger subsystem concepts

Criterion	Weight	Score			Comment
		S	C	R	
Cost	3	3	3	2	Estimated costs of S and C are R476 and R404, respectively, with R costing R775.
Ease of assembly	2	3	2	1	S is easiest to assemble, followed by C, and R.
Precision	2	1	1	3	S and C can misalign when picking up styluses. R can draw in same location and orientation as previous stylus.
Maintenance requirements	1	3	2	1	S requires very little maintenance, C's gears will need replacement, and R has extra motors and bearings to maintain.
Stylus exchange speed	3	1	1	3	R can exchange styluses much quicker with no need to move to and from a stylus stand.
Programming complexity	3	1	1	3	C and S require coordinates of styluses and an exchange sequence, while R only moves a stepper motor to the next index.
Total	14	12	10	13	
Weighted Total	42	26	23	33	

From both the qualitative and quantitative evaluations, the belt driven movement subsystem and revolver stylus exchanger subsystem concepts were selected as the best options for the final design.

# Chapter 4

## Detailed Design and Implementation

The concepts selected in the previous chapter were integrated into a detailed design for the system. Design decisions, such as material and component selection, are discussed in this chapter. Calculations to support these design decisions can be found in Appendix D. The physical construction of the system is also described.

### 4.1 System Overview

The final design of the whole system is shown in the CAD model in Figure 4.1. Electrical cables and their management have been omitted for clarity. CAD models of off-the-shelf components, such as motors, pulleys and electronic components, were sourced from GrabCAD. The artists of these models are credited in Appendix B.

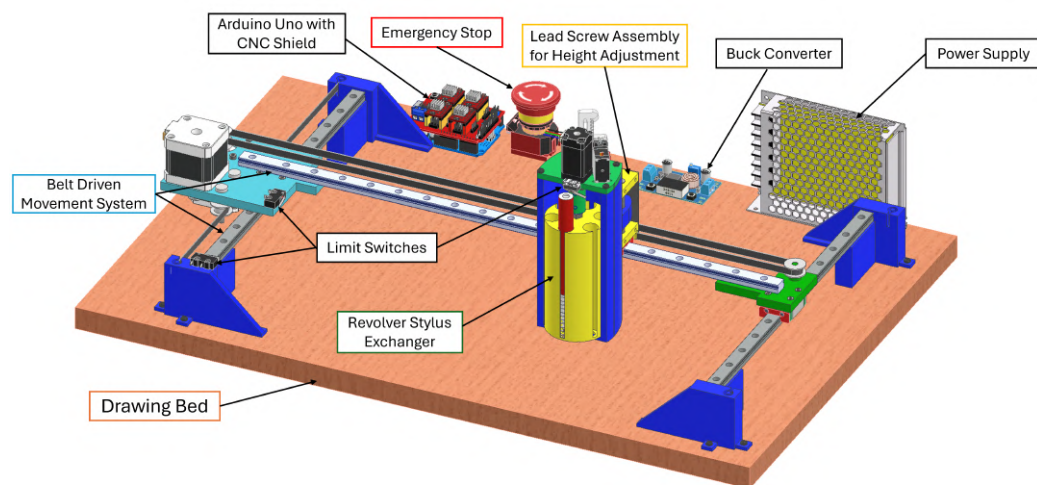


Figure 4.1: CAD model of final design of CNC drawing machine

As shown, the whole machine mounts onto a drawing bed. The drawing bed, a 600 by 400 mm board cut from 16 mm thick medium-density fibreboard (MDF), was sourced from Lumber King in Stellenbosch. This provides a sturdy base that the user can carry around, as well as a flat surface for drawing. The movement subsystem mounts onto this drawing bed, and the stylus exchanger mounts onto the movement subsystem.

The system is outfitted with an emergency stop button, which cuts power to all motors and the CNC shield when pressed. This feature prevents injury to an operator or damage to the system if it were to make unexpected movements. A safety guard installed on the power supply (not shown in the CAD model), prevents users from touching live electrical connections and potentially shocking themselves. Three mechanical limit switches are installed to home each axis of movement and to prevent the machine from moving outside its intended drawing area. Soft limits are defined in software with reference to these switches. This means that all axes have a defined zero- and maximum position, which the machine cannot move beyond.

## 4.2 Movement Subsystem

The movement subsystem in the final design functions as described in Section 3.3.2. This subsystem utilises some components sourced from a previous final year project: Design and Construction of a Kinetic Art Table by Mr Andrew Pienaar (2024). Pienaar's project was carefully disassembled and usable components were salvaged for this project to reduce costs and material waste. These components include Nema 17 stepper motors, GT2 timing belts and GT2 toothed pulleys.

Linear rails were acquired from DIY Electronics. Due to the high cost of these rails, the most affordable option was to purchase two 300 mm MGN12C rails for the y-axis, and one 480 mm MGN12H rail for the x-axis. The C and H designations refer to the size of the carriage blocks, with the H block being larger than the C block. For each rail, its deflection and bending moments were calculated to ensure that the planned loading would not exceed rated limits. These calculations, in Appendix D, show that the rails will experience negligible deformation and that they are resistant enough to bending moments caused by offset components, with the smallest safety factor being 6.8.

It was decided to use the salvaged Nema 17 stepper motors to drive the movement subsystem, as they are commonly used in hobby CNC machines and 3D printers. Calculations in Appendix D show that these motors can effectively drive the x- and y-axes with torque safety factors of 89.1 and 35.8, respectively. Weaker motors could have been used, but the Nema 17s were already available and their weight did not demand design changes to support them. The only condition for using them was that the mounting plate for the motors be rigid enough to support their weight.

Inspiration for the belt system layout, as described in Section 3.3.2, was drawn from an existing design in Dejan (2021). This specifically refers to the mounting of both stepper motors onto the y-axis carriage instead of fixing one to the drawing bed. While unconventional, this design reduces the moment about the x-axis that the x-axis rail would experience from the weight of one motor offset from it. The design is also more compact and aesthetically pleasing. Therefore, it was decided to implement this design, as long as the motor mounting plate is rigid enough to support the weight of both motors.

It was decided to make use of 3D printing to create the supports and mount plates for the movement subsystem. This is because 3D printing allows for the quick manufacture of complex shapes, and produces lightweight parts. The parts were printed using polylactic acid (PLA) filament, with a 20% infill density. With a plate thickness of 7.5 mm, the motor mounting plate was found to have a safety factor of 179 against the bending stress exerted on it, as shown in Appendix D. This thickness was chosen as it allows for the shortest cap screws (6 mm) available at the MMW to be counterbored into the plates, ensuring strong connection while not getting in the way of the x-axis rail.

As mentioned, GT2 timing belts and pulleys were salvaged from Pienaar's project. As these are commonly used in hobby CNC machines and 3D printers, they were deemed suitable. Two smooth idler pulleys and one toothed idler pulley were purchased from DIY Electronics to complete the two belt systems. For the y-axis belt system, belt clamps were designed as rounded grooves extruded into the 3D printed supports. This allows the belt ends to be clamped securely by folding them over themselves, with teeth interlocking, and pushing them down into the grooves. For the x-axis belt system, the tool mount was designed with two toothed grooves to clamp the belt on either side of it.

### 4.3 Stylus Exchanger Subsystem

The stylus exchanger in the final design functions as described in Section 3.4.3, although some design changes have been made to cut down on material cost, weight and complexity. This final design is shown in Figure 4.2. From the figure, it can be seen that the housing was redesigned to be more compact and rounder, reducing its weight. The servo motor's orientation was changed to be vertical instead of horizontal, which reduces its footprint on the mounting plate. It was also angled relative to the stepper motor to allow a tighter fit on the mounting plate, while still being able to reach the styluses within the housing. Lastly, the square shaft that couples to the stepper motor was shortened to only reach halfway into the revolving cylinder, as this is sufficient to turn it. A cylindrical protrusion was added to the bottom of the revolving cylinder that slips into the bearing seated at the bottom of the housing, to provide support and easy rotation.

Due to the complexity of the parts in the stylus exchanger subsystem and the need to keep weight low, it was decided to 3D print the housing, revolving

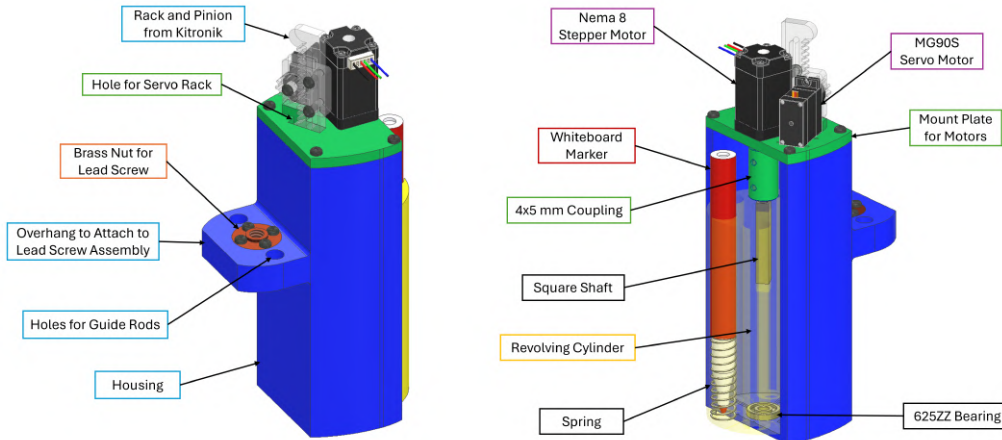


Figure 4.2: CAD model of final stylus exchanger subsystem

cylinder and mount plate. These parts were printed from PLA filament with a 20% infill density. To ensure that the mount plate is rigid enough to support the weight of the two motors, it was printed with a thickness of 5 mm. The bottom of the housing has to be very thin to allow the styluses to reach the drawing surface, so it was printed with a thickness of 3 mm. Since this bottom part carries the weight of the revolving cylinder, styluses and bearing, it has to be sufficiently strong too. Calculations in Appendix D show that the bottom of the housing can resist the bending stress exerted on it with a safety factor of 150, proving that 3 mm thickness is sufficient.

A Parrot Products Slimline Whiteboard marker was modelled in CAD to develop concepts to a realistic scale in Section 3.4. It was decided to use this marker as the drawing stylus for the final design. This is because the forces required to write with a whiteboard marker are low in comparison to pens, pencils or fineliners. The specific marker was chosen as it has a fine tip, comes in a variety of colours, and is widely available in most stationery stores. These markers come in inexpensive (R44.99) packs of six, which include the colours black, blue, red, green, purple and orange. They also feature a flat surface at their non-writing end, which allows the servo motor to push them down effectively. The dimensions of these markers were used to design the revolving cylinder and its housing to the right height and diameter to hold six styluses. Each chamber in the revolving cylinder is only 0.8 mm wider than the widest part of the marker, ensuring vertical alignment.

Each marker is supported by a spring in its chamber. These springs were custom made by Gellini Spring Manufacturers after springs from various suppliers were found to be unsuitable. A spring found in the Mechatronics Workshop was used as reference to design the custom springs. Each spring has a free length of 40 mm, an inner diameter of 11 mm to ensure a snug fit over the marker, and a wire diameter of 0.6 mm. From these parameters, the spring constant was calculated to be 0.065 N/mm (see Appendix D). This means

that the weight of the markers compress the springs by approximately 1.8 mm, which is acceptable and does not lead to snagging when the revolving cylinder turns.

An MG90S servo motor was selected to push the markers down onto the drawing surface. Its metal gearbox makes it stronger than standard plastic geared servos, giving it a stall torque of 0.18 Nm (Communica, 2025). This servo motor must resist the spring force of the spring it compresses, as well as the normal force exerted by the drawing surface on the marker tip. A marker was dragged over a sheet of paper on a precision scale to determine this normal force, which was found to be at most 2 N. More details on this procedure can be found in Appendix E. The maximum force that the servo motor can transfer through the rack and pinion to the marker was calculated to be 4.8 times greater than required, as shown in Appendix D. This provides a comfortable safety factor to resist drag forces when drawing on rough surfaces. The rack-and-pinion assembly that attaches to the servo motor's face, was bought from RS Components as a set designed by Kitronik for use with micro servos. It consists of a pinion gear, a rack and a mounting bracket, all cut from 5 mm thick acrylic. The rack allows for 20 mm of travel, which is sufficient to push the markers down far enough out of the housing to reach the drawing surface.

A Nema 8 stepper motor was chosen to rotate the revolving cylinder. It was chosen over a servo motor due to its ability to rotate 360° and hold its position without drawing power. Standard hobby servo motors can only rotate up to 180° and they can be prone to backlash. The Nema 8 was specifically chosen as it was the smallest and lightest stepper motor available from local suppliers. With its rated torque of 0.018 Nm, it can rotate the revolving cylinder with a safety factor of 3.8, as shown in Appendix D. A small 625ZZ radial ball bearing was acquired from Microrobotics to support the revolving cylinder at the bottom of the housing. At the top of the revolving cylinder, a 6 by 6 mm square shaft was designed to couple it to the stepper motor, through an aluminium coupling. The shaft was manufactured by the MMW from key steel and press fits into the revolving cylinder. Its one end was machined down to a 5 mm diameter round shaft to fit into the 4x5 mm aluminium shaft coupler, which was acquired from Microrobotics.

To interface the stylus exchanger system with the movement system, a lead screw assembly was designed. This assembly, shown in Figure 4.3, allows the user to adjust the height of the stylus exchanger system by up to 20 mm to accommodate for different drawing surfaces with different thicknesses. A short, 70 mm, TR8 lead screw and matching brass nut were used, as they were available from a previous project. The brass nut bolts into the stylus exchanger housing, while the lead screw is held in place by two 608ZZ radial ball bearings acquired from RS Components, one at the top and one at the bottom. The lead screw is turned by a hand knob, which was 3D printed from PLA filament. Two 8 mm thick guide rods (50 mm long) were cut to size from a longer rod from Pienaar's project to press fit into the toolmount and top

plate. The toolmount and top plate were also 3D printed from PLA filament. A thin stainless steel plate was cut from scrap metal to serve as the backing plate for the lead screw assembly. The interface was designed so that there is minimal tolerance between the stylus exchanger housing and the 3D printed plates, as well as between the housing and the backing plate. This means that the housing is held in place by friction, preventing the lead screw from turning by itself.

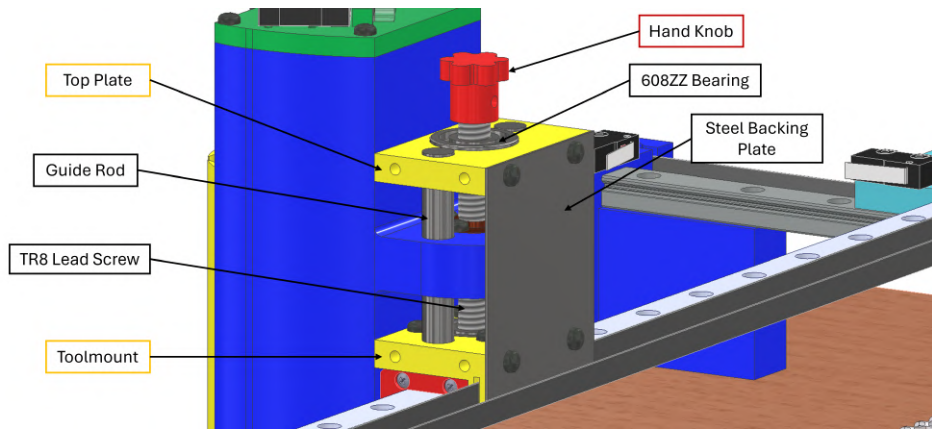


Figure 4.3: CAD model of lead screw assembly to adjust height of stylus exchanger

## 4.4 Electronics

The electronics of the CNC drawing machine include a microcontroller, CNC shield, motor drivers, power supply, buck converter, limit switches and an emergency stop button. A wiring diagram is shown in Appendix F to illustrate how all the electronic components connect to each other. Some of these electronics, such as the microcontroller, CNC shield and motor drivers were salvaged from Pienaar's project to reduce costs.

Pienaar (2024) used an Arduino Uno R3 with a CNC shield V3 to control his kinetic art table. Since these components are commonly used in hobby CNC projects and the author is familiar with programming Arduino Unos, it was decided that these components would be suitable for this project too. The CNC shield, which fits onto the Arduino, translates G-code commands from the Arduino Uno into step and direction pulses for the stepper motor drivers that attach to it. It allows for up to four stepper motors to be controlled at a time, one for each of the three Cartesian axes, and one for a duplicate axis. The CNC shield also has headers for positive and negative endstops for each axis, as well as spindle control pins that can be repurposed to control a servo motor (AZ-Delivery, n.d.). Therefore, all control functionality of the CNC drawing machine can be achieved with this microcontroller and shield setup.

Each stepper motor is driven by a stepper driver that plugs into the CNC shield. The CNC shield supports A4988 and DRV8825 stepper drivers (AZ-

Delivery, n.d.). Due to their superior microstepping capabilities and higher current ratings, the DRV8825 drivers were chosen. They could also be reused from Pienaar’s project, cutting costs and lead time. The drivers have adjustable current limits that can be set by turning a potentiometer that controls the driver’s reference voltage. Appropriate values for these reference voltages were calculated for each motor in Appendix D, according to the rated current of each motor. Initial reference voltages of 0.6 V and 0.25 V were set for the Nema 17 and Nema 8 stepper motors, respectively. It was also decided to enable 1/16 microstepping for all drivers, as this is common practice and allows for smooth movement of the motors.

The CNC shield requires a power supply of at least 12 V to drive the stepper motors (AZ-Delivery, n.d.). Therefore, it was needed to acquire a 12 V power supply with enough current capacity to drive all three stepper motors, the servo motor and the Arduino Uno. Calculations in Appendix D show that the required current rating for a power supply is around 1.4 A. An LRS-100-12 power supply rated for 12 V and 8.5 A was chosen and acquired from Microrobotics, as it is compact, not too expensive, and was available at the time of purchase. Weaker supplies were considered, but were not available at the time.

The servo motor cannot be powered with 12 V, as it is rated for 4.8 V to 6 V (Communica, 2025). Therefore, an inexpensive buck converter was acquired from Microrobotics, capable of stepping 4–38 V down to 1.25–36 V and with a similar current rating to the power supply (Microrobotics, 2025c). This specific buck converter was chosen as it has a seven-segment display that shows the output voltage, allowing for easy adjustment. It was adjusted to provide 5 V to the servo motor.

## 4.5 System Assembly

The full system was assembled in the Mechatronics Workshop by following an incremental approach. Subsystems and components were tested individually before being integrated into the system as a whole. The completed assembly is shown in Figure 4.4. It was nicknamed the “Rainbow Plotter”, after its ability to draw colourful pictures. As shown, a cable drag chain was installed to the left of the machine to manage cables going to the moving gantry. Between the motor mount on the left y-axis rail and the stylus exchanger, a strip of laminated paper was installed to keep the cables going to the stylus exchanger from snagging in the belt system. This strip is flexible enough to bend as the stylus exchanger moves, but stiff enough to support the cables attached to it. A magnetic whiteboard sheet was acquired from Takealot and placed on the drawing bed to provide both a surface to draw on and a way to hold drawing paper in place with magnets.

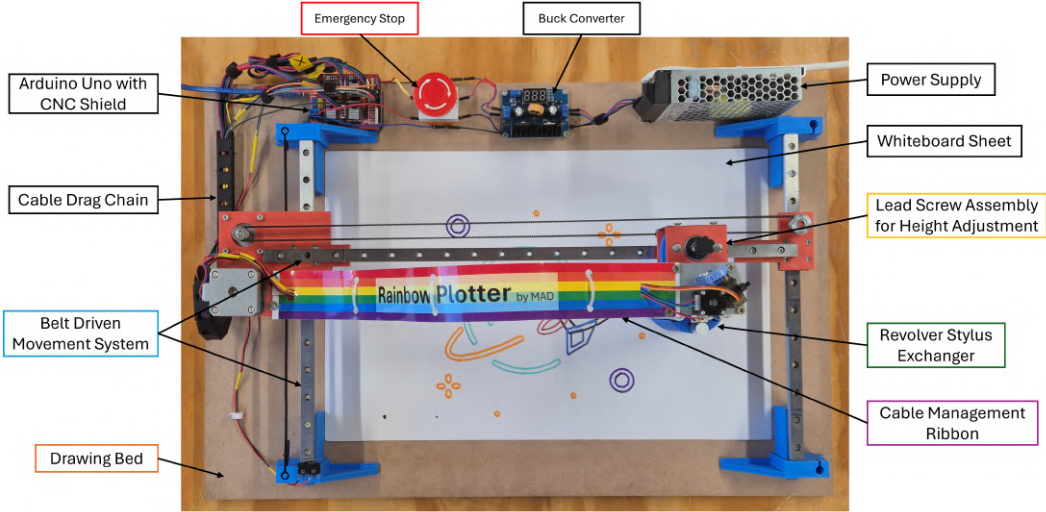


Figure 4.4: Photo of assembled CNC drawing machine

During the assembly process, some difficulties had to be overcome. Firstly, it proved difficult to align the two y-axis rails perfectly parallel to each other. The supports would “walk” significantly when the x-axis rail was moved back and forth. This was solved by using a large metal square to align the rails, as shown in Figure G.1 in Appendix G, and then only tightening the bolts on the x-axis rail tightly. Another issue was that the bolt holes in the motor mounting plate were infringing on the space where the x-axis rail needed to be. This was solved by adding counterbores to those holes so that the bolt heads would sit below the surface of the plate and not interfere with the x-axis rail. After some testing, it was found that the Nema 17 motors became too hot to touch. Out of concern that they may soften their PLA mount, the motor currents were limited further by setting the reference voltage to 0.5 V instead of 0.6 V. This reduced their temperature significantly, and did not affect their performance noticeably. When implementing homing for the revolving cylinder (which is connected as the CNC shield’s z-axis), it was found that the z-axis limit switch and spindle enable pins on the CNC shield were swapped, as the z-axis would not home at all. This was solved by plugging the limit switch for the z-axis into the spindle enable pin instead.

Once successfully assembled, the machine was found to weigh 5.8 kg. Its overall size was measured to be 600 mm in length, 400 mm in width and 238 mm in height. The machine’s drawing area was measured by moving the stylus exchanger to its furthest points along each axis and measuring the distance travelled along the linear rails. This results in a drawing area of 215 mm by 345 mm. The soft limits of each axis were defined in software accordingly.

# Chapter 5

## Software

The CNC drawing machine is controlled by software that sends instructions to the Arduino microcontroller. This software runs on a computer and interfaces with the Arduino via USB connection. It consists of two parts: the image to G-code converter program and the G-code sender application. Both parts are outlined in this chapter.

### 5.1 Overview

A flow diagram of the software elements and their interactions is shown in Figure 5.1. Elements in blue are scripts and applications executed on the user's computer, while elements in purple are hardware components. Solid line arrows indicate the flow of information, while dashed line arrows indicate voltage signals.

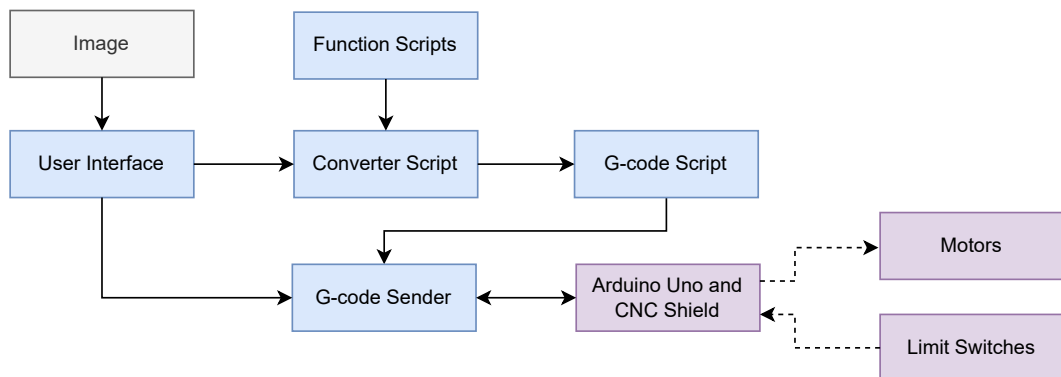


Figure 5.1: Flow diagram of software elements

As shown, the user starts by uploading an image to the user interface. The image is then sent to the image to G-code converter script, which was written in Python. This script utilises external libraries and function scripts to process the image, extract drawing paths and write G-code instructions to a text file. These libraries and function scripts were downloaded from a GitHub

repository, as explained in Section 5.3. The text file containing the G-code is then saved to the user's computer. From the user interface, the user can then open the G-code sender application and connect to the Arduino Uno. The G-code sender application has its own user interface, which allows the user to upload the G-code text file that they previously saved. Once the file has been uploaded, the user can home the machine and start a drawing job. The G-code sender application sends the uploaded G-code instructions line by line to the Arduino Uno via USB serial communication. In response to these instructions, the Arduino sends voltage signals to the stepper motor drivers and the servo motor to control the movement of the machine. The Arduino also receives input signals from the limit switches when they are triggered, which it then communicates back to the G-code sender application. This allows the application to home the machine and stop the drawing job if a limit switch is triggered. The software pipeline is demonstrated in the tutorial video in the project's [GitHub repository](#).

## 5.2 User Interface

The user interface that the user interacts with to upload their image, save the G-code file and open the G-code sender application is shown in Figure 5.2. It was written in Python using the Tkinter package and pops up in a separate window when the image converter script is run.

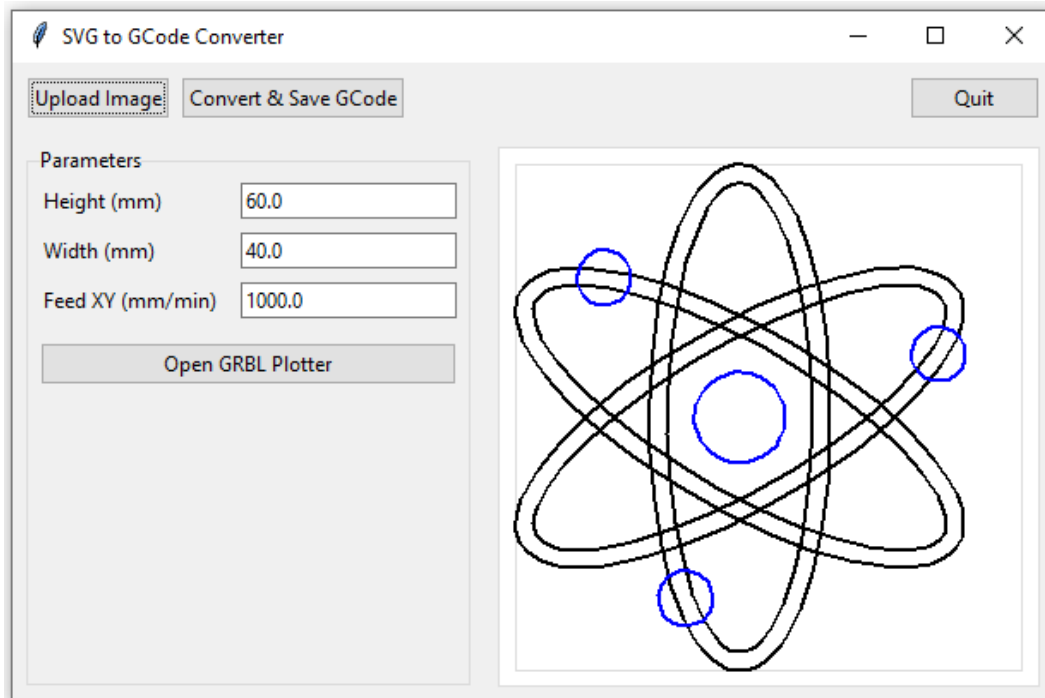


Figure 5.2: Screenshot of user interface for image converter

As shown in Figure 5.2, the interface has four buttons and three fields for user input. The “Upload Image” button opens the user’s file explorer, allowing them to select an SVG image file from their computer. Once selected, the image appears in a viewbox on the right side of the interface. The displayed image is a representation of the paths that will be drawn by the machine, in their assigned colours.

The “Convert & Save GCode” button activates the image to G-code conversion process with the parameters specified in the input fields. This process is outlined in the next section. The user can specify the drawing height, width and feed rate (“Feed XY”) in the respective input fields. Height and width refer to the dimensions of the drawing on the physical drawing surface, while feed rate refers to the speed at which the machine will move while drawing. The default values shown in Figure 5.2 are used if the user does not change them. Drawings are scaled proportionally to fit within the specified height and width, meaning aspect ratio is maintained. After the conversion process has completed and a G-code text file has been generated, the user’s file explorer opens and they are prompted to save the file on their computer. A pop-up message appears upon saving, informing the user where on their computer the file has been saved.

A shortcut to open the G-code sender application is provided in the form of the “Open GRBL Plotter” button. This button opens the GRBL-Plotter application, which is the G-code sender application used to control the machine and send instructions to the Arduino. Lastly, once the user is satisfied with the created G-code file, they can close the user interface by clicking the “Quit” button.

### 5.3 Image to G-code Converter

The image to G-code converter script was written in Python and takes an SVG image file as input. At first, the converter was planned to take raster image files, such as .png or .jpg, as input. However, raster images blend colours together, especially along the edges of shapes. This means that some pixels along the edges of shapes may not be the colour of the shape itself, but a blend of the shape’s colour and the background colour. When each pixel is matched to the nearest colour in the drawing machine’s palette, these blended pixels are matched to the wrong colour. This is shown in Figure 5.3 where a raster image of a green rectangle and a blue circle on a white background is compared to the G-code path generated from it. GRBL-Plotter’s native image converter was used to generate this path. As shown, some pixels along the edges of the blue circle are incorrectly mapped to green. The solution to this problem is to vectorise the image, which converts it into an SVG file. Therefore, it was decided that the converter would take SVG files as input instead of raster images. It should also be noted that the converter does not fill shapes with hatching or other fill patterns. Only the outlines of shapes are drawn.

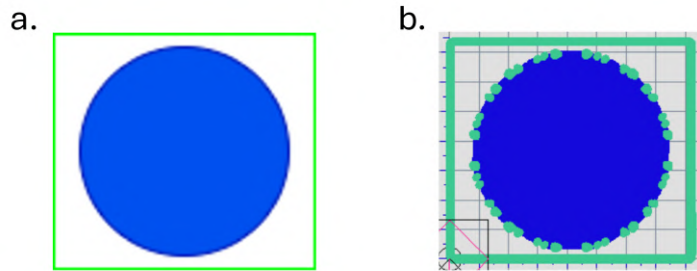


Figure 5.3: Comparison of (a.) a raster image and (b.) the G-code path generated from it

A repository called `svg2gcode_grbl` was found on GitHub with a script that converts SVG files to G-code for GRBL-based CNC machines. This script, written by arcadeperfect (2020), could only convert single-colour SVG files to G-code and had a tendency to crop images when converting, neglecting some shapes in the SVG. The repository, with its function scripts and libraries, was downloaded and the image converter script was modified significantly. Changes were made to allow for multicolour SVG files, improve path extraction, improve unit conversions, accommodate the servo motor and add the user interface. The function scripts and libraries from the repository remained largely unchanged, but the main script was essentially rewritten.

The main functions in the image converter script are represented by the blue blocks in the flow diagram in Figure 5.4. Once the user uploads an SVG image and clicks the “Convert & Save GCode” button, the script opens the SVG file and stores its XML text. This text defines all the paths contained within the file, along with their styles. The user-specified parameters are also read in from the user interface’s input fields and passed to the subsequent functions.

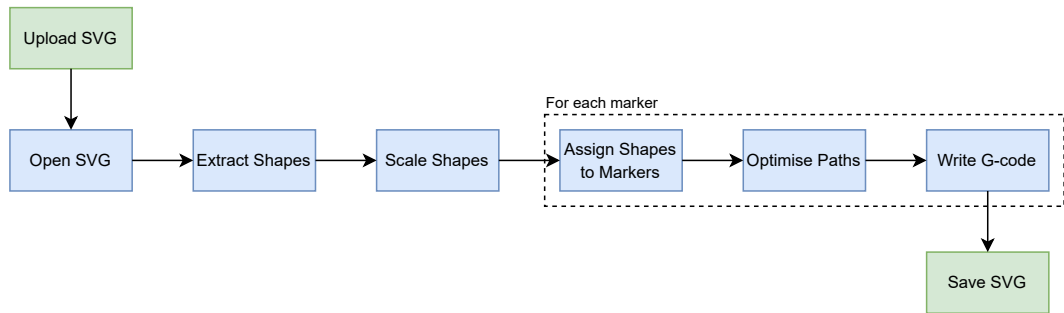


Figure 5.4: Flow diagram of image to G-code converter script

Next, the SVG text is parsed to extract all the geometric shapes and their styles. The script iterates through every element in the SVG text and checks if it is a defined shape that can be drawn: line, rectangle, circle, ellipse, polyline,

polygon or path. If it is, the shape's parameters and style (colour) are extracted from the XML text and stored in a list. Each shape's path is then parsed into a cubic-spline representation, defined by Bézier curves. The Bézier curves are then recursively subdivided into smaller and smaller straight line segments until they sufficiently approximate the original curves. Each line segment is defined by its start and end coordinates, which are stored in a list for each shape. The result being a list of polylines (shapes made up of straight line segments) and their styles.

Once a list of all shapes and their styles is extracted from the SVG text, the shapes are scaled to fit within the user-specified height and width. Scaling is done proportionally, meaning the script determines the limiting dimension and scales the other accordingly. Before this is done, the script first converts the units of the shapes into millimetres, as SVG files can contain shapes defined in various units, such as pixels, centimeters or inches. Various conversion factors are defined in the script for each possible unit conversion case. With all units in millimetres, the script scales all shapes within the list by the determined scaling factor. If necessary, the y-coordinates of the shapes are inverted, as some SVG files have their origin in the top-left corner and the machine's origin is in the bottom-right corner.

The six markers in the drawing machine's palette are defined in the script according to their number, RGB colour space values and Lab space values. They are arranged in order as follows: 1. Black, 2. Red, 3. Blue, 4. Green, 5. Orange and 6. Purple. For the last three functions in the flow diagram in Figure 5.4, the script iterates through these colours in order. First, the style of each shape extracted from the SVG text is matched to the nearest colour in the palette. This is done by converting the style to Lab colour space and then calculating the Euclidean distance between that style and each colour in the machine's palette. The shape is assigned to whichever colour in the palette has the shortest distance to the shape's style. Once all shapes are assigned to a colour, shapes are grouped according to their assigned colour.

Next, the script iterates through the paths in each shape assigned to each colour and attempts to optimise the drawing order. This is done using the greedy nearest neighbours algorithm, as described in Section 2.4. The algorithm ensures that within each colour group, the nearest shape is drawn next. If it is beneficial to flip a shape so that its start point becomes its end point and vice versa, this is also done. This flipping of start- and endpoints is a form of 2-opt optimisation, as described in Section 2.4. By finding the optimal drawing order of paths, the total distance travelled by the machine is reduced, saving time.

Finally, once all drawing paths are optimised, the script writes G-code instructions to a text file. This is done with a preamble specifying the feed rate (speed of drawing), followed by G-code instructions for each shape within each colour group. Before each new colour group, a tool change command is written in the following format: M6 Tn, where n is the marker's number in the

palette. All shapes in a colour group are drawn before moving on to the next colour group. This saves time by reducing the number of tool changes. Before each shape, a command is sent to actuate the servo motor to push the marker down onto the drawing surface. Once the shape is drawn, another command is sent to retract the servo motor and lift the marker off the drawing surface before moving to the next shape. After each servo motor command, a short dwell time is added with the G4 P0.5 command, where 0.5 is the dwell time in seconds. This allows time for the servo motor to fully actuate before the machine starts moving, preventing missed lines. The G-code file ends with a postamble that sends the machine to home position.

The image converter is available in the project's [GitHub repository](#) as an executable file named `SVGtoGcode.exe`. It is compatible with Windows and macOS operating systems. The Python scripts that make up the image converter are also included in the repository.

## 5.4 G-code Sender Application

The G-code sender application used to communicate with the Arduino is called GRBL-Plotter. It is a free, open-source application that can be downloaded from GitHub (svenhb, 2025). The application has its own user interface, as shown in Figure 5.5. In order to use the application, GRBL firmware must first be uploaded to the Arduino Uno. This firmware interprets G-code commands and translates them into pulses that the stepper motor drivers can understand. Since this project utilises a servo motor to push markers down, an adapted version of GRBL firmware was installed. This adapted version modifies the pulse width modulation (PWM) signals meant to control a spindle, to control a servo motor instead. However, this adapted version does not support 3-axis homing by default, which the project requires. Therefore, the homing sequence in the GRBL source code (written in C++) was modified to allow for homing of the z-axis (the revolving cylinder), using a limit switch.

As shown in Figure 5.5, the application shows the paths contained in an uploaded G-code file on a simulated drawing bed. The user can simulate the drawing job before executing it, read the G-code contained within the file, or apply offsets to move the drawing to a different position on the drawing bed. Machine controls are found at the top and right side of the interface, with buttons to home the machine, set the current position as zero, jog the machine in different directions and reset the controller if needed. A few custom buttons are also defined for this project. The “Pen Up” and “Pen Down” buttons send M3 S550 and M3 S0 PWM commands to retract and actuate the servo motor, respectively. The M3 S0 command moves the servo motor's rack to its lowest position, pushing the markers down. M3 S550 retracts the servo motor's rack to a safe position above the markers, as determined experimentally. For each of the colours in the drawing machine's palette, a custom button is defined to move the z-axis to the correct index for that colour.

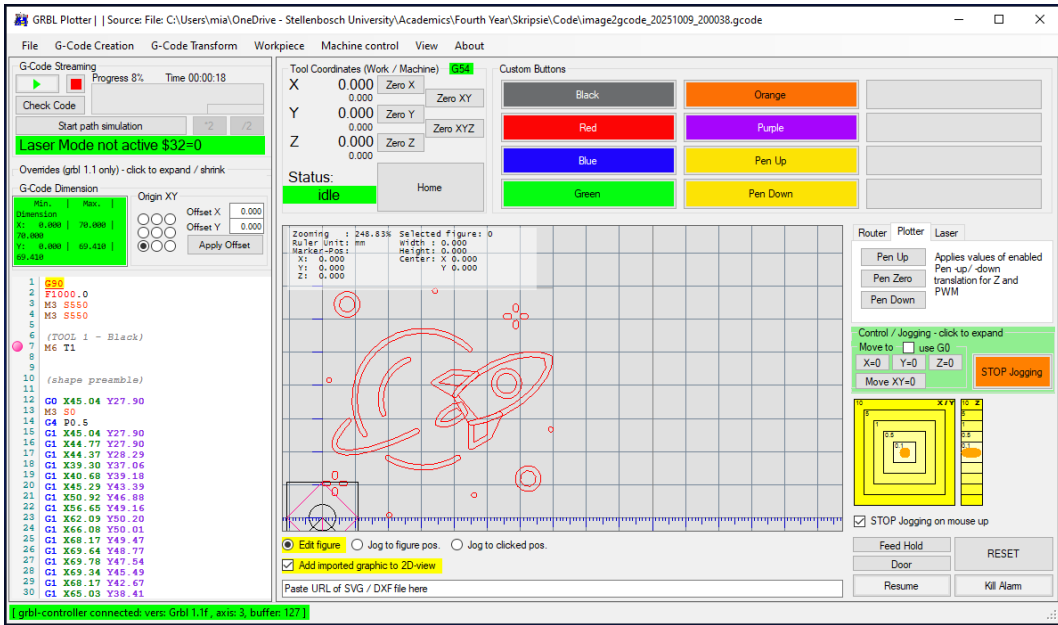


Figure 5.5: Screenshot of GRBL-Plotter user interface

GRBL-Plotter accommodates tool changes, making it ideal for this project. However, the application assumes that styluses are located in a repository next to the drawing bed and that the machine has to move to the repository, drop the current stylus in its slot, locate the next stylus, pick it up and move back to the drawing bed. Since this is not the case for this project, the scripts defining this tool change operation were modified. The provided tool table in GRBL-Plotter was populated with the six markers and their z-axis positions. A simple tool change command was then defined to replace the default operations, with reference to the positions defined in the tool table.

# Chapter 6

## Calibration, Testing and Validation

After the machine was assembled, its movement axes were calibrated and values for speed and acceleration were chosen. Thereafter, a series of tests were done to determine the machine's performance, accuracy, repeatability and precision. Calibration and testing procedures and the results thereof are described in this chapter, followed by a discussion of the machine's validation against the design requirements laid out in Section 3.1.

### 6.1 Calibration

The x- and y-axes of the machine were calibrated by calculating the steps/mm value for the stepper motors and belt setup. Since both the x- and y-axes use the same size belts (GT2) and pulleys (16 tooth), the same steps/mm value could be used for both. This value was calculated using the following equation adapted from Maker Store (2023):

$$\text{steps/mm} = \frac{\text{Steps} \times \text{Microsteps}}{\text{Belt pitch} \times \text{No. of pulley teeth}} \quad (6.1)$$

where *Steps* is the number of steps in one full revolution of the stepper motor (200 for a bipolar Nema 17), and *Beltpitch* is the distance between adjacent teeth on the belt (2 mm for a GT2 belt). Microstepping was set to 1/16 for all motors, making the *Microsteps* value 16. The calculated steps/mm value of 100 steps/mm was entered into the GRBL-Plotter machine setup. It was then confirmed by commanding the machine to move 10, 50 and 100 mm along both axes and measuring the actual distance travelled. Measurements were taken by marking the start and end position of the machine on the linear rails and measuring the distances between the marks with a caliper, as shown in Figure G.2 in Appendix G. These measurements were accurate to within 0.1 mm of the commanded distance, and so the calculated steps/mm value was left unchanged.

The revolving cylinder was calibrated by doing a similar calculation, but the denominator of the equation was replaced with  $360^\circ$ , which resulted in a value of 8.89 steps/ $^\circ$ . This value was entered into the GRBL-Plotter machine setup and confirmed visually by inspecting whether the next chamber in the revolving cylinder lined up with the position of the previous one when the z-axis was commanded to move  $60^\circ$ . The positions of the markers along the z-axis were calibrated by homing the machine and then moving the z-axis in increments of  $1^\circ$  until the first chamber was aligned with the hole in the bottom of the housing. This was confirmed by checking the perpendicularity of the chamber's centreline with the x-axis, using a protractor as shown in Figure G.3 in Appendix G. The z-axis value was then recorded as the position of marker 1 and incremented by  $60^\circ$  for each subsequent marker. Before a drawing operation is undertaken, the correct height for the stylus exchanger must be set manually. This is done by selecting any colour in the GRBL-Plotter software and actuating the servo motor to lower the marker. The stylus exchanger must then be lowered manually by twisting the height adjustment knob until the marker just makes contact with the drawing surface, as shown in Figure G.4 in Appendix G.

Values for maximum speed and acceleration were chosen experimentally by gradually increasing them from GRBL-Plotter's default conservative values until the machine started to miss steps or felt unsafe. For the x- and y-axis, the maximum speed was set to 2500 mm/min. Although the machine's drawing speed can be adjusted lower than that in the image conversion software, this value is used for rapid moves when the marker is lifted above the drawing surface. The x- and y-axes acceleration was set to 100 mm/s $^2$ . This is also the acceleration used for the z-axis, which was determined by gradually increasing the value until the revolving cylinder moved smoothly without visible stepping. The maximum speed for the z-axis was set to  $800^\circ/\text{min}$ , which was found to move the cylinder quickly and smoothly without causing the markers to rattle in their chambers.

## 6.2 Testing

Several tests were performed to determine the drawing machine's performance, accuracy, repeatability and precision. All tests, except for the functionality and software tests, were done on tracing paper taped to the drawing bed, as shown in Figure G.5 in Appendix G. Tracing paper was chosen as it does not allow markers to bleed into the paper and marker lines do not smudge easily. All physical tests were performed with the same set of brand new markers and measurements were taken with a Mitutoyo digital caliper with an accuracy of  $\pm 0.02\text{ mm}$  (RS Components, 2025a). The tests and their results are described in the following subsections.

### 6.2.1 Functionality Test

For this test, a complex multicolour image was drawn on multiple different surfaces to test the machine's ability to draw complex multicolour geometries and to compare its performance on different surfaces. The SVG image used was downloaded from IconPacks (2025) and its XML text was modified to change the colours of some of the shapes so that all six markers would be used. This modified SVG file was then converted to G-code and drawn on six different surfaces: a whiteboard sheet, an MDF board, a white paper sheet, a piece of cardboard, a scrap of cotton pillowcase fabric and a piece of felt. The machine was homed between each run and the height of the stylus exchanger was adjusted before each run to accommodate for the different surface thicknesses. All of the surfaces were taped down onto the drawing bed, with the fabrics stretched tight. The results of each of these runs are shown in Figure 6.1.

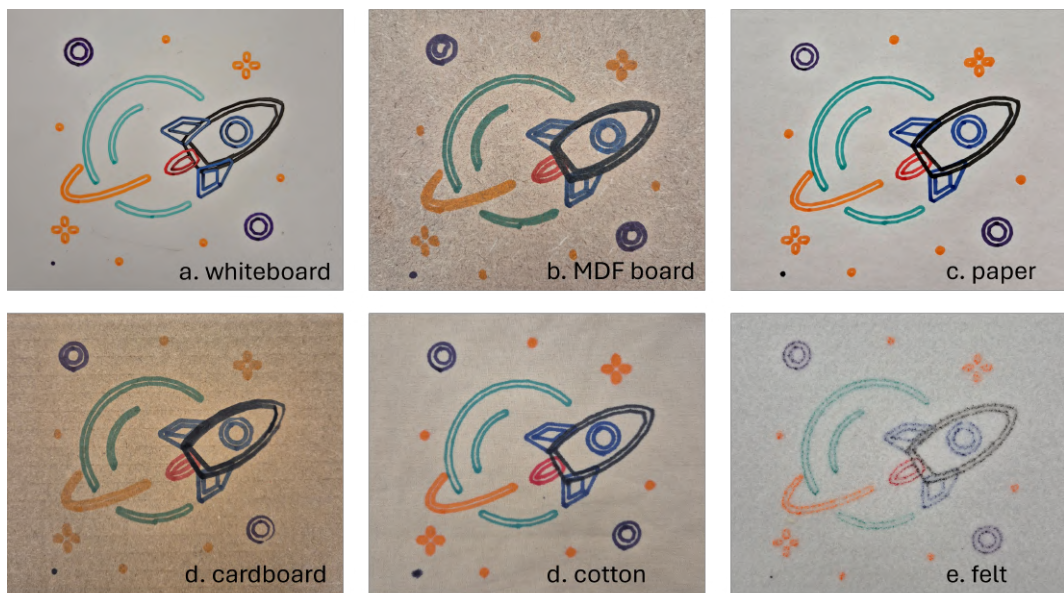


Figure 6.1: Results of functionality test on different surfaces: (a.) whiteboard, (b.) MDF board, (c.) white paper, (d.) cardboard, (e.) cotton fabric, (f.) felt fabric

The machine could successfully draw the image on all six surfaces, maintaining good line quality on most surfaces. Results appeared fairly similar for the whiteboard sheet, the paper sheet and the two fabrics. The MDF board showed thicker lines and some distortion of shapes, most likely due to the increased roughness of the surface. For the cardboard test, the markers bled into the surface, resulting in thicker lines and some loss of detail. Some lines toward the right side of the cardboard drawing were also much lighter. This is due to the cardboard being thinner towards its edges, resulting in the markers not making contact with its surface there. However, the machine demonstrated excellent performance and repeatability on the other surfaces, with no observable distortion of shapes or variation in line thickness.

### 6.2.2 Resolution Test

The average resolution (or line thickness) of the drawing machine was determined by drawing a test pattern onto tracing paper. This test pattern, shown in Figure 6.2, was created based on the instructions from Pasma (n.d.). It consists of seven lines drawn from one starting point at different angles so that the vertical distance between adjacent lines is 5 mm after 50 mm of horizontal travel. This means that the lines move 1 mm apart for every 10 mm of horizontal travel. Therefore, the horizontal distance from the starting point of each line to the point where adjacent lines become differentiable can be measured, and this value can be divided by 10 to obtain the average line thickness. As shown in Figure 6.2, the test pattern was drawn in three different colours (black, red and green) and the line thickness for each was determined. The average line thickness for all three colours was found to be 1.89 mm, with a maximum deviation of 0.091 mm between colours.

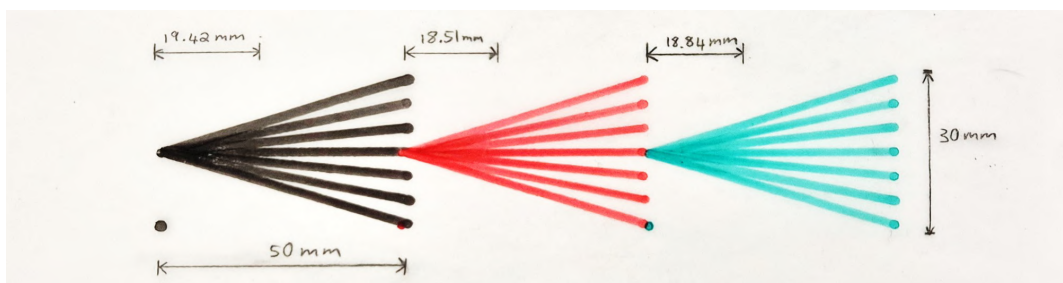


Figure 6.2: Resolution test results for three different colours

### 6.2.3 Repeatability Test

The drawing machine's repeatability and precision were tested by drawing the same black rectangle five times on the same sheet of tracing paper and measuring the dimensions of the rectangle after each run. Figure G.6 in Appendix G shows the rectangle after all five runs. Before each run, the machine was switched off and on again to reset its position, and homed. The rectangle was drawn close to the centre of the drawing bed and had dimensions of 40 mm by 20 mm. Both the inside and outside dimensions of the rectangle were measured after each run, and the deviation from the first run was calculated for each measurement. Figure 6.3 shows a plot of the absolute deviations for each measurement, with H and B denoting the outside heights and widths, and h and b denoting the inside heights and widths of the rectangle. As shown in the figure, deviations increased with each subsequent run, but remained small, with the maximum deviation being 0.1 mm. This indicates that the machine exhibits good repeatability and precision, performing well within the target precision of 0.5 mm.

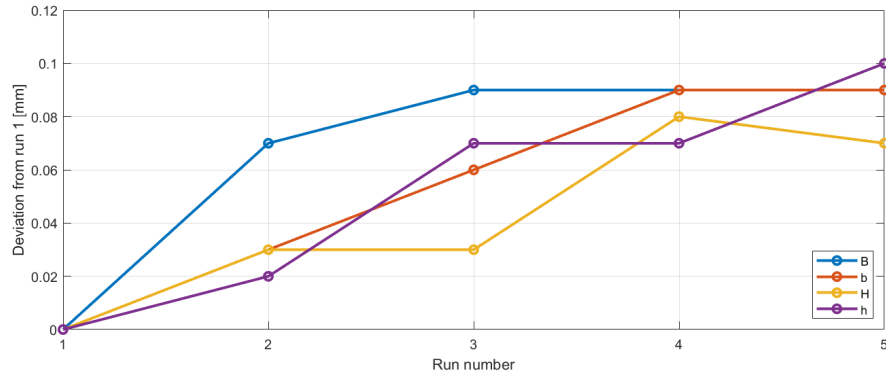


Figure 6.3: Repeatability test results showing absolute deviations from first run

#### 6.2.4 Accuracy Test

Accuracy for the movement system was tested by drawing a 320 by 200 mm grid with 40 by 40 mm squares on tracing paper and measuring the height and width of each square. The grid, created in Draw.io, was drawn in black and the measurements were taken on the inside of each square, as shown in Figure G.7 in Appendix G. With an assumed line thickness of 2 mm, the expected height and width of each square was 38 mm. The absolute deviation of each square's height and width from this expected value was calculated and plotted on the heatmaps shown in Figure 6.4, where colours range from white (0 mm deviation) to blue (maximum target deviation of 0.5 mm). Squares that exceeded the maximum target deviation are outlined in black.

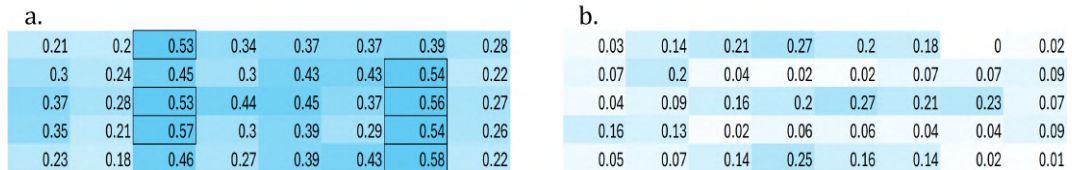


Figure 6.4: Heatmaps of deviations in (a.) width and (b.) height for each square in the accuracy test

As shown in the figure, all of the height measurements were well within the target deviation, with an average deviation of 0.109 mm and a maximum deviation of 0.27 mm. The width measurements deviated more, with an average deviation of 0.364 mm and a maximum deviation of 0.58 mm. Seven squares exceeded the target deviation, all of which were located in the third and seventh columns from the left. This may indicate that the marker's line thickness varied slightly, or that the x-axis belt tension is not perfectly uniform across the length of the axis. However, the machine demonstrated good overall accuracy, with its average deviations being well within the target accuracy of 0.5 mm.

### 6.2.5 ATC Precision Test

The precision of the ATC was tested by drawing four circles of diameter 40 mm, with each quadrant of each circle a different colour, and measuring the change in radius between quadrants. This was done to determine how precisely the ATC can position each marker relative to the others. The allocation of colours to quadrants was randomised to avoid repeating the same tool order, which could introduce bias in the alignment results. Figure 6.5 shows two of the circles drawn by the machine during this test. The other two circles are shown in Figure G.8 in Appendix G. Black vertical and horizontal lines were drawn that intersect at the center of each circle, providing reference lines to measure the radii along for each quadrant. Two measurements were taken along each reference line for each quadrant: one for each colour that meets at that line. The difference between these two measurements was calculated to determine the change in radius between quadrants.

For all four circles, the maximum change in radius was found to be 0.96 mm, with an average change in radius of 0.389 mm. However, all measured changes except three were below 0.45 mm. These three outliers (0.96 mm, 0.89 mm and 0.56 mm) were all found to be from colour changes involving the blue marker. On further inspection, it was observed that when the blue marker is in use, the servo motor's rack would hit the indexing screw for the z-axis limit switch, causing the revolving cylinder to rotate slightly and misalign the blue marker. This issue can be solved by using a shorter indexing screw or by attaching it to a lower point on the shaft coupling. However, even with these outliers, the ATC demonstrates good overall precision, with most of its tool changes being precise to within the 0.5 mm target.

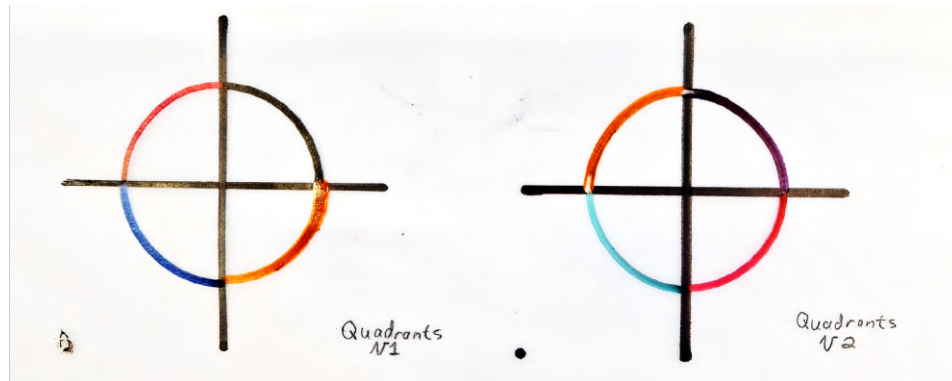


Figure 6.5: Two of the circles drawn during the ATC precision test

### 6.2.6 Software Test

To test the image conversion software's performance and optimisation, four different SVG images of varying complexity were converted to G-code. These images consisted of GRBL-Plotter's recommended test image (GRBL-Plotter,

2025), the grid image used in the accuracy test, the multicolour rocket image used in the functionality test, and an image of six identical, but differently coloured, squares arranged in a grid. The GRBL-Plotter test image and the six squares image are shown in Figures G.9 and G.10 in Appendix G, respectively. For each image, the time taken to convert the image to G-code and the RAM (random access memory) usage during the conversion process were recorded. These measurements are built into the image conversion software.

None of the images took more than a second to convert, with the most complex image (the rocket) only taking 0.112 seconds. The others took around 0.008 to 0.020 seconds. This indicates that the software is very efficient. The RAM usage for each image conversion operation was roughly the same, at around 101.4 to 104.9 MB. This is a tiny portion of modern computers' RAM capacities, indicating that the software could easily run on small computers or microcontrollers.

To verify the path optimisation of the image converter, each generated G-code file was compared to one generated by GRBL-Plotter's built-in image conversion tool. The same SVG images were uploaded to GRBL-Plotter, with the same size and feed rate settings as specified in the custom image converter. GRBL-Plotter shows the path length for G-code files uploaded to it, so it was used to determine the path lengths of both the custom and GRBL-Plotter generated G-code files. Table 6.1 shows the path lengths for each image as generated by the two different converters, along with the percentage difference between them. Positive percentage differences indicate that the custom software produced a shorter path length, while negative percentage differences indicate that GRBL-Plotter produced a shorter path length, and thus a more optimised path. As shown in the table, the custom image converter performed better for two of the images, while GRBL-Plotter performed better for the other two. However, the percentage differences were all relatively small, with the largest being 7.657%. This indicates that the performance of the path optimisation algorithm used in the custom image converter is comparable to GRBL-Plotter's built-in tool. It is worth noting that the custom image converter is more user-friendly and simpler to understand than GRBL-Plotter's tool, which contains many settings with unclear functions.

Table 6.1: G-code path lengths for each image

Image	Path Lengths [mm]		% Difference
	Custom software	GRBL-Plotter	
GRBL-Plotter test image	1337.959	1335.766	-0.164%
Grid	4397.384	4151.525	-5.922%
Multicolour rocket	4015.743	4348.723	7.657%
Six squares	1817.258	1830.391	0.717%

## 6.3 Validation

The drawing machine was validated against the design requirements identified in Section 3.1, which included stakeholder requirements, functional requirements and performance requirements. As confirmed by the functionality test, the machine can automatically draw complex multicolour images on a variety of surfaces, meeting SR3, SR5, SR6 and SR9. Its software can convert user-defined images into CNC instructions and includes a neat user interface, thus satisfying SR1, SR7 and SR8.

Many of the machine's functional requirements are met by its software and control system. The machine can process user instructions through its image conversion software and GRBL-Plotter (FR1), generate G-code from images (FR2), assign markers to image colours (FR4), change between markers automatically (FR5) and offers an easy-to-use interface (FR11). It draws images by moving a stylus over a drawing surface (FR3) and it can be adjusted to draw on different surfaces (FR10) by turning a height adjustment knob. While most of the machine's moving parts are not fully enclosed as required by FR7, its components are easy to access for maintenance, satisfying FR13.

The machine's performance requirements were validated through tests and measurements as described in this chapter and Chapter 4. These requirements are repeated in Table 6.2, along with the machine's actual quantitative performance for each requirement. As shown in the table, most of the performance requirements were met successfully. While the machine's overall length (PR1) does exceed the target range, its width (PR2), height (PR3) and weight (PR4) are all within specification. This means that the machine is compact and lightweight enough to be portable, satisfying SR2, FR8 and FR9. Unfortunately, the drawing area length (PR5) and width (PR6) are both below the target range to cover the full area of an A3 drawing sheet. However, the drawing bed is still large enough to place an A3 sheet of paper on it, thus satisfying SR4.

The total procurement cost (PR7) of the machine remained within budget, meeting SR12 and FR12. However, this cost was higher than expected and is discussed in detail in the techno-economic analysis in Appendix H. Thanks to its inexpensive components and open design, the machine will be easy and inexpensive to maintain, satisfying SR11. The machine's stylus exchanger can hold six different markers, which is perfectly on target for PR8. For PR9, compliance with the ISO 12100 Safety of Machinery standard (International Organization for Standardization, 2010) was considered. A risk assessment, as required by the standard, is included in Appendix J. Whilst all rotating and moving parts are not fully enclosed, the machine operates at low speeds and forces, reducing the risk of injury from operating it. Safeguards such as an emergency stop button, a power supply cover and insulated wiring were implemented, as suggested by the safety standard. Thus, the machine is considered to meet SR10.

Table 6.2: Validation of performance requirements

PR	Description	Performance	Target	Range	Unit
PR1	Overall machine length	600	480	430–500	mm
PR2	Overall machine width	400	400	330–450	mm
PR3	Overall machine height	238	130	40–350	mm
PR4	Machine weight	5.8	10	1–16	kg
PR5	Drawing area length	345	420	420–480	mm
PR6	Drawing area width	215	300	297–400	mm
PR7	Total procurement cost	4,110.98	3500	0–5000	R
PR8	Number of colours	6	6	2–10	colours
PR9	Compliance with safety standards	90	100	-	%
PR10	Adjustable drawing height	20	10	2–20	mm
PR11	Drawing precision	0.96	0.5	0.5–2	mm
PR12	Recyclable and reusable parts	82	80	60–90	%
PR13	Power consumption	9.72	15	2–50	W
PR14	Image processing time	0.11	60	0–300	s
PR15	Maximum RAM usage	0.105	2	0.01–4	GB

The machine's adjustable drawing height (PR10) is more than sufficient to accommodate different drawing surface thicknesses. For PR11, the machine's worst ATC precision was reported. This exceeds the target value, but still falls within the acceptable range. However, it is worth noting that most tool changes tested were precise to within 0.45 mm, and that the repeatability test revealed less than 0.1 mm deviation after five runs. Furthermore, the machine exhibited accuracies within 0.60 mm across its entire drawing area, as shown in the accuracy test results. Therefore, it successfully meets FR14.

Based on the amount of parts in the machine assembly, it was estimated that about 60% of it is reusable and about 44% is recyclable. With roughly 82% of parts falling into either category, the machine meets PR12, and subsequently FR6. As explained in the project's responsible use of resources and end-of-life strategy (Appendix I), the machine was designed to be easily disassembled so that parts may be reused, thus meeting SR13. The machine's maximum power consumption was determined by measuring the current drawn from the power supply during a drawing job. The measured 9.72 W falls well within the target range for PR13. Finally, the image conversion software's performance for PR14 and PR15 were confirmed during the software test, where both measurements were found to be far better than their target values.

# Chapter 7

## Conclusions

### 7.1 Objectives Achieved

This project aimed to design, build and test a multicolour CNC drawing machine. It was to be completed over the course of nine months, with an available procurement budget of R5,000.00. The main objectives included the formulation of requirements and specifications for the machine, which is outlined in Section 3.1. Thereafter, various concept designs were generated and evaluated for both the machine's movement system and its stylus exchanger, as described in Sections 3.3 to 3.5. Following the concept evaluation, a final design was selected and developed in detail, as discussed in Chapter 4. Suitable materials and components were sourced from local suppliers, and custom parts were 3D printed or manufactured in the MMW. The machine was then assembled in the Mechatronics Workshop by following an incremental approach, whereby subsystems were built and tested separately before being integrated into the system as a whole. During and after assembly, software was developed to convert SVG images into G-code files, and firmware was adapted to control the machine. This was detailed in Chapter 5. Finally, the completed system (hardware and software) was tested to determine its performance, accuracy, repeatability and precision, as described in Chapter 6. The machine's performance could be verified through the successful production of complex multicolour drawings. It was confirmed that all requirements, except FR7, PR1, PR5 and PR6, were met successfully, as explained in Section 6.3.

### 7.2 Recommendations for Future Work

Although the machine achieved an acceptable level of accuracy and repeatability, its ATC precision was negatively impacted by the setup of the z-axis homing switch. A better setup could have been devised to improve this, had the problem been identified earlier in the project timeline. The custom image converter software performed comparably well to existing tools, while being more user-friendly. However, it does not have the capability to add hatching

or fill patterns to solid shapes, which would be a useful feature to implement in future work. Since the image conversion software uses very little computer memory, the program can be shifted to a microcontroller with a user interface, instead of running on the user's computer. This would allow the machine to be freestanding, increasing its versatility. The developed ATC of the drawing machine (the revolver) is considered novel, as no similar systems were found during the literature review phase of the project. This design can be improved further to increase its accuracy and flexibility for use with different types of drawing styluses. There may also be potential to adapt this project's ATC concept for use in other CNC machines that require tool changes. As discussed in the techno-economic analysis (Appendix H), the machine has potential to be commercialised with further investment.

### 7.3 Closing Remarks

One of the main motivations behind this project was the development of a low-cost multicolour CNC drawing machine that could be used by artists, hobbyists, small businesses and educational institutions. With its total component cost of approximately R5,200.00, it succeeds in being more affordable than commercial alternatives, which do not offer automatic tool changes. The project's return on investment is therefore considered to be high, as it produced a functional machine with more capabilities than commercial options, at a fraction of the cost.

The project was completed on 22 October 2025 within the allocated timeline and budget. All objectives were met to a satisfactory level and the majority of the project requirements were achieved. The final drawing machine is capable of automatically producing complex multicolour images from user-defined SVG files, with an acceptable level of accuracy and repeatability. Therefore, the project is considered to be a success, not only in the prototype that it produced, but also in the skills and knowledge that were gained throughout its development.

# Appendix A

## Decision Rationale

### A.1 Performance Requirements

**PR1** The average forearm to forearm breadth of humans is 468.5 mm for females and 546.1 mm for males (Gordon *et al.*, 1988). Based on these numbers, a maximum length of 500 mm was chosen, as this would still allow women to carry the machine. The minimum length of 430 mm was chosen from the requirement that the machine must have an A3-sized drawing surface (length = 420 mm) and the assumption that the movement system components will take up at least 10 mm on the side.

**PR2** The average elbow to hand length of humans is 442.9 mm for females and 484.0 mm for males (Gordon *et al.*, 1988). Thus, a maximum machine width of 450 mm was chosen. This measurement is also limited by the size of an A3 (width = 297 mm) and so the minimum width was chosen as 330 mm to also allow at least 10 mm for components.

**PR3** The average elbow to shoulder length of humans is 335.8 mm for females and 369.0 mm for males (Gordon *et al.*, 1988). Therefore the machine height should not exceed 350 mm, for a person to still carry the machine comfortably and see where they are walking. The machine would be at least 40 mm tall, as that is the height of many small motors, such as Nema 17 stepper motors. A standard whiteboard marker measures about 130 mm in length. Thus, the target height was set to that, with the goal of not exceeding it by much.

**PR4** Female humans can safely lift and handle up to 16 kg in their arms, while males can handle up to 25 kg (Health and Safety Executive, 2020). Therefore the weight of the drawing machine is limited to 16 kg, but the target weight was set lower, to 10 kg.

**PR5** The drawing area must be at least 420 mm long to accommodate A3 drawing sheets. The maximum drawing area length (480 mm) is limited by the target set for the overall machine length. To limit overall machine length, the target for this requirement was set to its minimum.

**PR6** An A3 sheet is 297 mm wide, meaning the drawing area has to be at least that wide. The maximum drawing area width (400 mm) is limited by

the target set for the overall machine width. Here, the target is also set to its minimum, rounded to the nearest 10 mm.

**PR7** The project was allocated a total budget of R5,000.00 for consumables. Therefore, that is the maximum total cost. The target cost was set to R3,500.00, to allow R1,500.00 leeway in case of unexpected expenses.

**PR8** For the drawing machine to produce multicolour images, at least two colours that can be exchanged are required. More than ten colours is excessive, as this would exceed the amount of markers or pencils in a standard store-bought drawing pack. The target amount was set to six, since markers mainly come in packs of six. This would also allow the three primary colours (red, blue, yellow) and their three complementary colours (green, orange, purple) to be included.

**PR9** Safety is non-negotiable. The drawing machine is required to be 100% compliant with safety standards as set out in the ISO12100 Safety of Machinery Standard (International Organization for Standardization, 2010).

**PR10** For the drawing machine to draw on different surfaces with different thicknesses, the height of the stylus with which it draws must be adjustable. The minimum adjustable height was determined by the thickness of stainless steel and aluminium sheets, which typically have thicknesses of 2 mm and up. To accommodate for wooden boards, the target adjustable height was set to 10 mm, as this is a typical thickness for medium-density fibreboard (MDF). While some wooden boards can be as thick as 20 mm, it was not expected that anything more than that would be required.

**PR11** Drawing precision was estimated by measuring the line thickness of a streak made by a whiteboard marker. It measured 2 mm and thus determined the maximum precision value. Due to the effect that varying pressure on the stylus tip will have on line thickness, it was not expected that a precision of less than 0.5 mm could be achieved. Therefore, the target was set to that value.

**PR12** It would not be possible to manufacture the machine 100% from recyclable parts, since markers for instance, are not fully recyclable. It was decided that at least 60% of the machine's components should be recyclable. The target was set to 80% and it was decided that anything above 90% would be unrealistic.

**PR13** The UUNA TEK 3.0 consumes roughly 20 W while it draws (UUNA TEK CO., LIMITED, 2025a). For comparison, a desktop inkjet printer typically consumes 30 to 50 W when printing (energyusecalculator.com, n.d.). It was decided to aim for lower power consumption than the UUNA TEK machine and the target value was set to 15 W. The drawing machine should not exceed the power consumption of an inkjet printer, capping the maximum power consumption at 50 W.

**PR14** It was assumed that users would not want to wait for longer than 5 minutes for an image to be processed and converted to G-code. A target processing time of 1 minute was chosen, as this is a more or less reasonable time for a person to wait.

**PR15** The maximum random access memory (RAM) usage of the machine's software was limited to 4 GB at its absolute maximum, as some low-end computers only have that amount of RAM available (Intel Corporation, 2025). Therefore, the target maximum RAM usage was set to 2 GB to allow the software to run on low-end computers without taking up more than half of the available RAM.

## A.2 Quantitative Evaluation Scoring System

**Cost** For the movement system concepts, total cost below R1,000.00 was awarded a 3, between R1,000.00 and R2,000.00 a 2, and above R2,000.00 a 1. A similar approach was followed for the stylus exchanger concepts, with below R500.00 awarded a 3, between R500.00 and R1,000.00 a 2, and above R1,000.00 a 1.

**Scalability** Concepts that could easily be scaled up by simply acquiring longer components were awarded a 3, those that could be scaled up with some design changes a 2, and those that would require a different approach due to component limitations a 1.

**Weight** Concepts that were estimated to be portable by most users (below 8 kg) were awarded a 3, those that were estimated to be portable, but on the heavier side (between 8 kg and 12 kg) a 2, and those that were estimated to be difficult to carry for most users (above 12 kg) a 1.

**Maintenance requirements** For both the movement system and stylus exchanger concepts, those that required virtually no maintenance were awarded a 3, those that required occasional maintenance (such as lubrication) a 2, and those that required regular maintenance or the replacement of parts a 1.

**Safety** Concepts that are safe to touch while operating were awarded a 3, those that can cause minor injuries (such as finger pinching) a 2, and those that were not considered safe without additional safety measures a 1.

**Ease of manufacture** Concepts consisting primarily of off-the-shelf components or simple parts that only require one manufacturing process (such as 3D printing) were awarded a 3, those that require multiple manufacturing processes (such as 3D printing and machining) a 2, and those that require technical manufacturing processes (such as welding) a 1.

**Ease of assembly** For both the movement system and stylus exchanger concepts, those that could be assembled by only using a screwdriver or similar tools were awarded a 3, those that required more measurement and alignment a 2, and those that required specialised processes (such as press-fitting) a 1.

**Reusable parts** The potential of using 3D printing for custom parts was considered. Concepts that require no custom parts and can be fully assembled from off-the-shelf components were awarded a 3, those that require some simple custom parts that cannot be reused a 2, and those that require complex material-intensive custom parts a 1.

**Precision** Concepts estimated to achieve high precision (below 0.5 mm) were awarded a 3, those that were estimated to achieve moderate precision (between 0.5 mm and 1 mm) a 2, and those that were estimated to exhibit poor precision (above 1 mm), or had the potential for misalignment a 1.

**Stylus exchange speed** Concepts that were estimated to exchange styluses within 5 seconds were awarded a 3, those that would take between 5 and 20 seconds a 2, and those that would take longer than 20 seconds a 1. Note that these times are estimates and depend on the machine's movement speed.

**Programming complexity** Concepts that required minimal programming to exchange styluses (such as one or two single commands) were awarded a 3, those that require moderate programming (such as defining coordinates) a 2, and those that require more complex programming (such as defining a control sequence) or additional scripts a 1.

# Appendix B

## Sources for CAD Models

CAD models of off-the-shelf parts, such as motors, pulleys and electronic components were downloaded from GrabCAD and used in this project's CAD models. The artists of these models are credited below.

- Nema 17 stepper motor: Lawton (2025*b*)
- KFL08 pillow block bearing: Güzel (2016)
- LM8UU linear bearing: Zdelarec (2014)
- MGN12 Linear rails and carriages: Shuja (2018)
- GT2 toothed pulley: Jeroen (2025)
- Smooth pulley: Černý (2020)
- SG90 servo motor: Velykyi (2023)
- Nema 8 stepper motor: Dell'Oro (2022)
- LRS-100-12 power supply: Leonarduzzi (2016)
- Buck converter: Pamplin (2025)
- Arduino Uno with CNC shield: Pednekar (2021)
- MG90S servo motor: Pryimachenko (2024)
- Limit switch: Lawton (2025*a*)
- Micro limit switch: Zhurov (2023)
- Emergency stop button: Santos (2024)

# Appendix C

## Cost Estimation

Figure C.1 shows a screenshot from the Microsoft Excel sheet used to estimate the cost of each concept during concept evaluation. Quotes from various local suppliers were taken from the internet, and the prices listed were accurate as of July 2025. Multiple quotes were recorded for some parts, and the cheapest option was used in the cost estimation.

Component Description	Name at Supplier	Supplier	Quantity	Unit Cost	Cost	Link
480mm Linear Rail	MGN12 Linear Guide Rail with Carriage - 480mm	DIYElectronics	1 R	R 714.00	R 714.00	<a href="https://www.diyelectronics.c">https://www.diyelectronics.c</a>
300mm Linear Rail	MGN12 Linear Guide Rail with Carriage - 300mm	DIYElectronics	2 R	R 443.00	R 886.00	<a href="https://www.diyelectronics.c">https://www.diyelectronics.c</a>
GT2 6mm Toothed Idler Pulley	GT2 Idler Pulley(5mm Bore / 20 Teeth / 6mm Belt)	Netram Technologies	1 R	R 45.00	R 45.00	<a href="https://www.netram.co.za/be">https://www.netram.co.za/be</a>
GT2 6mm Smooth Idler Pulley	Idler Pulley (5mm Bore / Smooth / 6mm Belt )	Netram Technologies	2 R	R 45.00	R 90.00	<a href="https://www.netram.co.za/be">https://www.netram.co.za/be</a>
GT2 6mm Smooth Idler Pulley	Smooth Idler Pulley (5mm Bore / 6mm Belt)	DIYElectronics	2 R	R 31.00	R 62.00	<a href="https://www.diyelectronics.c">https://www.diyelectronics.c</a>
GT2 6mm Toothed Idler Pulley	Toothed Idler Pulley (5mm Bore, 20 Teeth / 6mm GT2 Belt )	DIYElectronics	1 R	R 33.00	R 33.00	<a href="https://www.diyelectronics.c">https://www.diyelectronics.c</a>
GT2 6mm Toothed Idler Pulley	GT2 Belt Idler Pulley, 20 Teeth, Bore 5mm, Width 6mm	Microrobotics	1 R	R 56.35	R 56.35	<a href="https://www.robotics.org.za/">https://www.robotics.org.za/</a>
GT2 6mm Smooth Idler Pulley	Smooth Idler Pulley , Bore 5mm, Width 7mm	Microrobotics	2 R	R 56.35	R 112.70	<a href="https://www.robotics.org.za/">https://www.robotics.org.za/</a>
GT2 6mm Smooth Idler Pulley	Idler Pulley GT2-6mm 20T 5mm Bore (smooth/no-teeth)	Next Dimension Electronics	2 R	R 31.00	R 62.00	<a href="https://nede3d.co.za/pulleys/">https://nede3d.co.za/pulleys/</a>
GT2 6mm Toothed Idler Pulley	Idler Pulley GT2-6mm 20teeth 5mm Bore	Next Dimension Electronics	1 R	R 31.00	R 31.00	<a href="https://nede3d.co.za/pulleys/">https://nede3d.co.za/pulleys/</a>
MDF Drawing Plate	500x600mm MDF Supawood 16 mm thick off-cut	Lumber King	1 R	R 105.00	R 105.00	
Nema 8 Motor	Stepper Motor 1.8 N.cm NEMA8 0.6A per Phase	Microrobotics	1 R	R 308.20	R 308.20	<a href="https://www.robotics.org.za/">https://www.robotics.org.za/</a>
4-5mm Shaft Coupling	Coupler Direct 5mm-4mm	Microrobotics	1 R	R 19.55	R 19.55	<a href="https://www.robotics.org.za/">https://www.robotics.org.za/</a>
4-5mm Shaft Coupling	4x5 D20 L25	Hobbytronics	1 R	R 65.90	R 65.90	<a href="https://www.hobbytronics.co">https://www.hobbytronics.co</a>
4-5mm Shaft Coupling	FLEXIBLE SHAFT COUPLING SH4-5mm 19x25	Mantech	1 R	R 38.51	R 38.51	<a href="https://www.mantech.co.za/">https://www.mantech.co.za/</a>
625 ball bearing	Radial Ball Bearing - 625RS - 5x16x5mm	DIYElectronics	1 R	R 10.00	R 10.00	<a href="https://www.diyelectronics.c">https://www.diyelectronics.c</a>
625 ball bearing	Bearing 5x16x5 Inner Diameter 5mm (4 Pack)	Microrobotics	1 R	R 25.30	R 25.30	<a href="https://www.robotics.org.za/">https://www.robotics.org.za/</a>
Kitronik Servo Kit	Kitronik Linear Actuator Kit	RS Components	1 R	R 179.32	R 179.32	<a href="https://za.rs-online.com/web">https://za.rs-online.com/web</a>
Kitronik Servo Kit	Kitronik (2595) Linear Actuator Kit, BBC micro:bit, 20mm Travel	Takealot	1 R	R 1,035.00	R 1,035.00	<a href="https://www.takealot.com/kit">https://www.takealot.com/kit</a>
Whiteboard Markers	Parrot Whiteboard Markers (6 Markers - Slimline Tip - Carded)	Takealot	1 R	R 69.00	R 69.00	<a href="https://www.takealot.com/pg">https://www.takealot.com/pg</a>
500 mm lead screw	TR8 Lead Screw 2mm Pitch - 500mm	Microrobotics	1 R	R 143.75	R 143.75	<a href="https://www.robotics.org.za/">https://www.robotics.org.za/</a>
300 mm lead screw	TR8 Lead Screw 2mm Pitch - 300mm	Microrobotics	1 R	R 102.35	R 102.35	<a href="https://www.robotics.org.za/">https://www.robotics.org.za/</a>
8mm pillow block bearing	KFL08 Flange Pillow Block	Netram Technologies	2 R	R 45.00	R 90.00	<a href="https://www.netram.co.za/be">https://www.netram.co.za/be</a>
Nema 17 Motor	Stepper Motor 0.28Nm 1.3A NEMA17	Microrobotics	2 R	R 193.20	R 386.40	<a href="https://www.robotics.org.za/">https://www.robotics.org.za/</a>
8mm guide rods	Linear Rod Rail 8mm Stainless Steel 500mm	Stelltron Electronics	4 R	R 59.98	R 239.92	<a href="https://stelltron.co.za/produc">https://stelltron.co.za/produc</a>
12mm guider rods	Linear Rail 12mm Stainless Steel Rod 1000mm	Stelltron Electronics	1 R	R 179.99	R 179.99	<a href="https://stelltron.co.za/produc">https://stelltron.co.za/produc</a>
12mm linear bearing	HKD LINEAR BALL BEARING 12MM	Communica	1 R	R 25.00	R 25.00	<a href="https://www.communica.co">https://www.communica.co</a>
Lead screw coupling	HKD SHAFT FLEXIBLE COUPLER 5X8MM	Communica	2 R	R 23.00	R 46.00	<a href="https://www.communica.co">https://www.communica.co</a>
Belt	GT2 Timing Belt, Open Ended - PU width 6mm	Microrobotics	1 R	R 36.80	R 36.80	<a href="https://www.robotics.org.za/">https://www.robotics.org.za/</a>
GT2 timing pulley	HKD GT2 TIMING PULLEY 20T 8MM	Communica	2 R	R 19.00	R 38.00	<a href="https://www.communica.co">https://www.communica.co</a>
Servo Motor	HKD MICRO SERVO 9G 4.8V-90D DIGT	Communica	1 R	R 70.00	R 70.00	<a href="https://www.communica.co">https://www.communica.co</a>
Foam Grip strips	Sellotape Foam Sealing Strip Black 5000 x 25 x 3 mm	Builders	1 R	R 72.00	R 72.00	<a href="https://www.builders.co.za/F">https://www.builders.co.za/F</a>
Perspex sheets	Duracryl Flat Perspex Sheet Clear 500 x 500 x 3 mm	Builders	1 R	R 229.00	R 229.00	<a href="https://www.builders.co.za/B">https://www.builders.co.za/B</a>

Figure C.1: Screenshot of the Microsoft Excel sheet used to estimate cost of concepts

# Appendix D

## Calculations

Design calculations done throughout the course of the project are included in this appendix. Unless otherwise indicated, all calculations are based on formulas and methods found in Shigley's Mechanical Engineering Design (Budynas and Nisbett, 2020). Calculations were done in an SMath Studio worksheet, with figures created using Draw.io. The full worksheet follows on the next few pages.

## Constants

### Masses

$m_{Nema17} := 230 \text{ g}$	(Microrobotics, 2025a)
$m_{Nema8} := 60 \text{ g}$	(Microrobotics, 2025b)
$m_{Servo} := 13.4 \text{ g}$	(Communica, 2025)
$m_{Yrail} := 258 \text{ g}$	(DIYElectronics, 2025a)
$m_{Xrail} := 376 \text{ g}$	(DIYElectronics, 2025b)
$m_{Pulley} := 6 \text{ g}$	(Microrobotics, 2025c)
$m_{Coupling} := 10 \text{ g}$	(Microrobotics, 2025d)
$m_{RevolverBearing} := 5 \text{ g}$	(Microrobotics, 2025e)
$m_{ScrewBearing} := 12 \text{ g}$	(RS Components, 2025)
$m_{Marker} := 12 \text{ g}$	(Incredible Connection, 2025)

$m_{Motormount} := 35 \text{ g}$	)	Weights calculated by Cura Slicer
$m_{Ysupport} := 10 \text{ g}$		
$m_{Toolmount} := 13 \text{ g}$		
$m_{Support} := 28 \text{ g}$		
$m_{Holster} := 107 \text{ g}$		

$m_{Revolver} := 69 \text{ g}$	)	Weights calculated by AutoCAD Inventor
$m_{GuideRod} := 24 \text{ g}$		
$m_{LeadScrew} := 25 \text{ g}$		
$m_{Motorrod} := 14 \text{ g}$		
$m_{BackingPlate} := 19 \text{ g}$		

$m_{Spring} := 3 \text{ g}$		
-----------------------------	--	--

### Moduli & Strengths

$E_{StainlessSteel} := 190 \text{ GPa}$	(Budynas and Nisbett, 2020)	$\sigma_{PLA} := 50 \text{ MPa}$	(Ranakoti et al., 2022)
$G_{StainlessSteel} := 69 \text{ GPa}$	(Budynas and Nisbett, 2020)	$E_{PLA} := 3.2 \text{ GPa}$	(Ranakoti et al., 2022)

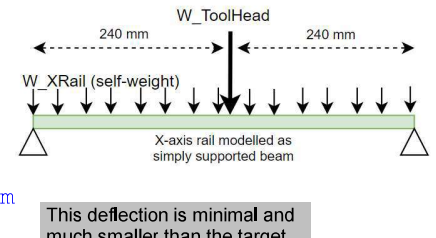
## Movement System

### Linear rail deflection, moments and loading

$$\begin{aligned} X_{rail\_length} &:= 480 \text{ mm} & Rail\_width &:= 12 \text{ mm} & w_{rail} &:= 0.65 \frac{\text{kg}}{\text{m}} \quad (\text{Hiwin Corporation, 2025}) \\ Y_{rail\_length} &:= 300 \text{ mm} & Rail\_height &:= 8 \text{ mm} & \\ I_{Rail} &:= \frac{1}{12} \cdot Rail\_width \cdot Rail\_height^3 = 5.12 \cdot 10^{-10} \text{ m}^4 & \\ m_{RevolverAssembly} &:= m_{Revolver} + m_{Holster} + m_{RevolverBearing} + 6 \cdot m_{Marker} + \dots + m_{Servo} + m_{Nema8} + m_{Coupling} + m_{Motorrod} + 6 \cdot m_{Spring} \\ m_{ToolHead} &:= m_{RevolverAssembly} + m_{LeadScrew} + 2 \cdot m_{GuideRod} + m_{BackingPlate} + \dots + m_{Toolmount} + m_{ScrewBearing} \end{aligned}$$

#### Deflection of x-axis rail

$$\begin{aligned} \delta_{X_{rail\_toolhead}} &:= \frac{(m_{ToolHead} g_e) \cdot X_{rail\_length}^3}{48 \cdot E_{StainlessSteel} \cdot I_{Rail}} = 0.0001 \text{ m} \\ \delta_{X_{rail\_selfweight}} &:= \frac{(5 \cdot w_{rail} g_e) \cdot X_{rail\_length}^4}{384 \cdot E_{StainlessSteel} \cdot I_{Rail}} = 4.5291 \cdot 10^{-5} \text{ m} \\ \delta_{X_{rail\_max}} &:= \delta_{X_{rail\_selfweight}} + \delta_{X_{rail\_toolhead}} = 0.0002 \text{ m} \end{aligned}$$



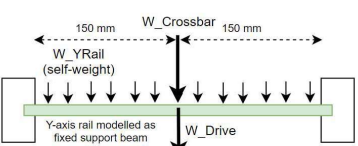
#### Deflection of driven y-axis rail

The non-driven y-axis rail is not analysed, as it experiences a much smaller loading.

$$\begin{aligned} m_{Crossbar} &:= m_{ToolHead} + m_{Xrail} = 0.8614 \text{ kg} \\ m_{Drive} &:= m_{Motormount} + 2 \cdot m_{Nema17} + 4 \cdot m_{Pulley} = 0.519 \text{ kg} \\ \delta_{Y_{rail\_selfweight}} &:= \frac{(w_{rail} g_e) \cdot X_{rail\_length}^4}{384 \cdot E_{StainlessSteel} \cdot I_{Rail}} = 9.0582 \cdot 10^{-6} \text{ m} \end{aligned}$$

$$\begin{aligned} \delta_{Y_{rail\_crossbar}} &:= \frac{(m_{Crossbar} g_e) \cdot 0.5 \cdot Y_{rail\_length}^3}{192 \cdot E_{StainlessSteel} \cdot I_{Rail}} = 6.1057 \cdot 10^{-6} \text{ m} \\ \delta_{Y_{rail\_drive}} &:= \frac{(m_{Drive} g_e) \cdot Y_{rail\_length}^3}{192 \cdot E_{StainlessSteel} \cdot I_{Rail}} = 7.3574 \cdot 10^{-6} \text{ m} \end{aligned}$$

$$\delta_{Y_{rail\_max}} := \delta_{Y_{rail\_crossbar}} + \delta_{Y_{rail\_drive}} + \delta_{Y_{rail\_selfweight}} = 2.2521 \cdot 10^{-5} \text{ m}$$

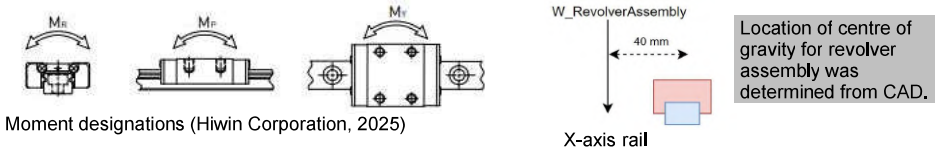


This deflection is minimal and much smaller than the target precision of 0.5 mm.

Moment on x-axis rail

$$Mr_{Xrail\_rated} := 38.22 \text{ N m}$$

(HiWIN Corporation, 2025)



$$Mr_{Xrail} := m_{RevolverAssembly} g_e \cdot 40 \text{ mm} = 0.1445 \text{ N m}$$

$$SF_{Xrail\_moments} := \frac{Mr_{Xrail\_rated}}{Mr_{Xrail}} = 264.4785$$

Therefore, the moment loading on the x-axis rail will not exceed the rated value.

Moment on y-axis rails

$$Mr_{Yrail\_rated} := 25.48 \text{ N m}$$

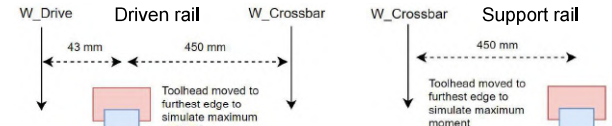
(HiWIN Corporation, 2025)

Locations of centre of gravity for drive plate and crossbar determined from CAD.

$$Mr_{Yrail\_driven} := (-m_{Drive}) g_e \cdot 43 \text{ mm} + m_{Crossbar} g_e \cdot 450 \text{ mm} = 3.5825 \text{ N m}$$

$$Mr_{Yrail\_support} := m_{Crossbar} g_e \cdot 450 \text{ mm} = 3.8014 \text{ N m}$$

$$SF_{Yrail\_moments} := \frac{Mr_{Yrail\_rated}}{Mr_{Yrail\_support}} = 6.7029$$



Therefore, the moment loading on the y-axis rail will not exceed the rated value.

**Motor Sizing**

Calculations in this section were done according to Collins (2019).

$$T_{Nema17} := 0.28 \text{ N m}$$

(Microrobotics, 2025a)

$$v_{max} := 4000 \frac{\text{mm}}{\text{s}}$$

$$a_{max} := 1000 \frac{\text{mm}}{\text{s}^2}$$

X-axis motor

$$r_{pulley} := \frac{D_{pulley}}{2} = 0.005 \text{ m}$$

$$Fa_{toolhead} := m_{ToolHead} g_e \cdot \mu_{rails} = 0.019 \text{ N}$$

$$Tc_{xmotor} := \frac{Fa_{toolhead} \cdot r_{pulley}}{\eta_{belt}} = 9.7146 \cdot 10^{-5} \text{ N m}$$

$\mu_{rails} := 0.004$  (Hiwin Corporation, 2025)

$$D_{pulley} := 10 \text{ mm}$$

$$\eta_{belt} := 0.98$$

(Budynas and Nisbett, 2020)

$$J_{Nema17} := 34 \frac{\text{g cm}^2}{\text{N m}^2}$$

(MotionKing, n.d.)

$$J_{Pulley} := 0.079 \frac{\text{kg mm}^2}{\text{N m}^2}$$

(CAD Model)

$$J_{rot\_x} := J_{Nema17} + 2 \cdot J_{Pulley} + J_{toolhead} = 1.5693 \cdot 10^{-5} \text{ kg m}^2$$

$$\alpha_{max} := \frac{a_{max}}{r_{pulley}} = 200 \cdot \frac{1}{2}$$

$$Tacc_{xmotor} := J_{rot\_x} \cdot \alpha_{max} + Tc_{xmotor} = 0.0032 \text{ N m}$$

Torque required during acceleration

$$SF_{xmotor\_torque} := \frac{T_{Nema17}}{Tacc_{xmotor}} = 86.5334$$

Motor is more than capable of moving x-axis load

Y-axis motor

$$m_{gantry} := m_{Crossbar} + m_{Drive} = 1.3804 \text{ kg}$$

$$Fa_{gantry} := m_{gantry} g_e \cdot \mu_{rails} = 0.0541 \text{ N}$$

$$Tc_{ymotor} := \frac{Fa_{gantry} \cdot r_{pulley}}{\eta_{belt}} = 0.0003 \text{ N m}$$

Torque required during constant velocity

$$J_{gantry} := m_{gantry} \cdot (r_{pulley})^2 = 3.451 \cdot 10^{-5} \text{ kg m}^2$$

$$J_{rot\_y} := J_{Nema17} + 3 \cdot J_{Pulley} + J_{gantry} = 3.8147 \cdot 10^{-5} \text{ kg m}^2$$

$$Tacc_{ymotor} := J_{rot\_y} \cdot \alpha_{max} + Tc_{ymotor} = 0.0079 \text{ N m}$$

Torque required during acceleration

$$SF_{ymotor\_torque} := \frac{T_{Nema17}}{Tacc_{ymotor}} = 35.4176$$

Motor is more than capable of moving y-axis load.

### 3D printed plate strength and deflection

$$t_{\text{plates}} := 7.5 \text{ mm}$$

$$l_{\text{motormountplate}} := 95 \text{ mm}$$

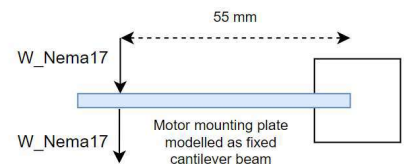
$$M_{\text{motormountplate}} := (m_{\text{Nema17}} \cdot 2 g_e) \cdot 55 \text{ mm} = 0.2481 \text{ N m}$$

$$I_y_{\text{motormountplate}} := \left( \frac{1}{12} \right) \cdot l_{\text{motormountplate}} \cdot t_{\text{plates}}^3 = 3.3398 \cdot 10^{-9} \text{ m}^4$$

$$\sigma_y_{\text{motormountplate}} := \frac{M_{\text{motormountplate}} \cdot t_{\text{plates}}}{I_y_{\text{motormountplate}} \cdot 2} = 2.7858 \cdot 10^5 \text{ Pa}$$

$$SF_{\text{motormountplate\_bending}} := \frac{\sigma_{\text{PLA}}}{\sigma_y_{\text{motormountplate}}} = 179.4832$$

$$\delta_{\text{motormountplate}} := \frac{(m_{\text{Nema17}} \cdot 2 g_e) \cdot 55 \text{ mm}}{3 \cdot E_{\text{PLA}} \cdot I_y_{\text{motormountplate}}} = 7.7383 \cdot 10^{-6} \text{ mm}$$



Therefore the plate will not bend.

The plate will experience very little deflection, much less than the targeted precision of 0.5 mm.

### Stylus Exchanger

#### Strength of 3D prints

##### Mount plate

$$l_{\text{mountplate}} := 60 \text{ mm}$$

$$b_{\text{mountplate}} := 40 \text{ mm}$$

$$t_{\text{mountplate}} := 5 \text{ mm}$$

$$F_{\text{RevMotors}} := (m_{\text{Nema8}} + m_{\text{Servo}} + m_{\text{Motorrod}} + m_{\text{Coupling}}) g_e = 0.9552 \text{ N}$$

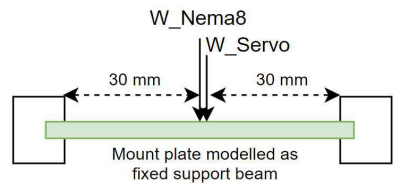
$$M_{\text{mountplate}} := \frac{F_{\text{RevMotors}} \cdot l_{\text{mountplate}}}{8} = 0.0072 \text{ N m}$$

$$I_{\text{mountplate}} := \left( \frac{1}{12} \right) \cdot b_{\text{mountplate}} \cdot t_{\text{mountplate}}^3 = 4.1667 \cdot 10^{-10} \text{ m}^4$$

$$\sigma_{\text{mountplate}} := \frac{M_{\text{mountplate}} \cdot t_{\text{mountplate}}}{I_{\text{mountplate}} \cdot 2} = 42982.547 \text{ Pa}$$

$$SF_{\text{mountplate\_bending}} := \frac{\sigma_{\text{PLA}}}{\sigma_{\text{mountplate}}} = 1163.2628$$

$$\delta_{\text{mountplate}} := \frac{F_{\text{RevMotors}} \cdot l_{\text{mountplate}}}{192 \cdot E_{\text{PLA}} \cdot I_{\text{mountplate}}}^3 = 8.0592 \cdot 10^{-7} \text{ m}$$



Therefore the plate will not bend.

The plate will experience very little deflection.

##### Housing bottom

$$l_{\text{housingbottom}} := 56 \text{ mm}$$

$$b_{\text{housingbottom}} := 20 \text{ mm}$$

$$t_{\text{housingbottom}} := 3 \text{ mm}$$

$$w_{\text{RevolverwithPens}} := (m_{\text{Revolver}} + 6 \cdot m_{\text{Marker}}) g_e = 1.3827 \text{ N}$$

$$F_{\text{RevolverPensBearing}} := w_{\text{RevolverwithPens}} + (m_{\text{RevolverBearing}}) g_e = 1.4318 \text{ N}$$

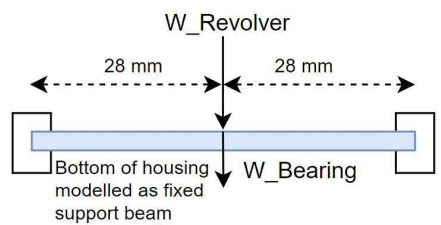
$$M_{\text{housingbottom}} := \frac{F_{\text{RevolverPensBearing}} \cdot l_{\text{housingbottom}}}{8} = 0.01 \text{ N m}$$

$$I_{\text{housingbottom}} := \left( \frac{1}{12} \right) \cdot b_{\text{housingbottom}} \cdot t_{\text{housingbottom}}^3 = 4.5 \cdot 10^{-11} \text{ m}^4$$

$$\sigma_{\text{housingbottom}} := \frac{M_{\text{housingbottom}} \cdot t_{\text{housingbottom}}}{I_{\text{housingbottom}} \cdot 2} = 3.3408 \cdot 10^5 \text{ Pa}$$

$$SF_{\text{housingbottom\_bending}} := \frac{\sigma_{\text{PLA}}}{\sigma_{\text{housingbottom}}} = 149.6648$$

$$\delta_{\text{housingbottom}} := \frac{F_{\text{RevolverPensBearing}} \cdot l_{\text{housingbottom}}}{192 \cdot E_{\text{PLA}} \cdot I_{\text{housingbottom}}}^3 = 9.0944 \cdot 10^{-6} \text{ m}$$



Therefore the housing bottom will not bend.

The housing bottom will experience very little deflection.

## Housing Overhang

$$l_{overhang} := 13.5 \text{ mm}$$

$$b_{overhang} := 50 \text{ mm}$$

$$t_{overhang} := 13.5 \text{ mm}$$

$$M_{overhang} := m_{RevolverAssembly} g_e \cdot l_{overhang} = 0.0488 \text{ N m}$$

$$I_{overhang} := \left( \frac{1}{12} \right) \cdot b_{overhang} \cdot t_{overhang}^3 = 1.0252 \cdot 10^{-8} \text{ m}^4$$

$$\sigma_{overhang} := \frac{M_{overhang} \cdot t_{overhang}}{I_{overhang} \cdot 2} = 32113.5099 \text{ Pa}$$

$$\tau_{overhang} := \frac{m_{RevolverAssembly} g_e}{b_{overhang} \cdot t_{overhang}} = 5352.2516 \text{ Pa}$$

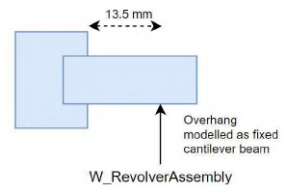
Shear stress is also calculated for the overhang.

$$\sigma_{overhang\_vonmises} := \sqrt{\sigma_{overhang}^2 + 3 \cdot \tau_{overhang}^2} = 33424.8008 \text{ Pa}$$

$$SF_{overhang\_strength} := \frac{\sigma_{PLA}}{\sigma_{overhang\_vonmises}} = 1495.8952 \quad \text{Therefore the overhang will not bend or shear.}$$

$$\delta_{overhang} := \frac{(m_{RevolverAssembly} g_e) \cdot l_{overhang}^3}{3 \cdot E_{PLA} \cdot I_{overhang}} = 9.0319 \cdot 10^{-8} \text{ m}$$

The deflection is minimal and will have negligible effect on the height adjustment.



## Springs

$$ID := 11 \text{ mm}$$

Max inner diameter from width of marker.

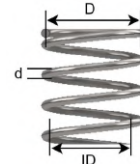
$$d := 0.7 \text{ mm}$$

Wire diameter from reference spring.

$$N := 11$$

Number of coils of reference spring.

$$D := ID + d = 11.7 \text{ mm}$$



$$k \approx \frac{d^4 G}{8D^3 N}$$

$$k := \frac{d^4 \cdot G_{StainlessSteel}}{8 \cdot D^3 \cdot N} = 0.1175 \frac{\text{N}}{\text{mm}}$$

Spring rate

$$\delta_{MarkerWeight} := \frac{(m_{Marker} g_e)}{k} = 1.0012 \text{ mm}$$

Distance spring will compress from marker's weight.

(Budynas and Nisbett, 2020)

## Motor sizing

### Servo motor

$$T_{servoRated} := 0.18 \text{ N m} \quad (\text{Communica, 2025})$$

$$r_{servoLever} := 11 \text{ mm} \quad \text{Distance from servo drive gear to centre of rack.}$$

$$F_{writingMax} := 2 \text{ N} \quad \text{Maximum force on drawing surface from marker.}$$

$$ymax := 12 \text{ mm} \quad \text{Distance to push markers down.}$$

$$F_{servoDownMax} := \frac{T_{servoRated}}{r_{servoLever}} = 16.3636 \text{ N}$$

$$F_{springPush} := k \cdot ymax = 1.4105 \text{ N}$$

$$F_{servoRequired} := F_{springPush} + F_{writingMax} = 3.4105 \text{ N}$$

$$SF_{servoPush} := \frac{F_{servoDownMax}}{F_{servoRequired}} = 4.798 \quad \text{Servo motor is strong enough to push markers down and resist drawing force.}$$

### Stepper motor

$$T_{nema8Rated} := 0.018 \text{ N m} \quad (\text{Microrobotics, 2025b})$$

$$r_{revolver} := 26.5 \text{ mm}$$

$$r_{markers} := 21 \text{ mm}^2 \quad \text{Radial distance to marker locations}$$

$$J_{nema8} := 4 \text{ g cm}^2 \quad (\text{Microrobotics, 2025b})$$

$$J_{coupler} := 0.248 \text{ kg mm}^2$$

$$J_{motorRod} := 0.076 \text{ kg mm}^2$$

$$J_{revolver} := \frac{1}{2} \cdot m_{Revolver} \cdot r_{revolver}^2 = 2.4228 \cdot 10^{-5} \text{ kg m}^2$$

$$J_{markers} := 6 \cdot m_{Marker} \cdot r_{markers}^2 = 3.1752 \cdot 10^{-5} \text{ kg m}^2$$

```

 $J_{nema8Total} := J_{coupler} + J_{markers} + J_{motorRod} + J_{nema8} + J_{revolver} = 5.6704 \cdot 10^{-5} \text{ kg m}^2$ 
time_toolchange := 0.5 s
θ_toolchange := 60 deg
α_revolver :=  $\frac{4 \cdot θ_{toolchange}}{time_{toolchange}^2} = 16.7552 \cdot \frac{1}{s^2}$ 
μ_PLA_in_bearing := 0.3 (Chisiu et al., 2021)
r_revolverBearing := 8 mm
m_weightOnBearing := m_Revolver + 6 · m_Marker + 6 · m_Spring = 0.159 kg
T_bearingFriction := m_weightOnBearing g_e · μ_PLA_in_bearing · r_revolverBearing = 0.0037 N m
T_nema8Required := J_nema8Total · α_revolver + T_bearingFriction = 0.0047 N m
SF_nema8_torque :=  $\frac{T_{nema8Rated}}{T_{nema8Required}} = 3.8361$  Nema 8 is strong enough to rotate revolver

```

---

## Electronics

### Current limits

#### Nema 17

$$I_{ratedNema17} := 1.3 \text{ A} \quad (\text{Microrobotics, 2025a})$$

$$V_{ref\_Nema17} := \frac{I_{ratedNema17}}{2} \cdot 1 \text{ ohm} = 0.65 \text{ V}$$

#### Nema 8

$$I_{ratedNema8} := 0.6 \text{ A} \quad (\text{Microrobotics, 2025b})$$

$$V_{ref\_Nema8} := \frac{I_{ratedNema8}}{2} \cdot 1 \text{ ohm} = 0.3 \text{ V}$$

The current limit is double the reference voltage, thus the reference voltages are set to half the rated currents of the motors (AZ-Delivery, n.d.).

### Power Supply

$$R_{Nema17} := 2.4 \text{ ohm} \quad (\text{MotionKing, n.d.})$$

$$R_{Nema8} := 5.6 \text{ ohm} \quad (\text{Microrobotics, 2025b})$$

$$I_{stallServo} := 0.75 \text{ A} \quad (\text{FDM 3D, n.d.})$$

$$V_{ratedServo} := 6 \text{ V} \quad (\text{Communica, 2025})$$

$$P_{ArduinoShield} := 2 \text{ W} \quad \text{Roughly 20% of motor's power for any losses or microcontroller overhead}$$

$$P_{Nema17} := R_{Nema17} \cdot I_{ratedNema17}^2 = 4.056 \text{ W}$$

$$P_{Nema8} := R_{Nema8} \cdot I_{ratedNema8}^2 = 2.016 \text{ W}$$

$$P_{servo} := V_{ratedServo} \cdot I_{stallServo} = 4.5 \text{ W}$$

$$P_{total} := 2 \cdot P_{Nema17} + P_{Nema8} + P_{servo} + P_{ArduinoShield} = 16.628 \text{ W}$$

$$I_{supply} := \frac{P_{total}}{12 \text{ V}} = 1.3857 \text{ A}$$

# Appendix E

## Estimation of Drawing Force

To estimate the normal force that the stylus exchanger experiences from a marker pressing and dragging on a surface, a simple test was performed. In this test, a sheet of white paper was taped to a CTS-30 portion scale and the scale was tared to zero. Then a marker was pressed down on the paper and dragged across it, while the weight reading on the scale was recorded. This was done at various force levels, from light pressure to heavy dragging. From the weight readings, the normal force was calculated by multiplying the weight reading (in kg) by the gravitational constant ( $9.81 \text{ m/s}^2$ ). The results of this test are shown in Table E.1.

Table E.1: Results of marker drawing force test

Description of pressure exerted	Weight (kg)	Normal force (N)
Light drag, barely visible line	0.007	0.069
Medium drag, visibly consistent line	0.020	0.196
Harder press, not dragging	0.060	0.589
Hard drag, thick dark line	0.100	0.981
Very hard press on paper	0.200	1.962

From the results in Table E.1, the maximum normal force that the stylus exchanger should be able to withstand whilst drawing was assumed to be 2 N. While it is unlikely that a user will draw with such a heavy force, this estimate provides a safety margin to ensure that additional force from increased friction of rougher surfaces or accidental hard presses will not damage the stylus exchanger.

# Appendix F

## Wiring Diagram

Figure F.1 below shows the wiring diagram of the CNC drawing machine. The diagram was created using Cirkit Designer.

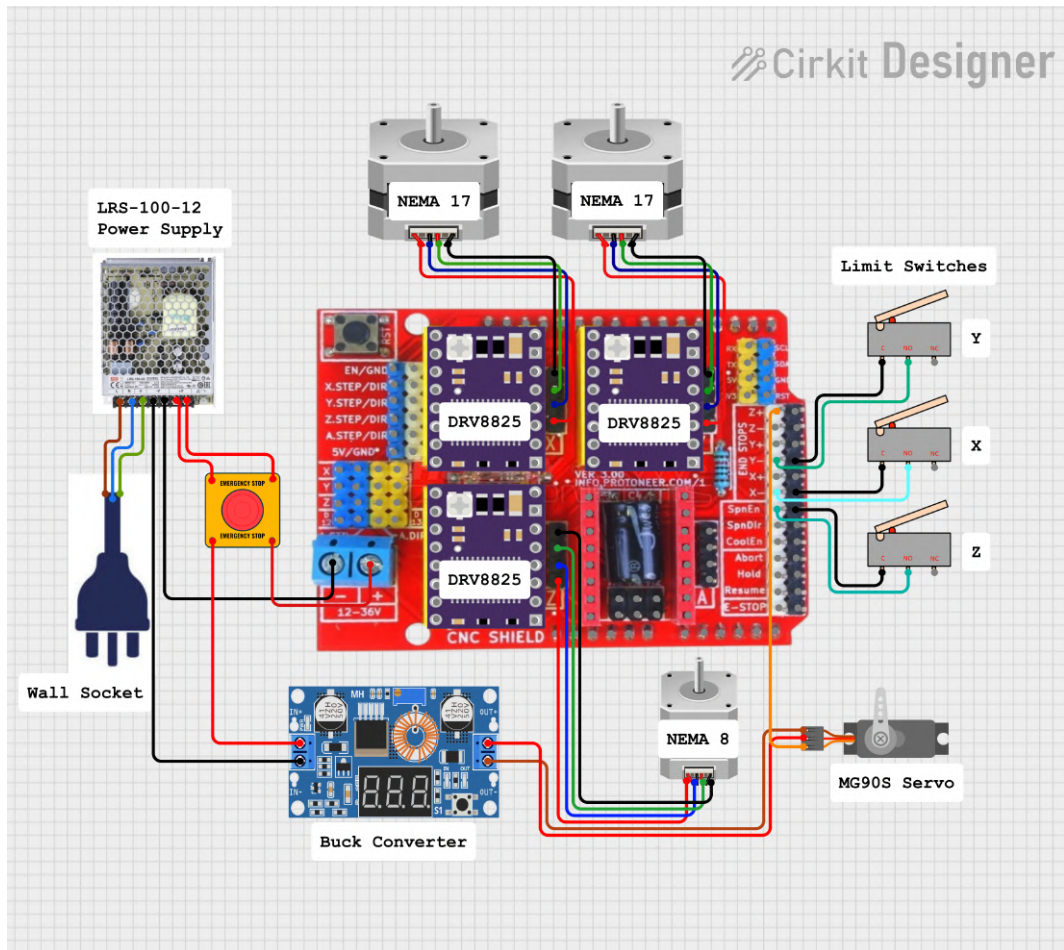


Figure F.1: Wiring diagram of the CNC drawing machine

# Appendix G

## Photographs

### G.1 Assembly and Calibration Photographs

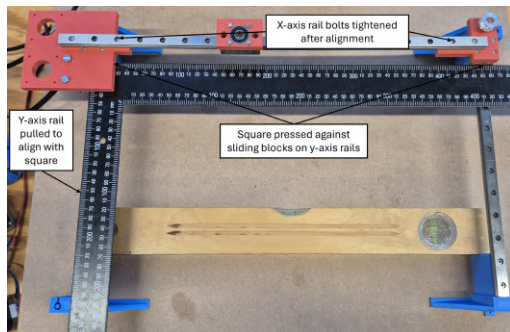


Figure G.1: Rail alignment using a square



Figure G.2: Calibration verification of x- and y-axes

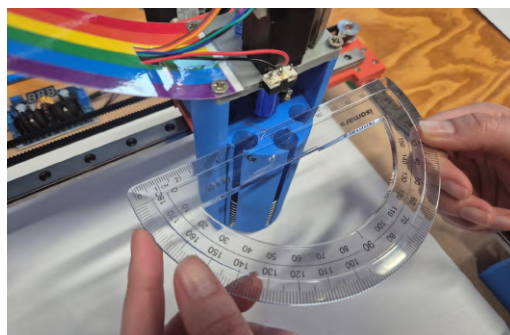


Figure G.3: Calibration of z-axis with protractor

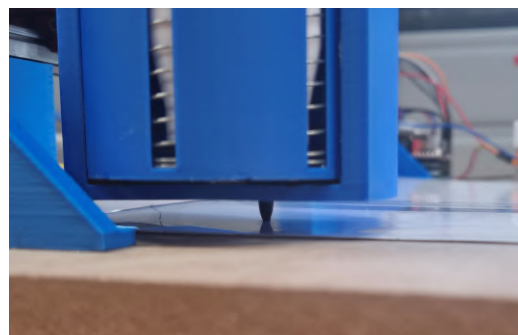


Figure G.4: Marker making contact with drawing surface

## G.2 Testing Photographs

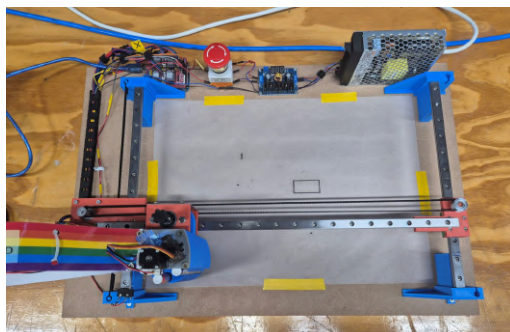


Figure G.5: Testing setup with tracing paper taped down

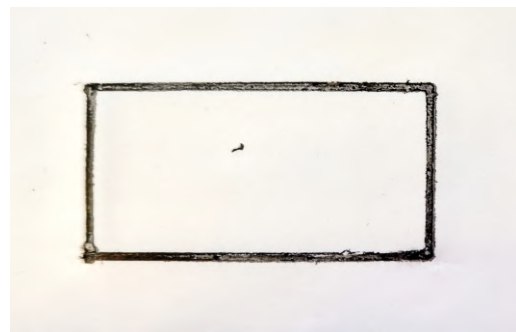


Figure G.6: Rectangle drawn in the repeatability test

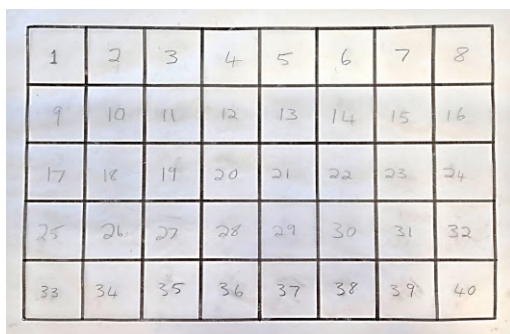


Figure G.7: Grid drawn in the accuracy test<sup>1</sup>

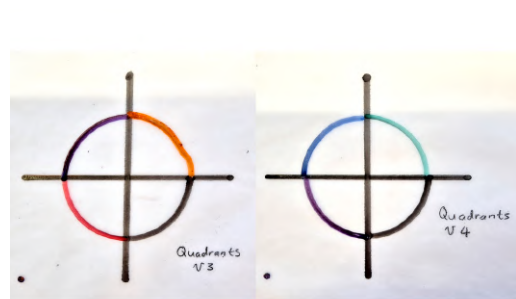


Figure G.8: Circles 3 and 4 drawn in the ATC accuracy test

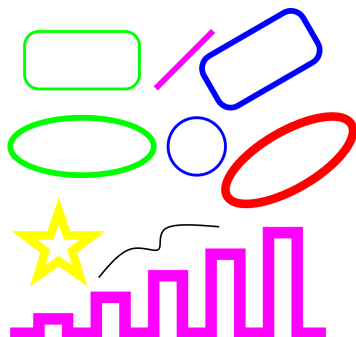


Figure G.9: GRBL-Plotter test image used in the software test

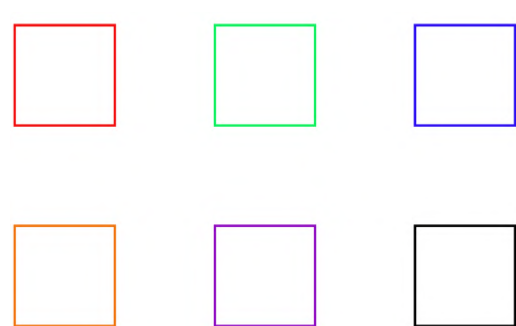


Figure G.10: Six squares image used in the software test

---

<sup>1</sup>Note: the tracing paper was not taped down for this photograph and shows wrinkles.

# Appendix H

## Techno-Economic Analysis

### H.1 Budget

The procurement budget for this project was R5,000.00. Originally, it was planned that R2,760.00 of that would be used to procure components and 3D print. Another R2,200.00 was allocated to buying a microcontroller, which counts as a capital cost. However, a working microcontroller could be salvaged from a previous project, eliminating that high cost. Other components, such as Nema 17 stepper motors, guide rods, belts and pulleys were also collected from previous projects, which further reduced the cost of components. The cost of all components used in the project is outlined in Figure H.1. Parts that were purchased are shaded in light grey.

Unfortunately, the cost of linear rails was much higher than anticipated. Due to their scarcity, these rails had to be ordered early in the project, before other components from the same supplier were decided on. This meant that shipping had to be paid for the second order. Another drawback was the cost of ordering two sets of springs from different suppliers (DIY Electronics and RS Components) before finding out that custom springs would be required. This was mainly because the spring constant of the springs from DIY Electronics was not known beforehand, and the RS Components springs were thinner than specified. The total cost of purchased components amounted to R4,110.98, which falls within the allocated budget of R5,000.00. This is largely thanks to the 3D printing of custom parts, as well as the amount of components that could be salvaged from previous projects. The total cost of all components used in the project was R5,515.60, indicating that about 25% of the component costs were saved by reusing parts.

The planned and actual budgets for the project are shown in Figures H.2 and H.3, respectively. As can be seen from the figures, MMW labour and material costs were significantly lower than planned. This is mainly due to the fact that most custom parts were 3D printed privately, and only large jobs were done at the MMW. Furthermore, MMW labour was only used for a 6-hour 3D print and one small manufacturing job, which took about half an hour. Run-

ning costs were higher than originally planned, mainly due to the high cost of linear rails. However, since there were no capital costs, procurement costs were lower than planned. Overall, the project went only R2,309.09 (1.08%) over budget due to more engineering time being required than originally anticipated. This is expanded on in the next section.

<b>Part</b>	<b>Supplier/Source</b>	<b>Unit cost</b>	<b>Quantity</b>	<b>Cost</b>
MGN12 linear rail - 300mm	DIY Electronics	R 443.00	2	R 886.00
MGN12 linear rail - 480mm	DIY Electronics	R 714.00	1	R 714.00
Drawing bed (MDF board)	Lumber King	R 105.00	1	R 105.00
Custom 3D prints	Private	R 300.00	0.286	R 85.80
Custom 3D prints	MMW	R -	0	R 194.80
Nema 17 motors	Previous project	R 193.20	2	R 386.40
Nema 8 motor	Microrobotics	R 308.20	1	R 308.20
MG90S servo motor	Previous project	R 59.00	1	R 59.00
Kironik linear actuator kit	RS Components	R 179.32	1	R 179.32
Custom springs	Gellini	R 25.00	10	R 250.00
Compression springs - 23 mm long	DIY Electronics	R 5.00	10	R 50.00
Compression springs - 54 mm long	RS Components	R 21.65	5	R 108.25
Whiteboard marker (6 pack)	PNA	R 44.99	1	R 44.99
Stainless steel plate	Previous project	R 38.00	1	R 38.00
Guide rod - 8mm thick, 300 mm long	Previous project	R 36.00	1	R 36.00
TR8-2 lead screw - 70 mm	Previous project	R 31.40	1	R 31.40
GT2 16-tooth pulley	Previous project	R 19.00	2	R 38.00
GT2 smooth idler pulley	DIY Electronics	R 31.00	2	R 62.00
GT2 toothed idler pulley	DIY Electronics	R 33.00	1	R 33.00
Motor coupling - 5x4 mm	Microrobotics	R 19.55	1	R 19.55
Square shaft	MMW	R 13.77	0.055	R 0.76
625ZZ bearings (4 pack)	Microrobotics	R 25.30	1	R 25.30
608-2RS bearings	RS Components	R 40.25	5	R 201.23
LRS-100-12 power supply	Microrobotics	R 342.70	1	R 342.70
Buck converter	Microrobotics	R 66.70	1	R 66.70
Limit switches	Microrobotics	R 13.80	3	R 41.40
Jumper wires (40 pack)	Microrobotics	R 79.35	1	R 79.35
Arduino Uno R3	Previous project	R 366.85	1	R 366.85
CNC shield v3	Previous project	R 43.00	1	R 43.00
DRV8825 stepper drivers	Previous project	R 43.70	3	R 131.10
Cable drag chain	Previous project	R 108.00	1	R 108.00
Fasteners	MMW	R 50.00	-	R 50.00
Magnetic whiteboard sheets (5 pack)	Takealot	R 350.00	1	R 350.00
Felt - 21x21 cm	PNA	R 6.99	1	R 6.99
Shipping	DIY Electronics	R 99.00	1	R 99.00
Shipping	RS Components	R 138.00	1	R 138.00
<b>Total procurement cost</b>				<b>R 4,110.98</b>
<b>Total project cost</b>				<b>R 5,680.08</b>

Figure H.1: Cost of all components used in project

Activity	Engineering Time		Running Costs	Facility Use	Capital Costs	MMW Labour		MMW Material	TOTAL
	hr	R	R	R	R	hr	R	R	R
1. Literature Review	35	15,750.00	400.00	0	-	0	-	-	16,150.00
2. Requirements and Specifications	10	4,500.00	-	0	-	0	-	-	4,500.00
3. Concept Design	30	13,500.00	-	0	-	0	-	-	13,500.00
4. Concept Evaluation and Final Design	45	20,250.00	-	0	-	0	-	-	20,250.00
5. Design Drawing	30	13,500.00	-	0	-	0	-	-	13,500.00
6. Component Selection and Procurement	20	9,000.00	1,800.00	0	2,200.00	0	-	-	13,000.00
7. Manufacture and Assembly	100	45,000.00	560.00	0	-	15	4,500.00	1,300.00	51,360.00
8. Software Development	55	24,750.00	-	0	-	0	-	-	24,750.00
9. User Interface Design	30	13,500.00	-	0	-	0	-	-	13,500.00
10. Testing and Verification	45	20,250.00	-	0	-	0	-	-	20,250.00
11. Report Consolidation	50	22,500.00	-	0	-	0	-	-	22,500.00
TOTAL	450	202,500.00	2,760.00	0	2,200.00	15	4,500.00	1,300.00	213,260.00

Figure H.2: Planned budget of project

Activity	Engineering Time		Running Costs	Facility Use	Capital Costs	MMW Labour		MMW Material	TOTAL
	hr	R	R	R	R	hr	R	R	R
1. Literature Review	20	9,000.00	-	0	-	0	-	-	9,000.00
2. Requirements and Specifications	10	4,500.00	-	0	-	0	-	-	4,500.00
3. Concept Design	45	20,250.00	-	0	-	0	-	-	20,250.00
4. Concept Evaluation and Final Design	35	15,750.00	-	0	-	0	-	-	15,750.00
5. Design Drawing	30	13,500.00	-	0	-	0	-	-	13,500.00
6. Component Selection and Procurement	7	3,150.00	4,110.98	0	-	0	-	-	7,260.98
7. Manufacture and Assembly	71	31,950.00	-	0	-	7	2,100.00	108.11	34,158.11
8. Software Development	45	20,250.00	-	0	-	0	-	-	20,250.00
9. User Interface Design	10	4,500.00	-	0	-	0	-	-	4,500.00
10. Testing and Verification	32	14,400.00	-	0	-	0	-	-	14,400.00
11. Report Consolidation	160	72,000.00	-	0	-	0	-	-	72,000.00
TOTAL	465	209,250.00	4,110.98	0	-	7	2,100.00	108.11	215,569.09

Figure H.3: Actual budget of project

## H.2 Planning

The planned and actual work hours for the project are shown in the project budgets on the previous page. Engineering time is valued at R450.00 per hour, and MMW labour is valued at R300.00 per hour. Project activities for the first half of the project were mostly consistent with the planned hours, except for concept design, which involved some redesign to cut material waste. For the second half of the project, most activities took less engineering time than planned, leading to lower overall engineering costs. However, this is offset by the fact that report consolidation took more than triple the amount of hours planned for it. This could be explained by the author's unfamiliarity with LaTeX, as well as the fact that other activities were inadvertently done while writing the report. Most other project activities were also completed three weeks before the project deadline, allowing ample time to perfect the report. Since the report accounts for the majority of the project's assessment, this was a worthwhile trade-off.

The project's planned and actual progression throughout the year is shown in the Gantt chart in Figure H.4. Grey bars indicate the planned schedule and duration of activities, while blue bars indicate their actual completion. Activities started in the first semester (literature review, requirements and specifications, and concept design) were stalled during the second term due to high workload. However, the project's pace picked up significantly in the third and fourth terms, with most activities completed in September and October. Although assembly started later than planned due to some redesigns and difficulties with sourcing springs, the mid-semester break was used effectively to get back on track. Software development and testing were completed in less time than planned, which allowed ample time for report consolidation. The report was also updated throughout project execution, which meant that very little work was still required on it after testing was completed.

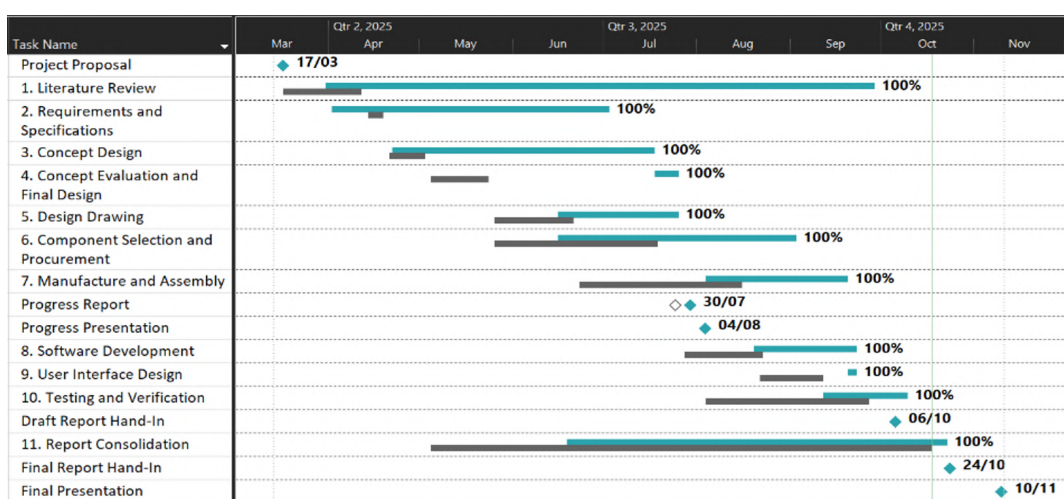


Figure H.4: Gantt chart of project planning

### H.3 Technical Impact

The technical impact of this project is significant, since it involved the design and development of a drawing machine capable of producing multicolour images automatically. This is a novel feature, as commercial drawing machines and pen plotters typically only support drawing with one colour at a time. The designed and implemented ATC system is different from existing systems, as it uses a revolving cylinder on the toolhead itself to exchange styluses. This can be adapted to other CNC applications, such as milling machines and 3D printers, to allow for quick tool changes without manual intervention. The precision of the machine is also noteworthy, especially considering its low cost in comparison to commercial alternatives, proving that high precision drawing machines can be built on a budget. Most importantly, a multicolour SVG to G-code converter was developed, which can be used with other multicolour drawing machines or pen plotters. The optimization approach followed in the converter can be very useful for any other CNC application where path length and minimising machine travel time is important.

### H.4 Return on Investment

With an investment of R215,569.09, this project produced a fully functioning prototype of a multicolour CNC drawing machine. In the short term, the machine will provide educational and marketing value to Stellenbosch University, as it can be displayed at the university's Open Day and its documentation can aid future students in their projects. The long-term return on investment of this project is its potential role as a stepping stone for future research and development in the field of low-cost desktop CNC machines. Since the machine was built using locally sourced components, it can be replicated and commercialised, generating profit not only for the future manufacturer, but also for the users of the machine. This is expanded on in the next section.

Further investment in the project would be focused on expanding the image converter software to produce fill patterns for solid shapes, as the software is currently only capable of tracing outlines. This would significantly increase the machine's usefulness and can be accomplished with an additional investment of about R22,500.00 for 50 hours of software development. A better homing mechanism for the z-axis could also be implemented with additional investment, such as an inductive or optical sensor. This would cost roughly R50.00 and an additional 5 hours of engineering time (R2,250.00). Finally, the machine's electronics can be enclosed in a custom 3D printed case to improve its aesthetics and protect the components. This would take about 10 hours of engineering time (R4,500.00) to design and cost about R100.00 to print.

## H.5 Potential for Commercialisation

This project has commercialisation potential, as it is a low-cost drawing machine that can be used for educational purposes, art, hobbyist projects and even small textile business applications. Drawing machines and pen plotters are commercially available, indicating that there is a market for this kind of product. This machine's ability to draw in multiple colours without manual intervention sets it apart from current commercial offerings. Its use of standard off-the-shelf components make it reproducible, scalable and repairable. Since it is constructed from roughly R5,200.00 worth of components, it can be sold at R10,000.00 to R15,000.00 (90% to 180% profit) and still be considered affordable compared to other commercial alternatives. Not only that, but small businesses can use the machine to make artwork or designs on textiles, wood, or other materials to sell at a profit. With further investment into the software and aesthetics, the machine can be sold as a complete package to hobbyists and small businesses, generating profit for both the manufacturer and the users.

# Appendix I

## Responsible Use of Resources and End-Of-Life Strategy

Due to the impending environmental crisis that the world is currently facing, innovation projects must consider using resources responsibly and plan for disposal of possible pollutants. Throughout the course of this project, as much as possible was done to minimise its environmental impact.

During the design phase, special attention was paid to opportunities for reusing components from older projects. For example, stepper motors, microcontrollers, belts, pulleys, lead screws and guide rods were salvaged from a previous project. Where it was possible, adjustments to the machine design were made to accommodate repurposed components without compromising on machine functionality.

In the manufacture and assembly phases, care was taken to not make use of permanent fasteners, such as glues. With the exception of 3D printing, minimal manufacturing of custom parts was required for this project, meaning the project's energy footprint is fairly low. The assembly process did not require energy-intensive machining and relied mostly on hand tools. During its operation, the machine consumes only about 10 W of power, which is very low compared to other household appliances.

The machine was designed in such a way that it can be disassembled with only a screwdriver at the end of its life cycle. This was done so that parts can be reused or recycled. All parts of the machine, except for insulation tape and 3D prints are reusable. The 3D printed parts were manufactured from PLA, a recyclable plastic. These parts will be taken to Stellenbosch Municipality's recycling plant at the end of the machine's life cycle.

Since the machine will remain within the Mechanical and Mechatronic Engineering department, its components can be reused for future final year projects, just as parts from previous projects were reused for this one. Care was taken not to cut motor cables shorter, so that future students can use them. The linear rails, lead screw, guide rods, pulleys and bearings can easily be reused in future mechanical designs, as they were not modified in any way.

# Appendix J

## Risk Assessment

The CNC drawing machine was assembled and tested in the Mechatronics Workshop at Stellenbosch University. A full risk assessment was conducted to identify potential hazards associated with the assembly and operation of the machine, as well as mitigating steps to ensure safety. The assembly procedure is briefly outlined below, followed by a table of the most significant risks identified in the assessment, taken from the submitted safety report for the Mechatronics Workshop.

### J.1 Assembly Procedure

The following steps were taken during the assembly of the CNC drawing machine:

1. **Preparation:** Gather all necessary tools and components. Ensure the workspace is clean and organised.
2. **Movement system assembly:** Assemble the linear rails, 3D printed parts, stepper motors and pulleys with screws and bolts. Tension belts and hook them into their clamps. Fasten assembly to drawing bed by drilling holes in the board and securing the assembly with screws.
3. **Stylus exchanger assembly:** Fit the motors and 3D printed parts and secure them with screws. Build the lead screw mechanism by fitting the bearings and guide rods into their respective slots in the 3D printed parts.
4. **Wiring:** Wire all motors and limit switches to the CNC shield, ensuring proper connections while avoiding solder burns or cuts from wire stripping. Use velcro straps to manage cables and prevent entanglement. Ensure the power supply is turned off during wiring.
5. **Tidy up:** Sweep up any debris from drilling and assembly. Ensure all tools and fasteners are accounted for and stored properly.

## J.2 Activity Based Risk Assessment

Activity	Risk	Risk Type* (P/E)	Classification of Risk Severity	Mitigating Steps
Physical Assembly				
Using drill	Eye injury from flying debris	P	Possible	Always wear safety glasses
	Hearing damage from prolonged use	P	Acceptable	Wear hearing protection when operating drill
	Dust inhalation	P	Possible	Wear mask when drilling into material that can generate dust (eg MDF). Ensure proper ventilation
	Entanglement with rotating drill/workpiece	P	Possible	Clamp part securely and never hold workpiece with hands. Keep loose clothing, jewellery and hair away
	Cutting hands on burrs and drill bits	P	Possible	Handle drill bits with care. File down rough burrs.
	Slipping of drill	P/E	Possible	Use centre punch to mark holes. Slowly and carefully start holes
Using craft knife	Cutting fingers	P	Possible	Cut away from body and do not cut close to hands
Electrical Wiring				
Cutting wires	Cutting fingers	P	Possible	Ensure wires are held securely in one hand while cutting with other hand, away from body
	Cutting other components	E	Acceptable	Remove any obstructing components before cutting wires
Soldering	Burning skin	P	Possible	Always assume soldering iron is hot. Only pick up soldering iron by its handle
	Causing a fire	P/E	Possible	Never leave soldering iron unattended and keep hot end away from flammable materials
	Creating short circuits, leading to shocks or fires	P/E	Possible	Ensure devices are switched off before soldering connections to them. Follow wiring diagram
Working with power supply	Electrical shock from touching wires	P/E	Possible	Ensure all live connections are properly insulated and well soldered. Do not touch exposed wires
	Short circuiting devices	E	Acceptable	Label wires clearly and follow wiring diagram
Testing				
Powering motors	Jamming fingers due to unexpected movement	P	Possible	Keep body parts clear of machine when actuators are powered. Enclose rotating parts. Include emergency stop.
	Motors getting stuck	E	Acceptable	Include emergency stop. Define limits of system with limit switches

\*P – personal, E - equipment

# List of References

- Abraham, J. (2023). Cnc tool changer guide: Benefits and cost. Accessed: 2025-07-26.  
Available at: <https://mellowpine.com/cnc-tool-changer>
- Aciu, R.-M. and Ciocarlie, H. (2014). G-code optimization algorithm and its application on printed circuit board drilling. In: *2014 IEEE 9th IEEE International Symposium on Applied Computational Intelligence and Informatics (SACI)*, pp. 43–47.
- arcadeperfect (2020). svg2gcode\_grbl: Svg to gcode converter for grbl pen plotter. Accessed: 2025-09-17.  
Available at: [https://github.com/arcadeperfect/svg2gcode\\_grbl](https://github.com/arcadeperfect/svg2gcode_grbl)
- Awati, R. (2024). Definition - g-code. Accessed: 2025-07-28.  
Available at: <https://www.techtarget.com/whatis/definition/G-code>
- AZ-Delivery (nd). Cnc shield v3 bundle. Tech. Rep., AZ-Delivery.
- Bantam Tools (2025a). Bantam tools nextdrawtm. Accessed: 2025-06-23.  
Available at: <https://bantamtools.com/collections/bantam-tools-nextdraw>
- Bantam Tools (2025b). Bantam tools nextdraw™ 1117. Accessed: 2025-06-23.  
Available at: <https://bantamtools.com/products/bantam-tools-nextdraw-1117>
- Barrington, H., McCabe, T.J.D., Donnachie, K., Fyfe, C., McFall, A., Gladkikh, M., McGuire, J., Yan, C. and Reid, M. (2024 10). Parallel and high throughput reaction monitoring with computer vision. *Angewandte Chemie International Edition*, vol. 64, p. e202413395.
- Budynas, R.G. and Nisbett, J.K. (2020). *Shigley's Mechanical Engineering Design*. 11th edn. McGraw-Hill Education, New York, NY. ISBN 978-0-07-339821-1.
- Businessresearchinsights.com (2025). Desktop cnc machines market size, growth | forecast 2033. Accessed: 2025-06-23.  
Available at: <https://www.businessresearchinsights.com/market-reports/desktop-cnc-machines-market-102832>
- Chisiu, G., Stoica, N.-A. and Stoica, A.-M. (2021). Friction behavior of 3d-printed polymeric materials used in sliding systems. *Materiale Plastice*, vol. 58, pp. 176–185.

- Choi, H.-J. and Lee, H.-G. (2020). A study on the design of drum type automatic tool changer. *Journal of the Korean Society of Manufacturing Process Engineers*, vol. 19, pp. 52–59.
- Collins, D. (2019). How to calculate motor drive torque for belt and pulley systems. Accessed: 2025-07-25.  
 Available at: <https://www.linearmotiontips.com/how-to-calculate-motor-drive-torque-for-belt-and-pulley-systems/>
- Communica (2025). Cmu micro servo 4.8v-6v mg90-360. Accessed: 2025-09-25.  
 Available at: <https://www.communica.co.za/collections/robotics/products/cmu-micro-servo-4-8v-6v-mg90-360>
- Darji, P. and Shil, S. (2017). Design, development and testing of 4 tool automatic tool changer. *International Journal of Engineering Sciences and Research Technology*, vol. 6, pp. 536–542.
- Das, U.C., Shaik, N.B., Suanpang, P., Nath, R.C., Mantrala, K.M., Benjapolakul, W., Gupta, M., Somthawinpongsai, C. and Nanthaamornphong, A. (2024). Development of automatic cnc machine with versatile applications in art, design, and engineering. *Array*, vol. 24, p. 100369.
- Dejan (2021). Diy pen plotter with automatic tool changer | cnc drawing machine. Accessed: 2025-06-15.  
 Available at: <https://howtomechatronics.com/projects/diy-pen-plotter-with-automatic-tool-changer-cnc-drawing-machine/>
- Dell’Oro, R. (2022). Nema 8 stepper motor. Accessed: 2025-06-15.  
 Available at: <https://grabcad.com/library/nema-8-stepper-motor-4>
- DIYElectronics (2025a). Mgn12 linear guide rail with carriage - 300mm. Accessed: 2025-09-25.  
 Available at: <https://www.diyelectronics.co.za/store/leadscrew-ballscrew/1643-mgn12-linear-guide-rail-with-carriage-300mm.html>
- DIYElectronics (2025b). Mgn12 linear guide rail with carriage - 480mm. Accessed: 2025-09-25.  
 Available at: <https://www.diyelectronics.co.za/store/spares/1931-mgn12-linear-guide-rail-with-carriage-480mm.html>
- energyusecalculator.com (nd). Electricity usage of a printer. Accessed: 2025-07-02.  
 Available at: [https://energyusecalculator.com/electricity\\_printer.htm](https://energyusecalculator.com/electricity_printer.htm)
- Evil Mad Scientist (2023). Axidraw writing and drawing machines. Accessed: 2025-06-23.  
 Available at: <https://axidraw.com/>
- FDM 3D (nd). Servo motor mg90s. Accessed: 2025-09-25.  
 Available at: <https://fdm3d.co.za/products/mg90s-servo-motor?variant=48545770864853>

Goodwin University (2024). What is cnc machining? Accessed: 2025-06-23.

Available at: <https://www.goodwin.edu/enews/what-is-cnc/>

Gordon, C.C., Churchill, T., Clauser, C.E., Bradtmiller, B., McConville, J.T., Tebbetts, I. and Walker, R.A. (1988 March). Anthropometric survey of u.s. army personnel: Summary statistics, interim report for 1988. Tech. Rep., United States Army Natick, Research, Development and Engineering Center, Natick, Massachusetts.

GRBL-Plotter (2025). Welcome to grbl-plotter. Accessed: 2025-10-18.

Available at: <https://grbl-plotter.de/?setlang=en>

Group, M. (2022). Choosing between timing belts and cogged drives. Accessed: 2025-07-25.

Available at: <https://megadyne-group.com/za/blog/choosing-between-timing-belts-and-cogged-drives>

Gökler, M.I. and Koç, M.B. (1997). Design of an automatic tool changer with disc magazine for a cnc horizontal machining center. *International Journal of Machine Tools and Manufacture*, vol. 37, no. 3, pp. 277–286. ISSN 0890-6955.

Güzel, E. (2016). Kfl08. Accessed: 2025-06-15.

Available at: <https://grabcad.com/library/kfl08-1>

Halim, A.H. and Ismail, I. (2019). Combinatorial optimization: Comparison of heuristic algorithms in travelling salesman problem. *Archives of computational methods in engineering*, vol. 26, no. 2, pp. 367–380. ISSN 1134-3060.

Health and Safety Executive, 2020 (2020). Health and safety executive manual handling at work a brief guide. Accessed: 2025-07-02.

Available at: <https://www.hse.gov.uk/pubns/INDG143.pdf>

Hiwin Corporation (2025). Linear guideway - technical information. Tech. Rep., Hiwin Corporation. Accessed: 2025-06-15.

Available at: <https://www.hiwin.com/wp-content/uploads/HIWIN-Linear-Guideway-Catalog.pdf>

IconPacks (2025). Free rocket svg, png icon, symbol. download image. Accessed: 2025-10-05.

Available at: <https://www.iconpacks.net/free-icon/rocket-9996.html>

Incredible Connection (2025). Parrot whiteboard marker slimline x 4 assorted. Accessed: 2025-09-25.

Available at: <https://www.incredible.co.za/parrot-whiteboard-marker-slimline-x-4-assorted>

Intel Corporation (2025). What is computer and laptop ram? Accessed: 2025-10-18.

Available at: <https://www.intel.com/content/www/us/en/tech-tips-and-tricks/computer-ram.html>

- International Organization for Standardization (2010). Iso 12100:2010 - safety of machinery — general principles for design — risk assessment and risk reduction. Accessed: 2025-10-18.
- Jeroen (2025). Gt2 16t pulley. Accessed: 2025-06-15.  
 Available at: <https://grabcad.com/library/gt2-16t-pulley-2>
- Khdeir, Y. and Awad, A. (2025). A comparison of heuristic algorithms for solving the traveling salesman problem. *An-Najah University Journal for Research - A (Natural Sciences)*, vol. 39, no. 1, pp. 73–80. ISSN 1727-2114.
- Lawton, D. (2025a). 20mm 2 pin limit switch. Accessed: 2025-06-15.  
 Available at: <https://grabcad.com/library/20mm-2-pin-limit-switch-1>
- Lawton, D. (2025b). Nema 17 42x40x5. Accessed: 2025-06-15.  
 Available at: <https://grabcad.com/library/nema-17-42x40x5-1>
- Leonarduzzi, A. (2016). Menawell lrs-100-12. Accessed: 2025-06-15.  
 Available at: <https://grabcad.com/library/menawell-lrs-100-12-1>
- Levin, A. and Yovel, U. (2013). Nonoblivious 2-opt heuristics for the traveling salesman problem. *Networks*, vol. 62, no. 3, pp. 201–219. ISSN 0028-3045.
- Maker Store (2023). Introduction to timing pulleys. Accessed: 2025-10-04.  
 Available at: <https://www.makerstore.com.au/blog/timing-pulleys/>
- Maqsood, S., Abbas, M., Hu, G., Ramli, A.L.A. and Miura, K.T. (2020). A novel generalization of trigonometric b閦ier curve and surface with shape parameters and its applications. *Mathematical Problems in Engineering*, vol. 2020, no. 1, p. 4036434.  
 Available at: <https://onlinelibrary.wiley.com/doi/abs/10.1155/2020/4036434>
- Melo, M. (2021). Understanding b閦ier curves. Accessed: 2025-09-28.  
 Available at: <https://mrrndev.medium.com/understanding-b%C3%A9zier-curves-f6eaa0fa6c7d>
- Microrobotics (2025a). Bearing 5x16x5 inner diameter 5mm (4 pack). Accessed: 2025-09-25.  
 Available at: <https://www.robotics.org.za/625ZZ>
- Microrobotics (2025b). Coupler direct 5mm-4mm. Accessed: 2025-09-25.  
 Available at: <https://www.robotics.org.za/CD0504>
- Microrobotics (2025c). Dc dc buck converter, vin 4-38v , vout 1.25-36v 8a. Accessed: 2025-09-25.  
 Available at: <https://www.robotics.org.za/XL4016?search=buck%20converter>
- Microrobotics (2025d). Gt2 belt idler pulley, 20 teeth, bore 5mm, width 6mm. Accessed: 2025-09-25.  
 Available at: <https://www.robotics.org.za/GT2-20T-B5-IDLER>

Microrobotics (2025e). Stepper motor 0.28nm 1.3a nema17. Accessed: 2025-09-25.

Available at: <https://www.robotics.org.za/17HS3401>

Microrobotics (2025f). Stepper motor 1.8 n.cm nema8 0.6a per phase. Accessed: 2025-09-25.

Available at: <https://www.robotics.org.za/20BYGH306>

Motion King (nd). Hb stepper motor catalog. Tech. Rep., MotionKing (China) Motor Industry Co., Ltd. Accessed: 2025-07-25.

Available at: <https://www.alldatasheet.com/datasheet-pdf/download/1137268/MOTIONKING/17HS3401.html>

Neumann, A. (2008). *Scalable Vector Graphics (SVG)*, pp. 1013–1021. Springer US, Boston, MA. ISBN 978-0-387-35973-1.

Available at: [https://doi.org/10.1007/978-0-387-35973-1\\_1159](https://doi.org/10.1007/978-0-387-35973-1_1159)

Nuraiman, D., Ilahi, F., Dewi, Y. and Hamidi, E.A.Z. (2018). A new hybrid method based on nearest neighbor algorithm and 2-opt algorithm for traveling salesman problem. In: *2018 4th International Conference on Wireless and Telematics (ICWT)*, pp. 1–4. IEEE.

Pamplin, C. (2025). Dc buck converter 1.25-36v. Accessed: 2025-06-15.

Available at: <https://grabcad.com/library/dc-buck-converter-1-25-36v-1>

Pantone (2025). Understanding different color spaces. Accessed: 2025-10-04.

Available at: <https://www.pantone.com/articles/color-fundamentals/understanding-different-color-spaces>

Pasma, P. (nd). Measure the line width of your pens with a plotter. Accessed: 2025-10-05.

Available at: <https://piterasma.nl/articles/line-test>

Pednekar, A. (2021). Arduino uno cnc shield. Accessed: 2025-06-15.

Available at: <https://grabcad.com/library/arduino-uno-cnc-shield-1>

Pienaar, A. (2024). Design and construction of a kinetic art table. *Department of Mechanical and Mechatronic Engineering Stellenbosch University*.

Pryimachenko, O. (2024). Tower pro mg90s micro servo. Accessed: 2025-06-15.

Available at: <https://grabcad.com/library/tower-pro-mg90s-micro-servo-2>

Ranakoti, L., Gangil, B., Mishra, S.K., Singh, T., Sharma, S., Ilyas, R. and El-Khatib, S. (2022). Critical review on polylactic acid: Properties, structure, processing, biocomposites, and nanocomposites. *Materials*, vol. 15, p. 4312.

Available at: <https://www.ncbi.nlm.nih.gov/pmc/articles/PMC9228835/>

Rathbone, E. (2020). What is g-code programming? Accessed: 2025-07-28.

Available at: <https://www.autodesk.com/products/fusion-360/blog/getting-started-with-g-code/>

- Rogelio, J.P. and Baldovino, R.G. (2014). Development of an automatic tool changer (atc) system for the 3-axis computer numerically-controlled (cnc) router machine: Support program for the productivity and competitiveness of the metals and engineering industries. In: *2014 International Conference on Humanoid, Nanotechnology, Information Technology, Communication and Control, Environment and Management (HNICEM)*, pp. 1–5.
- Rossing, C. (2014). Xy coordinates, 2 axis motion? Accessed: 2025-06-23.  
Available at: <https://mekatronikgruppe6.wordpress.com/2014/04/04/xy-coordinates-2-axis-motion/>
- RS Components (2025a). Mitutoyo 150mm, 6in digital caliper 0.01 mm resolution, imperial, metric. Accessed: 2025-10-04.  
Available at: <https://za.rs-online.com/web/p/calipers/2455676>
- RS Components (2025b). Rs pro 608-2rs single row deep groove ball bearing- both sides sealed 8mm i.d, 22mm o.d. Accessed: 2025-09-25.  
Available at: <https://za.rs-online.com/web/p/ball-bearings/2612600>
- Santos, N. (2024). emergency stop button. Accessed: 2025-06-15.  
Available at: <https://grabcad.com/library/emergency-stop-button-12>
- Shuja, H. (2018). Mgn12 linear guide subassembly, configurable rail length from 100 mm to 2000 mm in increments of 50 mm. Accessed: 2025-06-15.  
Available at: <https://grabcad.com/library/mgn12-linear-guide-subassembly-configurable-rail-length-from-100-mm-to-2000-mm-in-increments-of-50-mm-1>
- Smoothy, L. (2024). The history of cnc machining. Accessed: 2025-06-23.  
Available at: <https://get-it-made.co.uk/resources/the-history-of-cnc-machining>
- svenhb (2025). Grbl-plotter. Accessed: 2025-09-17.  
Available at: <https://github.com/svenhb/GRBL-Plotter>
- Trajkovski, S. (1985). Automatic tool changers for nc machining centres. In: Bullinger, H.-J. and Warnecke, H.J. (eds.), *Toward the Factory of the Future*, pp. 95–100. Springer Berlin Heidelberg, Berlin, Heidelberg. ISBN 978-3-642-82580-4.
- UUNA TEK CO., LIMITED (2025a). All products. Accessed: 2025-06-23.  
Available at: <https://uunatek.com/collections/all-products>
- UUNA TEK CO., LIMITED (2025b). About uuna tek®. Accessed: 2025-06-23.  
Available at: <https://uunatek.com/pages/how-it-all-began-share-the-best-with-you>
- UUNA TEK CO., LIMITED (2025c). Uuna tek 3.0 - a3/a2/a1/a0 size preassembled highend all-in-one pen plotter drawing robot drawing machine writing machine signature machine. Accessed: 2025-06-23.  
Available at: <https://uunatek.com/collections/all-products/products/>

[uuna-tek-3-0-pen-plotter-drawing-robot-drawing-machine-homework-machine-handwriting-robot](https://grabcad.com/library/uuna-tek-3-0-pen-plotter-drawing-robot-drawing-machine-homework-machine-handwriting-robot)

Velykyi, O. (2023). Servomotor sg90. Accessed: 2025-06-15.

Available at: <https://grabcad.com/library/servomotor-sg90-1>

Xiaohong, L., Zhenyuan, J., Xudong, H., Wentao, W., Pengzhuo, H., Zongjin, R. and Likun, S. (2014). Reliability oriented performance testing system of chain-type magazine and atc. *Sensors & Transducers*, vol. 177, pp. 113–121.

Zdelarec, I. (2014). 12mm linear bearings. Accessed: 2025-06-15.

Available at: <https://grabcad.com/library/12mm-linear-bearings-1>

Zhurov, K. (2023). Dm1 series micro switch. Accessed: 2025-06-15.

Available at: <https://grabcad.com/library/dm1-series-micro-switch-1>

Černý, J. (2020). Gates powergrip® 2gt smooth idler 6mm belt - 12mm od - 5mm id, e3d. Accessed: 2025-06-15.

Available at: <https://grabcad.com/library/gates-powergrip-2gt-smooth-idler-6mm-belt-12mm-od-5mm-id-e3d-1>